ISSN 2218-4333 (online)

World Journal of *Clinical Oncology*

World J Clin Oncol 2022 November 24; 13(11): 866-942

Published by Baishideng Publishing Group Inc

WJCO

World Journal of Clinical Oncology

Contents

Monthly Volume 13 Number 11 November 24, 2022

World Journal of Clinical Oncology

Monthly Volume 13 Number 11 November 24, 2022

Contents

ABOUT COVER

Editorial Board Member of *World Journal of Clinical Oncology*, Mamdouh M El-Shishtawy, Professor, Department of Biochemistry, Faculty of Pharmacy, Mansoura University, Mansoura, 35516, Dakahlia Governorate, Egypt. mshisht@mans.edu.eg

AIMS AND SCOPE

The primary aim of *World Journal of Clinical Oncology* (*WJCO*, *World J Clin Oncol*) is to provide scholars and readers from various fields of oncology with a platform to publish high-quality basic and clinical research articles and communicate their research findings online.

WJCO mainly publishes articles reporting research results and findings obtained in the field of oncology and covering a wide range of topics including art of oncology, biology of neoplasia, breast cancer, cancer prevention and control, cancer-related complications, diagnosis in oncology, gastrointestinal cancer, genetic testing for cancer, gynecologic cancer, head and neck cancer, hematologic malignancy, lung cancer, melanoma, molecular oncology, neurooncology, palliative and supportive care, pediatric oncology, surgical oncology, translational oncology, and urologic oncology.

INDEXING/ABSTRACTING

The *WJCO* is now abstracted and indexed in PubMed, PubMed Central, Emerging Sources Citation Index (Web of Science), Reference Citation Analysis, China National Knowledge Infrastructure, China Science and Technology Journal Database, and Superstar Journals Database. The 2022 edition of Journal Citation Reports® cites the 2021 Journal Citation Indicator (JCI) for *WJCO* as 0.35.

RESPONSIBLE EDITORS FOR THIS ISSUE

NAME OF JOURNAL
World Journal of Clinical Oncology

ISSN
ISSN 2218-4333 (online)

LAUNCH DATE
November 10, 2010

FREQUENCY
Monthly

EDITORS-IN-CHIEF
Hiten RH Patel, Stephen Safe, Jian-Hua Mao, Ken H Young

EDITORIAL BOARD MEMBERS
https://www.wjgnet.com/2218-4333/editorialboard.htm

PUBLICATION DATE
November 24, 2022

INSTRUCTIONS TO AUTHORS
https://www.wjgnet.com/bpg/gerinfo/204

GUIDELINES FOR ETHICS DOCUMENTS
https://www.wjgnet.com/bpg/GerInfo/287

GUIDELINES FOR NON-NATIVE SPEAKERS OF ENGLISH
https://www.wjgnet.com/bpg/gerinfo/240

PUBLICATION ETHICS
https://www.wjgnet.com/bpg/GerInfo/288

PUBLICATION MISCONDUCT
https://www.wjgnet.com/bpg/gerinfo/208

ARTICLE PROCESSING CHARGE
https://www.wjgnet.com/bpg/gerinfo/242

STEPS FOR SUBMITTING MANUSCRIPTS
https://www.wjgnet.com/bpg/GerInfo/239

ONLINE SUBMISSION
https://www.f6publishing.com

World Journal of Clinical Oncology

Submit a Manuscript: https://www.f6publishing.com

World J Clin Oncol 2022 November 24; 13(11): 866-879

DOI: 10.5306/wjco.v13.i11.866

ISSN 2218-4333 (online)

REVIEW

Influence of *Helicobacter pylori* oncoprotein CagA in gastric cancer: A critical-reflective analysis

Fabrício Freire de Melo, Hanna Santos Marques, Samuel Luca Rocha Pinheiro, Fabian Fellipe Bueno Lemos, Marcel Silva Luz, Kádima Nayara Teixeira, Cláudio Lima Souza, Márcio Vasconcelos Oliveira

Specialty type: Oncology

Provenance and peer review: Invited article; Externally peer reviewed.

Peer-review model: Single blind

Peer-review report's scientific quality classification

Grade A (Excellent): 0
Grade B (Very good): B, B, B
Grade C (Good): C
Grade D (Fair): 0
Grade E (Poor): 0

P-Reviewer: Bataga SM, Romania; Fujimori S, Japan; Kirkik D, Turkey; SathiyaNarayanan R, India

Received: August 6, 2022
Peer-review started: August 6, 2022
First decision: September 5, 2022
Revised: September 20, 2022
Accepted: October 11, 2022
Article in press: October 11, 2022
Published online: November 24, 2022

Fabrício Freire de Melo, Samuel Luca Rocha Pinheiro, Fabian Fellipe Bueno Lemos, Marcel Silva Luz, Cláudio Lima Souza, Márcio Vasconcelos Oliveira, Instituto Multidisciplinar em Saúde, Universidade Federal da Bahia, Vitória da Conquista 45029-094, Brazil

Hanna Santos Marques, Campus Vitória da Conquista, Universidade Estadual do Sudoeste da Bahia, Vitória da Conquista 45029-094, Brazil

Kádima Nayara Teixeira, Campus Toledo, Universidade Federal do Paraná, Toledo 85919899, Brazil

Corresponding author: Fabrício Freire de Melo, PhD, Professor, Instituto Multidisciplinar em Saúde, Universidade Federal da Bahia, Estrada do Bem Querer, 3293-3391 - Candeias, Vitória da Conquista 45029-094, Brazil. freiremeloufba@gmail.com

Abstract

Gastric cancer is the fifth most common malignancy and third leading cancer-related cause of death worldwide. *Helicobacter pylori* is a Gram-negative bacterium that inhabits the gastric environment of 60.3% of the world's population and represents the main risk factor for the onset of gastric neoplasms. CagA is the most important virulence factor in *H. pylori*, and is a translocated oncoprotein that induces morphofunctional modifications in gastric epithelial cells and a chronic inflammatory response that increases the risk of developing precancerous lesions. Upon translocation and tyrosine phosphorylation, CagA moves to the cell membrane and acts as a pathological scaffold protein that simultaneously interacts with multiple intracellular signaling pathways, thereby disrupting cell proliferation, differentiation and apoptosis. All these alterations in cell biology increase the risk of damaged cells acquiring pro-oncogenic genetic changes. In this sense, once gastric cancer sets in, its perpetuation is independent of the presence of the oncoprotein, characterizing a "hit-and-run" carcinogenic mechanism. Therefore, this review aims to describe *H. pylori*- and CagA-related oncogenic mechanisms, to update readers and discuss the novelties and perspectives in this field.

Key Words: *Helicobacter pylori*; Virulence factors; CagA; Gastric cancer; EPIYA motifs; Hit-and-run carcinogenesis

Core tip: CagA is a translocated effector protein that induces morphofunctional modifications in gastric epithelial cells and persistent chronic gastric inflammation. Upon translocation, the bacterial oncoprotein acts as a promiscuous scaffold or hub protein, which is capable of disrupting multiple host signaling pathways, thereby inducing precancerous cellular alterations. This review aims to describe *Helicobacter pylori*- and CagA-related oncogenic mechanisms, as well as to discuss the novelties and perspectives in this field.

Citation: Freire de Melo F, Marques HS, Rocha Pinheiro SL, Lemos FFB, Silva Luz M, Nayara Teixeira K, Souza CL, Oliveira MV. Influence of *Helicobacter pylori* oncoprotein CagA in gastric cancer: A critical-reflective analysis. *World J Clin Oncol* 2022; 13(11): 866-879
URL: https://www.wjgnet.com/2218-4333/full/v13/i11/866.htm
DOI: https://dx.doi.org/10.5306/wjco.v13.i11.866

INTRODUCTION

The multiple virulence mechanisms of *Helicobacter pylori* confer an ability to colonize the hostile gastric environment[1]. This pathogen infects > 50% of the global population and is a major health concern due to the serious repercussions related to its colonization[2]. Among the diseases predisposed by *H. pylori* infection, gastric adenocarcinoma is the fifth most common malignancy and third leading cancer-related cause of death worldwide[3]. Of note, the close relationship between *H. pylori* and gastric cancer has led the World Health Organization International Agency for Research on Cancer Working Group to consider the bacterium as a class 1 carcinogen based on epidemiological evidence and biological plausibility[4].

Various virulence factors contribute to successful *H. pylori* colonization and pathogenicity[5]. Among these factors is *cagA*, a well-known gene that encodes an oncogenic protein that seems to be a determining agent in *H. pylori*-related gastric carcinogenesis[6]. CagA seropositivity, regardless of *H. pylori* status, is associated with increased gastric cancer risk. The *cagA* gene is located in the pathogenicity island *cag* (*cag*PAI), a nucleic acid sequence that encodes the type IV secretion system (T4SS), which is a bacterial apparatus that delivers the CagA protein and peptidoglycans into gastric epithelial cells. Inside host cells, that virulence factor suffers phosphorylation at a Glu-Pro-Ile-Tyr-Ala (EPIYA) motif, a variable C-terminal region and, subsequently, promotes the activation of the SH2-containing protein tyrosine phosphatase (SHP2)[7,8]. SHP2, in turn, triggers various mechanisms that lead to important cell changes, including alterations in cellular morphology through the disturbing of cell polarity, which leads to a "hummingbird" phenotype, as well as carcinogenesis-related changes in cytoskeleton[9].

Despite the extensive number of studies on the relationship between CagA and *H. pylori* infection, much still has to be done in order to better understand the role of this oncoprotein in gastric carcinogenesis. Recent investigations have explored multiple host–pathogen interactions in this setting and found other CagA-triggered pathways that probably influence cancer development[10]. Moreover, the action of small RNAs in CagA post-transcriptional regulation has been investigated, showing a broad field to be explored[11]. This review aims to describe *H. pylori*- and CagA-related oncogenic mechanisms, and to discuss the novelties and perspectives in this field.

PATHOGENESIS OF *H. PYLORI* GASTRIC INFECTION

The capacity to resist severe stomach acid conditions is a notable aspect of *H. pylori*. To provide successful colonization, the pathogen uses various mechanisms, such as enhanced motility, adherence to gastric epithelial cells, enzymatic machinery, and virulence factors[12]. Besides that, the host immune system also plays an essential role during the infection, mainly by a Th1 response against the bacteria [13].

The bacterial flagella are crucial for reaching the protective mucus layer at the exterior of the gastric mucosa. After entering the stomach, *H. pylori* uses its flagella for swimming in gastric content, allowing the pathogen to arrive at the mucus layer[14]. Some studies have shown that the ferric uptake regulator performs an important role in bacterial colonization, positively regulating the flagellar motility switch in *H. pylori* strain J99[15]. Another factor described as a motility modulator is HP0231, a Dsb-like protein. It cooperates in redox homeostasis and is fundamental for gastric establishment[16].

H. pylori also depends on chemotaxis for its colonization. The essential pathogen chemoreceptors are T1pA, B, C, D, a CheA kinase, a CheY responsive regulator, and numerous coupling proteins, playing a pivotal role in bacteria pathogenesis[17]. The aggregation of the coupling proteins CheW and CheV1 culminates in the formation of the CheA chemotaxis complex, activating CheA kinase and optimizing the chemotaxis function[18].

An ideal balance between nickel absorption and incorporation is indispensable for *H. pylori* colonization, since nickel is an essential metal for bacterial survival and infection[12,19]. This metal is a cofactor for two significant enzymes: urease and hydrogenase. Both of them have a role in gastric infection, contributing, respectively, to bacterial colonization and metabolism signaling cascade to produce energy[20,21].

Adherence and outer membrane gastric cell receptors are also relevant in bacterial pathogenesis. The blood group antigen binding adhesin (BabA) is the best-studied molecule of *H. pylori*[22]. This protein sequence affects acid sensitivity and plays a critical role in bacterial acid adaptation during infection [12]. Pathogens with high BabA expression levels have increased virulence, leading to duodenal cancer and gastric adenocarcinoma[23]. Another adhesin has been described: HopQ. This molecule binds to cell adhesion molecules related to the carcinoembryonic antigen (carcinoembryonic antigen-related cell adhesion molecules, CEACAMs) 1, 3, 5 and 6, promoting cell signaling guided by this interaction, allowing the translocation of the oncoprotein CagA, the most important *H. pylori* virulence factor, and rising proinflammatory mediators in the infected cells[24,25].

Additionally, besides CagA, a wide range of virulence factors like vacuolating cytotoxin A (VacA), DupA and OipA have been reported as determinant molecules for *H. pylori* pathogenicity[26]. VacA, whose gene is found in most bacterial strains, promotes the formation of acidic vacuoles in gastric epithelial cells and modulate the immune response, leading to an immune tolerance and enduring *H. pylori* infection, due to its role in the activity of T cells and antigen-presenting cells [27,28]. These VacA functions can lead to gastritis and duodenal ulcer and gastric cancer development. The bacterial protein DupA provides acid resistance to the pathogen, and seems to cooperate with the production of interleukin (IL)-8, enhancing its levels in the gastric mucosa[29]. The outer membrane protein OipA contributes to the adhesion and activation of IL-8 production, increasing inflammation. OipA is a significant virulence factor on the infection outcome, resulting in increased development of gastric cancer and peptic ulcers[30].

H. pylori infection produces complex host immune responses, through diverse immune mechanisms [31]. During the first contact with the bacteria, a wide range of antigens like lipoteichoic acid and other lipoproteins bind to stomach cell receptors, known as Toll-like receptors (TLRs)[32]. After this interaction, NF-B and c-Jun N-terminal kinase activation takes place, among the proinflammatory cytokine release as signaling pathways[33]. Neutrophils and mononuclear cells infiltrate the gastric surface, producing nitric oxide and reactive oxygen species (ROS), and recruiting $CD4^+$ and $CD8^+$ T cells [34]. Finally, a Th1-polarized response occurs, with enhanced levels of IFN-γ, IL-1β, Il-6, IL-7, IL-8, IL-10 and IL-18[35,36].

A correlation has been shown between Th17 cells, a proinflammatory subset of $CD4^+$ T cells, and their affiliated cytokines (IL-17A, IL-17F, IL-21, IL-22 and IL-26) in persistent *H. pylori*-mediated gastric inflammation and the subsequent gastric cancer development[36,37]. We have demonstrated in a previous study that an IL-17 T-cell response predominates in *H. pylori*-associated gastritis in adults, whereas, in children, there is predominance of a T regulatory (Treg) cell response. IL-17A is known to play an important role in the recruitment and activation of polymorphonuclear cells that are vital for *H. pylori* clearance. Treg and Th17 cells are mutually controlled. Therefore, these findings could explain the higher susceptibility of children to the infection and bacterial persistence[38].

IL-27 expression differs between *H. pylori*-related diseases. Accordingly, we have shown that there is a high expression of IL-27 in the gastric mucosa and serum of *H. pylori*-positive duodenal ulcer patients. In contrast, IL-27 is absent in the gastric mucosa and serum of patients with gastric cancer. Consistent with the immunosuppressive role of IL-27 in Th17 cells and IL-6 expression, we observed that expression of Th17-cell-associated cytokines was lower in the patients with duodenal ulcer, which secreted a large concentration of proinflammatory Th1 representative cytokines. We demonstrated that there is high levels of IL-1β, IL-6, IL-17A, IL-23, and transforming growth factor-β, involved in IL-17A expression, on the gastric mucosa and in the serum of gastric cancer patients. Therefore, IL-27 may be involved in the development of different patterns of *H. pylori*-induced gastritis and its progression. Taking into account that IL-27 has evident antitumor activity, our results point to a possible therapeutic use of IL-27 as an anticancer agent[39].

Recently, the role of the interaction between *H. pylori* infection and the gastrointestinal microbiome in gastric carcinogenesis has also been investigated. In this regard, researchers explored the diversity and composition of the gastric microbiome at different stages of disease, including normal gastric mucosa, chronic gastritis, atrophic gastritis, intestinal metaplasia, and gastric cancer[40]. A recent meta-analysis indicated that *H. pylori*-positive gastric samples exhibit reduced microbial diversity, altered microbial community, composition, and bacterial interactions. An increased abundance of opportunistic pathogens (*e.g.*, *Veillonella* and *Parvimonas*) was observed concomitantly with a decrease in putative probiotics (*e.g.*, *Bifidobacterium*) throughout the stages of disease progression[41]. Another study has suggested that successful eradication of *H. pylori* could reverse the tendency towards gastric microbiota

dysbiosis and show beneficial effects on the gastric microbiota[42]. The next step in this field could be to conduct a prospective, multicenter, crosscultural study to validate these results and explore the mechanisms underlying the *H. pylori*–gastric microbiota interaction and its role in gastric cancer development[43].

CAGA — *H. PYLORI* TRANSLOCATED ONCOPROTEIN

CagA is a translocated effector protein that induces morphofunctional modifications in gastric epithelial cells and inflammatory responses, whose balance allows successful colonization of the acidic stomach environment[44,45]. The CagA gene is located in the *cag*PAI; a 40-kb DNA fragment that contains about 31 genes and confers virulence to some strains of *H. pylori*. Some genes of the island encode proteins that form a T4SS, which is responsible for the translocation of CagA into the cytoplasm of gastric epithelial cells through interaction of bacterial and host cell components[46-48]. The oncoprotein has a molecular weight of 128–145 kDa and its tertiary structure is characterized by a structured N-terminal region, split into Domains I–III and an unstructured C-terminal tail[49].

Injection of CagA depends on the recognition of its N-terminal and C-terminal portions by T4SS, which can occur simultaneously or not[50]. However, several other mechanisms are also required for its inoculation. We highlight the binding between T4SS CagL and CagY to human β1-integrins[51,52], along with the CEACAMs and *H. pylori* outer membrane protein Q (HopQ) interaction, that allow the translocation of CagA into the host cells[53]. A recent study noted that the instability of the relationship between *H. pylori* HopQ and mouse CEACAMs may explain why the pathogenesis of infection in the stomach of rodents infected with CagA positive *H. pylori* strains occurs differently from infection by the same strain in humans. The authors also demonstrated that the presence of functional T4SS is associated with a time-dependent reduction in human CEACAM1 levels after CagA-positive *H. pylori* infection [54]. However, it is still unclear whether the instability of the HopQ–CEACAMs relationship favors the host or the bacterium, so more studies are needed to investigate the possibility of these interactions being beneficial in favor of the patient infected with *H. pylori*. BabA is apparently also capable of increasing T4SS activity[55].

CagA is known to possess multiple phosphorylation segments in its tertiary structure. The phosphorylation sites are denominated EPIYA sequences; regions consisting of five amino acids (Glu-Pro-Ile-Tyr-Ala) located in the C-terminal portion of the oncoprotein. Four different EPIYA segments have been described according to the different amino acid sequences surrounding each motif, designated EPIYA-A (32 amino acids), B (40 amino acids), C (34 amino acids) and D (42 amino acids). EPIYA-A and EPIYA-B motifs have been identified in almost all CagA-positive *H. pylori* strains, followed by one, two, or three EPIYA-C sequences in western strains, or an EPIYA-D segment in East Asian strains[56,57]. Figure 1A summarizes the main structural domain differences between East Asian and western CagA.

Once inside the gastric epithelial cells, the EPIYA segments are selectively tyrosine-phosphorylated by different kinases of the Src family (s-Src, Fyn, Lyn and Yes) or by Abl kinase of the host cells[58-61]. After the phosphorylation process, CagA moves to the cell membrane and acts as a promiscuous scaffold protein that simultaneously disturbs multiple signaling pathways, involved in the regulation of a large range of cellular processes, including proliferation, differentiation and apoptosis[62].

In this sense, a better understanding of the molecular structure of CagA and the interactions promoted by CagA-positive *H. pylori* strains to prevail in the host organism may be essential in identifying variations in prognosis, disease severity, and mechanisms that may be beneficial to the host, according to infections by different *H. pylori* strains.

ROLE OF CagA IN GASTRIC CARCINOGENESIS

The translocated effector protein CagA was found to be associated with gastric cancer development even before the initial elucidation of its pathogenic mechanisms[63,64]. Initially, the correlation between infection with CagA-positive *H. pylori* strains and carcinogenesis *in vivo* was established by experiments in Mongolian gerbil models[65-67]. More recently, transgenic expression of CagA in mice and zebrafish has also been shown to be associated with the development of gastric and hematopoietic neoplasms[68, 69]. Thereby, the oncogenic potential of the bacterial protein has become increasingly evident and, at the same time, different studies have sought to clarify its underlying mechanisms. Nowadays, CagA is considered a pathological analog of a scaffold or hub protein capable of disrupting multiple host signaling pathways and promoting a pro-oncogenic microenvironment[70].

Upon translocation, CagA localizes to the inner surface of the plasmatic membrane, where it undergoes tyrosine phosphorylation by multiple members of the Src family kinases and c-Abl kinases[8, 10,59,61]. As mentioned above, four different EPIYA segments were described according to the different amino acid sequences surrounding each motif, designated EPIYA-A–EPIYA-D[56,57]. Strains containing EPIYA-D or at least two EPIYA-C motifs are known to be associated with an increased risk of

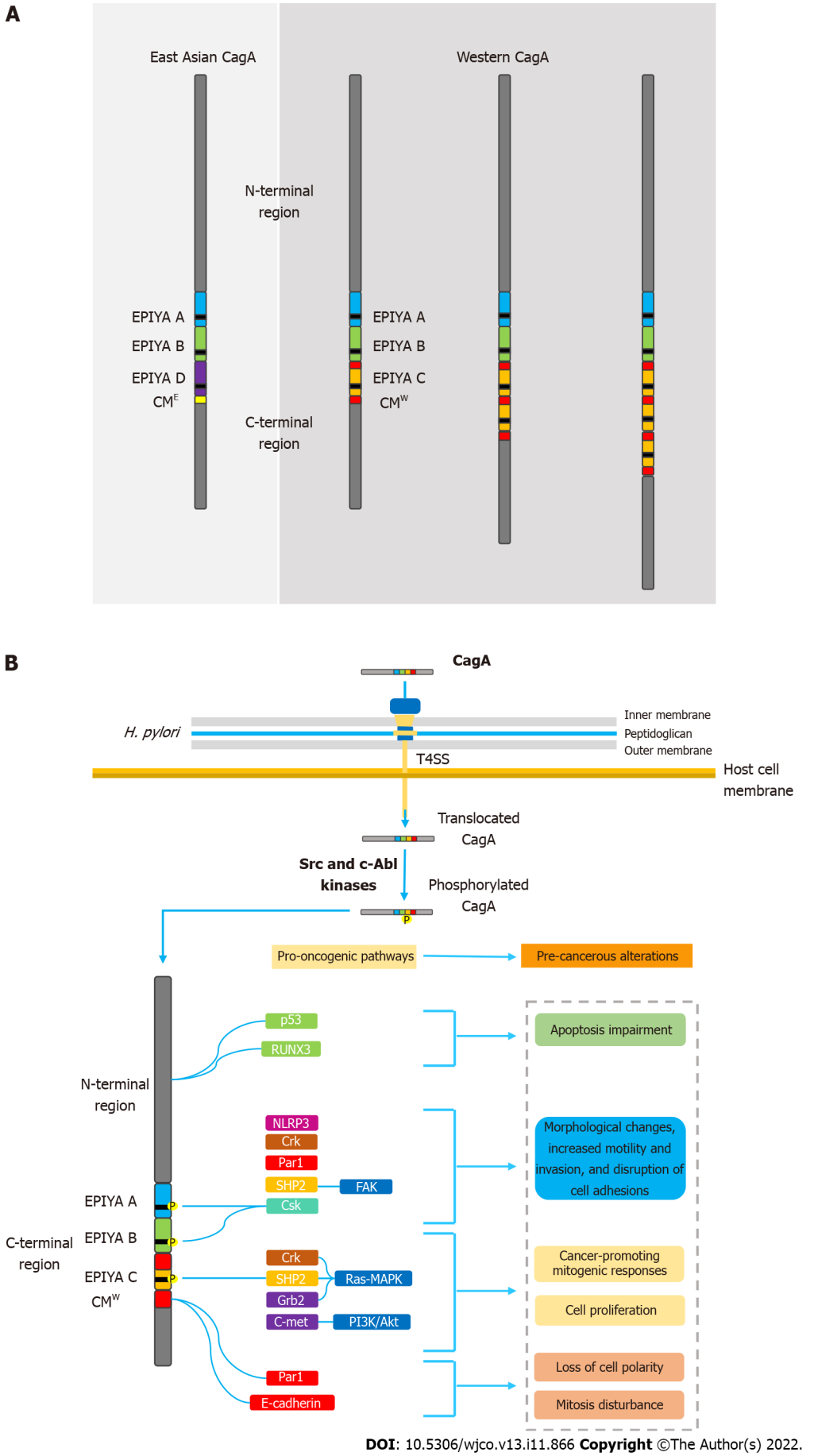

DOI: 10.5306/wjco.v13.i11.866 **Copyright** ©The Author(s) 2022.

Figure 1 *Helicobacter pylori* oncoprotein: molecular structure and CagA-mediated carcinogenesis underlying mechanisms. A: Structural

domain differences between East Asian and western CagA. CagA tertiary structure is characterized by a structured N-terminal region and an unstructured C-terminal tail. The oncoprotein contains repetitive sequences in its C-terminal polymorphic region, known as the EPIYA motifs and CM motif. EPIYA-A and EPIYA-B motifs were identified in almost all CagA-positive *H. pylori* strains, followed by one, two, or three EPIYA-C sequences in western strains, or an EPIYA-D segment in East Asian strains. The CM motif, although highly conserved, possesses a 5-amino-acid difference between East Asian and western strains, hence distinguishing East Asian and Western CagA; B: Molecular mechanisms of CagA-mediated carcinogenesis. Upon translocation, CagA EPIYA motifs are tyrosine-phosphorylated by Src family or c-Abl kinases of the host cell. After phosphorylation, CagA localizes to the inner leaflet of the plasmatic membrane and acts as a promiscuous scaffold or hub protein that simultaneously disturbs multiple host signaling pathways, involved in regulation of a large range of cellular processes, including proliferation, differentiation and apoptosis. Ultimately, the disharmonic interaction between CagA and host proteins leads to pro-oncogenic cellular alterations. CM: CagA-multimerization; CM^{W}: western CagA.

developing precancerous lesions and gastric cancer[71-75]. Queiroz *et al*[75] demonstrated in a Brazilian population that first-degree relatives of patients with gastric cancer were significantly and independently more frequently colonized by *H. pylori* strains with higher numbers of CagA EPIYA-C segments, which may be associated with an enhanced risk of developing this neoplasm[76].

Following tyrosine phosphorylation, EPIYA-C and D motifs acquire the ability to interact with SHP2 and induce pathological intracellular signaling[9]. Abnormal SHP2 activity leads to aberrant activation of the Ras–MAPK pathway, which has been associated with accelerated cell cycle progression and enhanced cell proliferation. CagA-activated SHP2 is also able to interact with proteins such as focal adhesion kinase, thence leading to cell elongation, increased motility, and cytoskeleton rearrangements [77,78]. All these pathological alterations in cell biology increase the risk of damaged cells acquiring precancerous genetic changes[79]. It is worth mentioning that CagA possessing EPIYA-D or a higher number of EPIYA-C segments binds more robustly to SHP2, which may explain their association with higher risk of gastric cancer development[8]. It has also been described that EPIYA-A and B motifs are able to interact with the SH2 domains of the tyrosine-protein kinase Csk, thereby inducing damage to actin binding proteins such as cortactin and vinculin. Consequently, rearrangements in the cytoskeleton reduce cell adhesion to the extracellular matrix and increase cell motility[80]. A recent study observed that *H. pylori*, through the T4SS encoded by *cag*PAI, interferes with the activity of cortectin binding partners, and stimulates overexpression of this molecule and promotes alterations in the actin cytoskeleton that may favor cell adhesion, motility and invasion of tumor cells contributing to the development of gastric cancer[81].

Recent studies have described that SHIP2, an SH2-containing phosphatidylinositol 5′-phosphatase, is a previously undiscovered CagA binding protein. Similar to SHP2, the SHIP2 protein is able to bind to EPIYA-C and D motifs in a tyrosine phosphorylation-dependent manner. In contrast, SHIP2 binds more robustly to EPIYA-C than to EPIYA-D sequences, thereby inducing changes in membrane phosphatidylinositol composition. This process enhances the subsequent delivery of CagA to the host cell, which binds to and dysregulates SHP2[82].

Other mechanisms have also been related to the aberrant induction of morphological changes, increased motility and cell proliferation[83]. In a tyrosine-phosphorylation-dependent manner, the interaction of CagA with the adapter molecule Crk is known to drive abnormal cell proliferation *via* MAPK signaling. Furthermore, the activation of Crk signaling pathways lead to the loss of cell–cell adhesion, hence inducing cell scattering/hummingbird phenotype and cell–cell dissociation[84]. It is important to mention that the EPIYA motif that corresponds to the binding site Csk has not been identified yet. In contrast, activation of the growth factor receptor-bound protein 2 (Grb2) protein and the *C-Met* oncogene in a tyrosine-phosphorylation-independent manner can also lead to similar pathological effects, highlighting the multiplicity of pro-oncogenic mechanisms of CagA[85,86]. Grb2 is an important regulator of Ras–MAPK pathway activation, capable of deregulating cell proliferation. Activation of C-Met-mediated PI3K/Akt signaling is associated with cancer-promoting mitogenic and inflammatory response[87-91].

The ability of CagA to disrupt the epithelial barrier has also been widely linked to its carcinogenic potential. In addition to the EPIYA sequences, the oncoprotein contains another repetitive sequence in its C-terminal polymorphic region, known as the CagA-multimerization (CM) motif[90]. With its number varying between different strains, the CM motif is composed of a 16-amino-acid sequence located downstream of the last EPIYA sequence[89]. This sequence, although highly conserved, possesses a 5-amino-acid difference between East Asian and western strains, hence distinguishing East Asian and western CagA (CM^{W})[91]. Thus, higher number of EPIYA-C motifs also increases the number of CM motifs in the CM^{W}. The CM motif is identified as the main mediator of the interaction between CagA and the partitioning-defective 1 (PAR1)/microtubule affinity-regulating kinase, which plays a pivotal role in establishing epithelial polarity. As a result, there is loss of cell polarity, as well as induction of morphological alterations also associated with the hummingbird phenotype[92]. CagA-mediated PAR1 inhibition also disrupts mitosis, causing increased cell division and impaired segregation of sister chromatids, thus leading to chromosomal instability (CI)[93]. Currently, CI is widely recognized for its multifactorial role in carcinogenesis and its microenvironment[94].

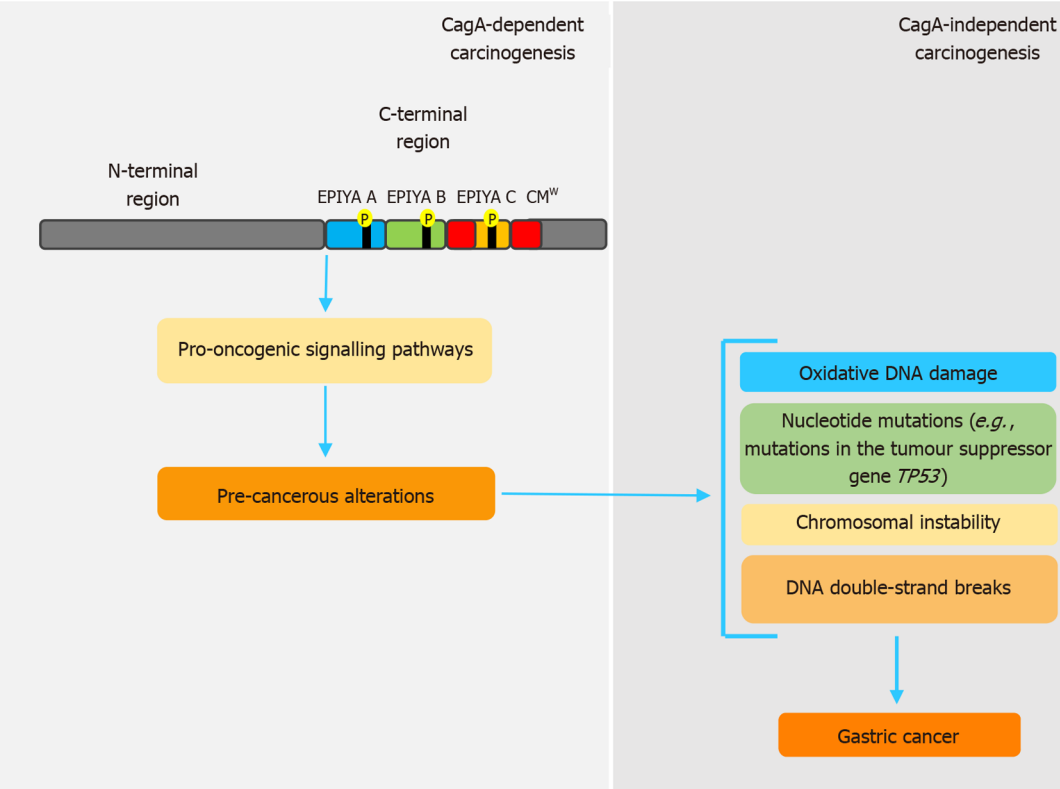

DOI: 10.5306/wjco.v13.i11.866

Figure 2 Simplified model of CagA-mediated hit-and-run carcinogenesis. The pro-oncogenic properties of CagA are already well established. However, genetic and epigenetic alterations caused by this oncoprotein provide a favorable environment for carcinogenesis, independently of its presence, in a hit-and-run carcinogenesis mechanism. In this sense, through interaction with various host proteins, CagA leads to chromosomal instability, double-strand breaks and repeated nucleotide mutations, which are correlated to gastric cancer development. CM^W: western CagA.

From a different perspective, there is also a dangerous association between CM motifs and E-cadherin, a key protein in establishing cell polarity and maintaining epithelial integrity and differentiation[95-97]. It has been described that the CagA–E-cadherin interaction downregulates the β-catenin signal that promotes intestinal transdifferentiation in gastric epithelial cells. Therefore, it was inferred that the oncoprotein plays an important role in the development of intestinal metaplasia, a precancerous transdifferentiation of gastric epithelial cells from which intestinal-type gastric adenocarcinoma emerges [98].

Also in this sense, a recent study observed that CagA seems to be able to induce gastric carcinogenesis by stimulating the migration of cancer cells through the activation of the NLR family pyrin domain containing 3 (NLRP3) inflammasome. The authors reported that CagA also participates in the generation of intracellular ROS and that ROS inhibition has the potential to disrupt the NLRP3 pathway and pyroptosis. With these findings, the authors concluded that NLRP3 plays a key role in the action of CagA on gastric cells and that silencing NLRP3 can limit the effects of migration and invasion of cancer cells caused by CagA[99].

It is worth emphasizing the ability of CagA to activate a variety of antiapoptotic pathways, upon interaction of its N-terminal portion with various tumor suppressor factors. For example, it is well described that CagA is able to impair the antiapoptotic activity of the tumor suppressor factor p53. CagA protein induces degradation of p53 protein in both ASPP2- and p14ARF-dependent manners[100, 101]. Furthermore, it is known that the interaction of the oncoprotein with Runt-related transcription factor 3 (RUNX3) is able to induce the ubiquitination and degradation of RUNX3 that blocks its antitumoral activity[102]. Figure 1B summarizes the main molecular mechanisms of CagA-mediated carcinogenesis.

Another important potential of CagA associated with gastric cancer pathogenesis is the ability to drive epithelial to mesenchymal transition (EMT); a phenomenon extensively related to carcinogenesis [103,104]. EMT is the result of a complex molecular program that allows cancer cells to suppress their epithelial characteristics, transforming themselves into mesenchymal epithelial cells. This change allows the cells to acquire motility, invasiveness, greater resistance to apoptosis, and the ability to migrate from the primary site[104,105]. In this regard, it has been shown that EMT gene expression is upregulated in gastric epithelial cells infected with *H. pylori* CagA-positive strains[106]. Nevertheless, multiple pathogenic mechanisms have been described, including reduction of glycogen synthase kinase-3 activity and triggering of the YAP oncogenic pathway, for example. However, the multiplicity of processes

involved in EMT and its role in gastric cancer development still requires further explanation[107,108].

Recent studies have not been limited to pathogen–host interactions in *H. pylori* infection, but have also investigated the mechanisms regulating bacterial virulence factors, such as CagA, and their relation to carcinogenesis. Eisenbart *et al*[11] identified a conserved, abundant nickel-regulated sRNA and named it NikS (nickel-regulated sRNA), whose expression is transcriptionally modulated based on the size of a variable thymine stretch in its promoter region. NikS, in dependence on nickel availability, directly represses several virulence factors of *H. pylori*, including the oncoprotein, CagA, and its effects on host cell internalization and epithelial barrier disruption. In this sense, multiple clinical repercussions of post-transcriptional modulation of CagA by NikS can be hypothesized, including decreased activation of procarcinogenic signaling. Kinoshita-Daitoku *et al*[109] described that NikS expression is lower in clinical isolates from gastric cancer patients than in isolates from noncancer patients, while the expression of virulence factors targeted by NikS, including CagA, is increased in isolates from gastric cancer patients. This field needs to be better explored, especially regarding the correlation of NikS with the multiple virulence factors of *H. pylori* and its potential clinical repercussions.

CAGA-MEDIATED HIT-AND-RUN CARCINOGENESIS

Even though CagA is notably a pro-oncogenic virulence factor, once gastric cancer sets in, its perpetuation is independent of the presence of this oncoprotein. In this sense, genetic and epigenetic changes caused by CagA seem to be responsible for this process, in a mechanism called "hit-and-run" carcinogenesis[58,92], firstly proposed by Skinner[110] for virus-induced cancers. Apparently, these changes are intrinsically related to disorders in the expression of activation-induced cytidine deaminase (AID), a crucial enzyme in the processes of somatic hypermutation and class-switch recombination of immunoglobulin genes in B cells[111,112]. Matsumoto *et al*[111] state that *cagA*-positive *H. pylori* induces disordered expression of AID *via* NF-B, which consequently leads to various nucleotide mutations, such as in the tumor suppressor gene *TP53*. *cagA*-positive *H. pylori* strains are also related to oxidative DNA damage, because they are able to promote increased levels of H_2O_2 and downregulation of heme oxygenase-1[89,113]. CagA also inhibits PAR1 kinase, leading to microtubule-based spindle dysfunction and consequent CI[93].

Some studies have shown that *H. pylori* can also promote DNA double-strand breaks (DSBs) in host cells[114,115], but whether or not this feature is CagA-related remains uncertain. However, a recent study showed that inhibition of PAR1b kinase by CagA hindered *BRCA1* gene phosphorylation, which leads to a BRCAness picture that, in turn, induces DSBs[116]. All these genetic and epigenetic changes support the hit-and-run mechanism, in which, regardless of the presence of CagA, the established pro-oncogenic environment maintains the acquired phenotype. Figure 2 summarizes the main features regarding CagA-mediated hit and run carcinogenesis mechanism.

CONCLUSION

In this study, we address the role of CagA in the development of *H. pylori*-mediated gastric carcinogenesis and discuss the perspectives in this field of study (Figure 3). CagA undergoes important translocation and tyrosine phosphorylation before disrupting several cell signaling pathways and promoting protein dysfunction. However, there is still much to be clarified regarding the steps involved in the role of CagA in gastric carcinogenesis. Recent discoveries such as the identification of the SHIP2 binding protein capable of binding to the EPIYA-C and D motifs and potentiating the delivery of CagA to infected cells, or discovery of the instability between the *H. pylori* HopQ and CEACAM relationship, are significant findings that can generate advances in the area, and therefore, need to be investigated in more depth. Exploration of the little-known field of regulatory RNAs seems promising for a broader understanding of the control mechanisms involved in *H. pylori* infection and CagA levels and has the potential to identify factors with important clinical repercussions for conditions such as gastric cancer. Finally, the ability of *H. pylori* to evolve as a pathogenic bacterium and as a carcinogen is undeniable, therefore, it is essential to clarify what is still unclear about the subject and periodically monitor the behavior of the bacterium in the infection, the molecular processes and elements such as CagA to advance the diagnosis and treatment of the disease.

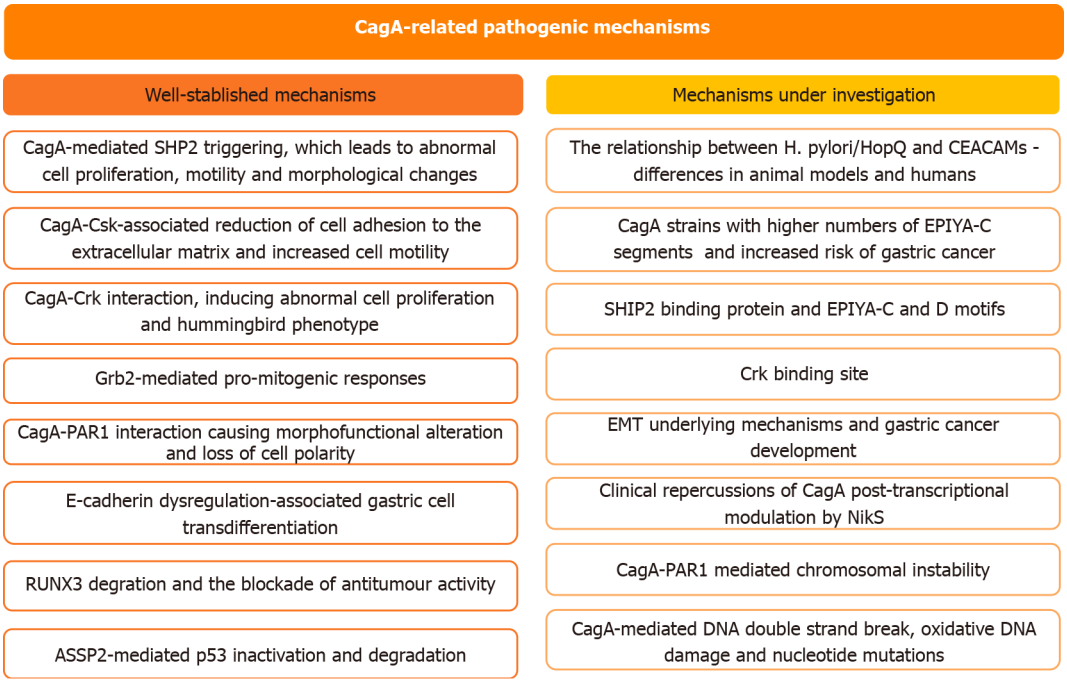

DOI: 10.5306/wjco.v13.i11.866

Figure 3 Status of the current understanding regarding CagA-related pathogenic mechanisms. EMT: Epithelial to mesenchymal transition; CEACAMs: Carcinoembryonic antigen-related cell adhesion molecules; Grb2: Growth factor receptor-bound protein 2; ASPP2: Apoptosis-stimulating protein of p53 2; SHP2: Domain-containing protein tyrosine phosphatase 2; SHIP2: Src homology 2 domain-containing inositol 5'-phosphatase 2; RUNX3: Runt-related transcription factor 3; PAR1: Partitioning-defective 1; NikS: Nickel-regulated sRNA.

FOOTNOTES

Author contributions: All authors equally contributed to this paper with conception and design of the study, literature review and analysis, drafting and critical revision and editing, and final approval of the final version; all authors agree to be accountable for all aspects of the work in ensuring that questions that are related to the accuracy or integrity of any part of the work are appropriately investigated and resolved.

Supported by National Council for Scientific and Technological Development, CNPq Brazil.

Conflict-of-interest statement: All the authors report no relevant conflicts of interest for this article.

Country/Territory of origin: Brazil

ORCID number: Fabrício Freire de Melo 0000-0002-5680-2753; Hanna Santos Marques 0000-0001-5741-1570; Samuel Luca Rocha Pinheiro 0000-0002-8877-892X; Fabian Fellipe Bueno Lemos 0000-0002-4686-7086; Marcel Silva Luz 0000-0003-1650-5807; Cláudio Lima Souza 0000-0002-8094-8357; Márcio Vasconcelos Oliveira 0000-0002-8959-0478.

S-Editor: Gao CC
L-Editor: Kerr C
P-Editor: Gao CC

REFERENCES

1 **Sitkin S**, Lazebnik L, Avalueva E, Kononova S, Vakhitov T. Gastrointestinal microbiome and *Helicobacter pylori*: Eradicate, leave it as it is, or take a personalized benefit-risk approach? *World J Gastroenterol* 2022; **28**: 766-774 [PMID: 35317277 DOI: 10.3748/wjg.v28.i7.766]
2 **Alzahrani S**, Lina TT, Gonzalez J, Pinchuk IV, Beswick EJ, Reyes VE. Effect of Helicobacter pylori on gastric epithelial cells. *World J Gastroenterol* 2014; **20**: 12767-12780 [PMID: 25278677 DOI: 10.3748/wjg.v20.i36.12767]

3 **Warsinggih**, Syarifuddin E, Marhamah, Lusikooy RE, Labeda I, Sampetoding S, Dani MI, Kusuma MI, Uwuratuw JA, Prihantono, Faruk M. Association of clinicopathological features and gastric cancer incidence in a single institution. *Asian J Surg* 2022; **45**: 246-249 [PMID: 34090784 DOI: 10.1016/j.asjsur.2021.05.004]

4 Schistosomes, liver flukes and Helicobacter pylori. *IARC Monogr Eval Carcinog Risks Hum* 1994; **61**: 1-241 [PMID: 7715068]

5 **Sgouras DN**, Trang TT, Yamaoka Y. Pathogenesis of Helicobacter pylori Infection. *Helicobacter* 2015; **20** Suppl 1: 8-16 [PMID: 26372819 DOI: 10.1111/hel.12251]

6 **Alipour M**. Molecular Mechanism of Helicobacter pylori-Induced Gastric Cancer. *J Gastrointest Cancer* 2021; **52**: 23-30 [PMID: 32926335 DOI: 10.1007/s12029-020-00518-5]

7 **Backert S**, Tegtmeyer N, Fischer W. Composition, structure and function of the Helicobacter pylori cag pathogenicity island encoded type IV secretion system. *Future Microbiol* 2015; **10**: 955-965 [PMID: 26059619 DOI: 10.2217/fmb.15.32]

8 **Selbach M**, Moese S, Hauck CR, Meyer TF, Backert S. Src is the kinase of the Helicobacter pylori CagA protein *in vitro* and in vivo. *J Biol Chem* 2002; **277**: 6775-6778 [PMID: 11788577 DOI: 10.1074/jbc.C100754200]

9 **Higashi H**, Tsutsumi R, Muto S, Sugiyama T, Azuma T, Asaka M, Hatakeyama M. SHP-2 tyrosine phosphatase as an intracellular target of Helicobacter pylori CagA protein. *Science* 2002; **295**: 683-686 [PMID: 11743164 DOI: 10.1126/science.1067147]

10 **Tammer I**, Brandt S, Hartig R, König W, Backert S. Activation of Abl by Helicobacter pylori: a novel kinase for CagA and crucial mediator of host cell scattering. *Gastroenterology* 2007; **132**: 1309-1319 [PMID: 17408661 DOI: 10.1053/j.gastro.2007.01.050]

11 **Eisenbart SK**, Alzheimer M, Pernitzsch SR, Dietrich S, Stahl S, Sharma CM. A Repeat-Associated Small RNA Controls the Major Virulence Factors of Helicobacter pylori. *Mol Cell* 2020; **80**: 210-226.e7 [PMID: 33002424 DOI: 10.1016/j.molcel.2020.09.009]

12 **Camilo V**, Sugiyama T, Touati E. Pathogenesis of Helicobacter pylori infection. *Helicobacter* 2017; **22** Suppl 1 [PMID: 28891130 DOI: 10.1111/hel.12405]

13 **Bamford KB**, Fan X, Crowe SE, Leary JF, Gourley WK, Luthra GK, Brooks EG, Graham DY, Reyes VE, Ernst PB. Lymphocytes in the human gastric mucosa during Helicobacter pylori have a T helper cell 1 phenotype. *Gastroenterology* 1998; **114**: 482-492 [PMID: 9496938 DOI: 10.1016/S0016-5085(98)70531-1]

14 **Eaton KA**, Morgan DR, Krakowka S. Motility as a factor in the colonisation of gnotobiotic piglets by Helicobacter pylori. *J Med Microbiol* 1992; **37**: 123-127 [PMID: 1629897 DOI: 10.1099/00222615-37-2-123]

15 **Lee AY**, Kao CY, Wang YK, Lin SY, Lai TY, Sheu BS, Lo CJ, Wu JJ. Inactivation of ferric uptake regulator (Fur) attenuates Helicobacter pylori J99 motility by disturbing the flagellar motor switch and autoinducer-2 production. *Helicobacter* 2017; **22** [PMID: 28402041 DOI: 10.1111/hel.12388]

16 **Zhong Y**, Anderl F, Kruse T, Schindele F, Jagusztyn-Krynicka EK, Fischer W, Gerhard M, Mejías-Luque R. Helicobacter pylori HP0231 Influences Bacterial Virulence and Is Essential for Gastric Colonization. *PLoS One* 2016; **11**: e0154643 [PMID: 27138472 DOI: 10.1371/journal.pone.0154643]

17 **Aizawa SI**, Harwood CS, Kadner RJ. Signaling components in bacterial locomotion and sensory reception. *J Bacteriol* 2000; **182**: 1459-1471 [PMID: 10692349 DOI: 10.1128/jb.182.6.1459-1471.2000]

18 **Abedrabbo S**, Castellon J, Collins KD, Johnson KS, Ottemann KM. Cooperation of two distinct coupling proteins creates chemosensory network connections. *Proc Natl Acad Sci U S A* 2017; **114**: 2970-2975 [PMID: 28242706 DOI: 10.1073/pnas.1618227114]

19 **Becker KW**, Skaar EP. Metal limitation and toxicity at the interface between host and pathogen. *FEMS Microbiol Rev* 2014; **38**: 1235-1249 [PMID: 25211180 DOI: 10.1111/1574-6976.12087]

20 **Eaton KA**, Brooks CL, Morgan DR, Krakowka S. Essential role of urease in pathogenesis of gastritis induced by Helicobacter pylori in gnotobiotic piglets. *Infect Immun* 1991; **59**: 2470-2475 [PMID: 2050411 DOI: 10.1002/ps.2016]

21 **Olson JW**, Maier RJ. Molecular hydrogen as an energy source for Helicobacter pylori. *Science* 2002; **298**: 1788-1790 [PMID: 12459589 DOI: 10.1126/science.1077123]

22 **Oliveira AG**, Santos A, Guerra JB, Rocha GA, Rocha AM, Oliveira CA, Cabral MM, Nogueira AM, Queiroz DM. babA2- and cagA-positive Helicobacter pylori strains are associated with duodenal ulcer and gastric carcinoma in Brazil. *J Clin Microbiol* 2003; **41**: 3964-3966 [PMID: 12904430 DOI: 10.1128/JCM.41.8.3964-3966.2003]

23 **Mahdavi J**, Sondén B, Hurtig M, Olfat FO, Forsberg L, Roche N, Angstrom J, Larsson T, Teneberg S, Karlsson KA, Altraja S, Wadström T, Kersulyte D, Berg DE, Dubois A, Petersson C, Magnusson KE, Norberg T, Lindh F, Lundskog BB, Arnqvist A, Hammarström L, Borén T. Helicobacter pylori SabA adhesin in persistent infection and chronic inflammation. *Science* 2002; **297**: 573-578 [PMID: 12142529 DOI: 10.1126/science.1069076]

24 **Javaheri A**, Kruse T, Moonens K, Mejías-Luque R, Debraekeleer A, Asche CI, Tegtmeyer N, Kalali B, Bach NC, Sieber SA, Hill DJ, Königer V, Hauck CR, Moskalenko R, Haas R, Busch DH, Klaile E, Slevogt H, Schmidt A, Backert S, Remaut H, Singer BB, Gerhard M. Helicobacter pylori adhesin HopQ engages in a virulence-enhancing interaction with human CEACAMs. *Nat Microbiol* 2016; **2**: 16189 [PMID: 27748768 DOI: 10.1038/nmicrobiol.2016.189]

25 **Königer V**, Holsten L, Harrison U, Busch B, Loell E, Zhao Q, Bonsor DA, Roth A, Kengmo-Tchoupa A, Smith SI, Mueller S, Sundberg EJ, Zimmermann W, Fischer W, Hauck CR, Haas R. Helicobacter pylori exploits human CEACAMs *via* HopQ for adherence and translocation of CagA. *Nat Microbiol* 2016; **2**: 16188 [PMID: 27748756 DOI: 10.1038/nmicrobiol.2016.188]

26 **de Brito BB**, da Silva FAF, Soares AS, Pereira VA, Santos MLC, Sampaio MM, Neves PHM, de Melo FF. Pathogenesis and clinical management of *Helicobacter pylori* gastric infection. *World J Gastroenterol* 2019; **25**: 5578-5589 [PMID: 31602159 DOI: 10.3748/wjg.v25.i37.5578]

27 **Atherton JC**, Peek RM Jr, Tham KT, Cover TL, Blaser MJ. Clinical and pathological importance of heterogeneity in vacA, the vacuolating cytotoxin gene of Helicobacter pylori. *Gastroenterology* 1997; **112**: 92-99 [PMID: 8978347 DOI: 10.1016/S0016-5085(97)70223-3]

28 **Djekic A**, Müller A. The Immunomodulator VacA Promotes Immune Tolerance and Persistent Helicobacter pylori

Infection through Its Activities on T-Cells and Antigen-Presenting Cells. *Toxins (Basel)* 2016; **8** [PMID: 27322319 DOI: 10.3390/toxins8060187]

29 **Farzi N**, Yadegar A, Aghdaei HA, Yamaoka Y, Zali MR. Genetic diversity and functional analysis of oipA gene in association with other virulence factors among Helicobacter pylori isolates from Iranian patients with different gastric diseases. *Infect Genet Evol* 2018; **60**: 26-34 [PMID: 29452293 DOI: 10.1016/j.meegid.2018.02.017]

30 **Miftahussurur M**, Yamaoka Y, Graham DY. Helicobacter pylori as an oncogenic pathogen, revisited. *Expert Rev Mol Med* 2017; **19**: e4 [PMID: 28322182 DOI: 10.1017/erm.2017.4]

31 **Yoshikawa T**, Naito Y. The role of neutrophils and inflammation in gastric mucosal injury. *Free Radic Res* 2000; **33**: 785-794 [PMID: 11237100 DOI: 10.1080/10715760000301301]

32 **Smith SM**. Role of Toll-like receptors in Helicobacter pylori infection and immunity. *World J Gastrointest Pathophysiol* 2014; **5**: 133-146 [PMID: 25133016 DOI: 10.4291/wjgp.v5.i3.133]

33 **Smith MF Jr**, Mitchell A, Li G, Ding S, Fitzmaurice AM, Ryan K, Crowe S, Goldberg JB. Toll-like receptor (TLR) 2 and TLR5, but not TLR4, are required for Helicobacter pylori-induced NF-kappa B activation and chemokine expression by epithelial cells. *J Biol Chem* 2003; **278**: 32552-32560 [PMID: 12807870 DOI: 10.1074/jbc.M305536200]

34 **Wilson KT**, Ramanujam KS, Mobley HL, Musselman RF, James SP, Meltzer SJ. Helicobacter pylori stimulates inducible nitric oxide synthase expression and activity in a murine macrophage cell line. *Gastroenterology* 1996; **111**: 1524-1533 [PMID: 8942731 DOI: 10.1016/S0016-5085(96)70014-8]

35 **Lindholm C**, Quiding-Järbrink M, Lönroth H, Hamlet A, Svennerholm AM. Local cytokine response in Helicobacter pylori-infected subjects. *Infect Immun* 1998; **66**: 5964-5971 [PMID: 9826379 DOI: 10.1111/j.1574-695X.1998.tb01224.x]

36 **Dixon BREA**, Hossain R, Patel RV, Algood HMS. Th17 Cells in Helicobacter pylori Infection: a Dichotomy of Help and Harm. *Infect Immun* 2019; **87** [PMID: 31427446 DOI: 10.1128/IAI.00363-19]

37 **Pinchuk IV**, Morris KT, Nofchissey RA, Earley RB, Wu JY, Ma TY, Beswick EJ. Stromal cells induce Th17 during Helicobacter pylori infection and in the gastric tumor microenvironment. *PLoS One* 2013; **8**: e53798 [PMID: 23365642 DOI: 10.1371/journal.pone.0053798]

38 **Freire de Melo F**, Rocha AM, Rocha GA, Pedroso SH, de Assis Batista S, Fonseca de Castro LP, Carvalho SD, Bittencourt PF, de Oliveira CA, Corrêa-Oliveira R, Magalhães Queiroz DM. A regulatory instead of an IL-17 T response predominates in Helicobacter pylori-associated gastritis in children. *Microbes Infect* 2012; **14**: 341-347 [PMID: 22155622 DOI: 10.1016/j.micinf.2011.11.008]

39 **Rocha GA**, de Melo FF, Cabral MMDA, de Brito BB, da Silva FAF, Queiroz DMM. Interleukin-27 is abrogated in gastric cancer, but highly expressed in other Helicobacter pylori-associated gastroduodenal diseases. *Helicobacter* 2020; **25**: e12667 [PMID: 31702083 DOI: 10.1111/hel.12667]

40 **Xiao W**, Ma ZS. Influences of Helicobacter pylori infection on diversity, heterogeneity, and composition of human gastric microbiomes across stages of gastric cancer development. *Helicobacter* 2022; **27**: e12899 [PMID: 35678078 DOI: 10.1111/hel.12899]

41 **Liu C**, Ng SK, Ding Y, Lin Y, Liu W, Wong SH, Sung JJ, Yu J. Meta-analysis of mucosal microbiota reveals universal microbial signatures and dysbiosis in gastric carcinogenesis. *Oncogene* 2022; **41**: 3599-3610 [PMID: 35680985 DOI: 10.1038/s41388-022-02377-9]

42 **Guo Y**, Cao XS, Guo GY, Zhou MG, Yu B. Effect of *Helicobacter Pylori* Eradication on Human Gastric Microbiota: A Systematic Review and Meta-Analysis. *Front Cell Infect Microbiol* 2022; **12**: 899248 [PMID: 35601105 DOI: 10.3389/fcimb.2022.899248]

43 **Chen CC**, Liou JM, Lee YC, Hong TC, El-Omar EM, Wu MS. The interplay between *Helicobacter pylori* and gastrointestinal microbiota. *Gut Microbes* 2021; **13**: 1-22 [PMID: 33938378 DOI: 10.1080/19490976.2021.1909459]

44 **Montecucco C**, Rappuoli R. Living dangerously: how Helicobacter pylori survives in the human stomach. *Nat Rev Mol Cell Biol* 2001; **2**: 457-466 [PMID: 11389469 DOI: 10.1038/35073084]

45 **Backert S**, Tegtmeyer N, Selbach M. The versatility of Helicobacter pylori CagA effector protein functions: The master key hypothesis. *Helicobacter* 2010; **15**: 163-176 [PMID: 20557357 DOI: 10.1111/j.1523-5378.2010.00759.x]

46 **Censini S**, Lange C, Xiang Z, Crabtree JE, Ghiara P, Borodovsky M, Rappuoli R, Covacci A. cag, a pathogenicity island of Helicobacter pylori, encodes type I-specific and disease-associated virulence factors. *Proc Natl Acad Sci U S A* 1996; **93**: 14648-14653 [PMID: 8962108 DOI: 10.1073/pnas.93.25.14648]

47 **Odenbreit S**, Püls J, Sedlmaier B, Gerland E, Fischer W, Haas R. Translocation of Helicobacter pylori CagA into gastric epithelial cells by type IV secretion. *Science* 2000; **287**: 1497-1500 [PMID: 10688800 DOI: 10.1126/science.287.5457.1497]

48 **Backert S**, Ziska E, Brinkmann V, Zimny-Arndt U, Fauconnier A, Jungblut PR, Naumann M, Meyer TF. Translocation of the Helicobacter pylori CagA protein in gastric epithelial cells by a type IV secretion apparatus. *Cell Microbiol* 2000; **2**: 155-164 [PMID: 11207572 DOI: 10.1046/j.1462-5822.2000.00043.x]

49 **Hatakeyama M**. Anthropological and clinical implications for the structural diversity of the Helicobacter pylori CagA oncoprotein. *Cancer Sci* 2011; **102**: 36-43 [PMID: 20942897 DOI: 10.1111/j.1349-7006.2010.01743.x]

50 **Takahashi-Kanemitsu A**, Knight CT, Hatakeyama M. Molecular anatomy and pathogenic actions of Helicobacter pylori CagA that underpin gastric carcinogenesis. *Cell Mol Immunol* 2020; **17**: 50-63 [PMID: 31804619 DOI: 10.1038/s41423-019-0339-5]

51 **Kwok T**, Zabler D, Urman S, Rohde M, Hartig R, Wessler S, Misselwitz R, Berger J, Sewald N, König W, Backert S. Helicobacter exploits integrin for type IV secretion and kinase activation. *Nature* 2007; **449**: 862-866 [PMID: 17943123 DOI: 10.1038/nature06187]

52 **Jiménez-Soto LF**, Kutter S, Sewald X, Ertl C, Weiss E, Kapp U, Rohde M, Pirch T, Jung K, Retta SF, Terradot L, Fischer W, Haas R. Helicobacter pylori type IV secretion apparatus exploits beta1 integrin in a novel RGD-independent manner. *PLoS Pathog* 2009; **5**: e1000684 [PMID: 19997503 DOI: 10.1371/journal.ppat.1000684]

53 **Couturier MR**, Tasca E, Montecucco C, Stein M. Interaction with CagF is required for translocation of CagA into the host *via* the Helicobacter pylori type IV secretion system. *Infect Immun* 2006; **74**: 273-281 [PMID: 16368981 DOI: 10.1128/IAI.74.1.273-281.2006]

54 **Shrestha R**, Murata-Kamiya N, Imai S, Yamamoto M, Tsukamoto T, Nomura S, Hatakeyama M. Mouse Gastric Epithelial Cells Resist CagA Delivery by the *Helicobacter pylori* Type IV Secretion System. *Int J Mol Sci* 2022; **23** [PMID: 35269634 DOI: 10.3390/ijms23052492]

55 **Sharafutdinov I**, Backert S, Tegtmeyer N. The Helicobacter pylori type IV secretion system upregulates epithelial cortactin expression by a CagA- and JNK-dependent pathway. *Cell Microbiol* 2021; **23**: e13376 [PMID: 34197673 DOI: 10.1111/cmi.13376]

56 **Hatakeyama M**. Oncogenic mechanisms of the Helicobacter pylori CagA protein. *Nat Rev Cancer* 2004; **4**: 688-694 [PMID: 15343275 DOI: 10.1038/nrc1433]

57 **Argent RH**, Hale JL, El-Omar EM, Atherton JC. Differences in Helicobacter pylori CagA tyrosine phosphorylation motif patterns between western and East Asian strains, and influences on interleukin-8 secretion. *J Med Microbiol* 2008; **57**: 1062-1067 [PMID: 18719174 DOI: 10.1099/jmm.0.2008/001818-0]

58 **Mueller D**, Tegtmeyer N, Brandt S, Yamaoka Y, De Poire E, Sgouras D, Wessler S, Torres J, Smolka A, Backert S. c-Src and c-Abl kinases control hierarchic phosphorylation and function of the CagA effector protein in Western and East Asian Helicobacter pylori strains. *J Clin Invest* 2012; **122**: 1553-1566 [PMID: 22378042 DOI: 10.1172/JCI61143]

59 **Stein M**, Bagnoli F, Halenbeck R, Rappuoli R, Fantl WJ, Covacci A. c-Src/Lyn kinases activate Helicobacter pylori CagA through tyrosine phosphorylation of the EPIYA motifs. *Mol Microbiol* 2002; **43**: 971-980 [PMID: 11929545 DOI: 10.1046/j.1365-2958.2002.02781.x]

60 **Tegtmeyer N**, Backert S. Role of Abl and Src family kinases in actin-cytoskeletal rearrangements induced by the Helicobacter pylori CagA protein. *Eur J Cell Biol* 2011; **90**: 880-890 [PMID: 21247656 DOI: 10.1016/j.ejcb.2010.11.006]

61 **Poppe M**, Feller SM, Römer G, Wessler S. Phosphorylation of Helicobacter pylori CagA by c-Abl leads to cell motility. *Oncogene* 2007; **26**: 3462-3472 [PMID: 17160020 DOI: 10.1038/sj.onc.1210139]

62 **Hatakeyama M**. Helicobacter pylori CagA and gastric cancer: a paradigm for hit-and-run carcinogenesis. *Cell Host Microbe* 2014; **15**: 306-316 [PMID: 24629337 DOI: 10.1016/j.chom.2014.02.008]

63 **Blaser MJ**, Perez-Perez GI, Kleanthous H, Cover TL, Peek RM, Chyou PH, Stemmermann GN, Nomura A. Infection with Helicobacter pylori strains possessing cagA is associated with an increased risk of developing adenocarcinoma of the stomach. *Cancer Res* 1995; **55**: 2111-2115 [PMID: 7743510]

64 **Parsonnet J**, Friedman GD, Orentreich N, Vogelman H. Risk for gastric cancer in people with CagA positive or CagA negative Helicobacter pylori infection. *Gut* 1997; **40**: 297-301 [PMID: 9135515 DOI: 10.1136/gut.40.3.297]

65 **Watanabe T**, Tada M, Nagai H, Sasaki S, Nakao M. Helicobacter pylori infection induces gastric cancer in mongolian gerbils. *Gastroenterology* 1998; **115**: 642-648 [PMID: 9721161 DOI: 10.1016/s0016-5085(98)70143-x]

66 **Peek RM Jr**, Wirth HP, Moss SF, Yang M, Abdalla AM, Tham KT, Zhang T, Tang LH, Modlin IM, Blaser MJ. Helicobacter pylori alters gastric epithelial cell cycle events and gastrin secretion in Mongolian gerbils. *Gastroenterology* 2000; **118**: 48-59 [PMID: 10611153 DOI: 10.1016/s0016-5085(00)70413-6]

67 **Ogura K**, Maeda S, Nakao M, Watanabe T, Tada M, Kyutoku T, Yoshida H, Shiratori Y, Omata M. Virulence factors of Helicobacter pylori responsible for gastric diseases in Mongolian gerbil. *J Exp Med* 2000; **192**: 1601-1610 [PMID: 11104802 DOI: 10.1084/jem.192.11.1601]

68 **Ohnishi N**, Yuasa H, Tanaka S, Sawa H, Miura M, Matsui A, Higashi H, Musashi M, Iwabuchi K, Suzuki M, Yamada G, Azuma T, Hatakeyama M. Transgenic expression of Helicobacter pylori CagA induces gastrointestinal and hematopoietic neoplasms in mouse. *Proc Natl Acad Sci U S A* 2008; **105**: 1003-1008 [PMID: 18192401 DOI: 10.1073/pnas.0711183105]

69 **Neal JT**, Peterson TS, Kent ML, Guillemin K. H. pylori virulence factor CagA increases intestinal cell proliferation by Wnt pathway activation in a transgenic zebrafish model. *Dis Model Mech* 2013; **6**: 802-810 [PMID: 23471915 DOI: 10.1242/dmm.011163]

70 **Amieva M**, Peek RM Jr. Pathobiology of Helicobacter pylori-Induced Gastric Cancer. *Gastroenterology* 2016; **150**: 64-78 [PMID: 26385073 DOI: 10.1053/j.gastro.2015.09.004]

71 **Yamaoka Y**, El-Zimaity HM, Gutierrez O, Figura N, Kim JG, Kodama T, Kashima K, Graham DY. Relationship between the cagA 3' repeat region of Helicobacter pylori, gastric histology, and susceptibility to low pH. *Gastroenterology* 1999; **117**: 342-349 [PMID: 10419915 DOI: 10.1053/gast.1999.0029900342]

72 **Basso D**, Zambon CF, Letley DP, Stranges A, Marchet A, Rhead JL, Schiavon S, Guariso G, Ceroti M, Nitti D, Rugge M, Plebani M, Atherton JC. Clinical relevance of Helicobacter pylori cagA and vacA gene polymorphisms. *Gastroenterology* 2008; **135**: 91-99 [PMID: 18474244 DOI: 10.1053/j.gastro.2008.03.041]

73 **Sicinschi LA**, Correa P, Peek RM, Camargo MC, Piazuelo MB, Romero-Gallo J, Hobbs SS, Krishna U, Delgado A, Mera R, Bravo LE, Schneider BG. CagA C-terminal variations in Helicobacter pylori strains from Colombian patients with gastric precancerous lesions. *Clin Microbiol Infect* 2010; **16**: 369-378 [PMID: 19456839 DOI: 10.1111/j.1469-0691.2009.02811.x]

74 **Batista SA**, Rocha GA, Rocha AM, Saraiva IE, Cabral MM, Oliveira RC, Queiroz DM. Higher number of Helicobacter pylori CagA EPIYA C phosphorylation sites increases the risk of gastric cancer, but not duodenal ulcer. *BMC Microbiol* 2011; **11**: 61 [PMID: 21435255 DOI: 10.1186/1471-2180-11-61]

75 **Queiroz DM**, Silva CI, Goncalves MH, Braga-Neto MB, Fialho AB, Fialho AM, Rocha GA, Rocha AM, Batista SA, Guerrant RL, Lima AA, Braga LL. Higher frequency of cagA EPIYA-C phosphorylation sites in H. pylori strains from first-degree relatives of gastric cancer patients. *BMC Gastroenterol* 2012; **12**: 107 [PMID: 22891666 DOI: 10.1186/1471-230X-12-107]

76 **Rocha GA**, Rocha AM, Gomes AD, Faria CL Jr, Melo FF, Batista SA, Fernandes VC, Almeida NB, Teixeira KN, Brito KS, Queiroz DM. STAT3 polymorphism and Helicobacter pylori CagA strains with higher number of EPIYA-C segments independently increase the risk of gastric cancer. *BMC Cancer* 2015; **15**: 528 [PMID: 26186918 DOI: 10.1186/s12885-015-1533-1]

77 **Segal ED**, Cha J, Lo J, Falkow S, Tompkins LS. Altered states: involvement of phosphorylated CagA in the induction of host cellular growth changes by Helicobacter pylori. *Proc Natl Acad Sci U S A* 1999; **96**: 14559-14564 [PMID: 10588744 DOI: 10.1073/pnas.96.25.14559]

78 **Tsutsumi R**, Takahashi A, Azuma T, Higashi H, Hatakeyama M. Focal adhesion kinase is a substrate and downstream

effector of SHP-2 complexed with Helicobacter pylori CagA. *Mol Cell Biol* 2006; **26**: 261-276 [PMID: 16354697 DOI: 10.1128/MCB.26.1.261-276.2006]

79 **Naito M**, Yamazaki T, Tsutsumi R, Higashi H, Onoe K, Yamazaki S, Azuma T, Hatakeyama M. Influence of EPIYA-repeat polymorphism on the phosphorylation-dependent biological activity of Helicobacter pylori CagA. *Gastroenterology* 2006; **130**: 1181-1190 [PMID: 16618412 DOI: 10.1053/j.gastro.2005.12.038]

80 **Tsutsumi R**, Higashi H, Higuchi M, Okada M, Hatakeyama M. Attenuation of Helicobacter pylori CagA x SHP-2 signaling by interaction between CagA and C-terminal Src kinase. *J Biol Chem* 2003; **278**: 3664-3670 [PMID: 12446738 DOI: 10.1074/jbc.M208155200]

81 **Tegtmeyer N**, Harrer A, Rottner K, Backert S. *Helicobacter pylori* CagA Induces Cortactin Y-470 Phosphorylation-Dependent Gastric Epithelial Cell Scattering *via* Abl, Vav2 and Rac1 Activation. *Cancers (Basel)* 2021; **13** [PMID: 34439396 DOI: 10.3390/cancers13164241]

82 **Fujii Y**, Murata-Kamiya N, Hatakeyama M. Helicobacter pylori CagA oncoprotein interacts with SHIP2 to increase its delivery into gastric epithelial cells. *Cancer Sci* 2020; **111**: 1596-1606 [PMID: 32198795 DOI: 10.1111/cas.14391]

83 **Stein M**, Ruggiero P, Rappuoli R, Bagnoli F. Helicobacter pylori CagA: From Pathogenic Mechanisms to Its Use as an Anti-Cancer Vaccine. *Front Immunol* 2013; **4**: 328 [PMID: 24133496 DOI: 10.3389/fimmu.2013.00328]

84 **Suzuki M**, Mimuro H, Suzuki T, Park M, Yamamoto T, Sasakawa C. Interaction of CagA with Crk plays an important role in Helicobacter pylori-induced loss of gastric epithelial cell adhesion. *J Exp Med* 2005; **202**: 1235-1247 [PMID: 16275761 DOI: 10.1084/jem.20051027]

85 **Mimuro H**, Suzuki T, Tanaka J, Asahi M, Haas R, Sasakawa C. Grb2 is a key mediator of helicobacter pylori CagA protein activities. *Mol Cell* 2002; **10**: 745-755 [PMID: 12419219 DOI: 10.1016/s1097-2765(02)00681-0]

86 **Churin Y**, Al-Ghoul L, Kepp O, Meyer TF, Birchmeier W, Naumann M. Helicobacter pylori CagA protein targets the c-Met receptor and enhances the motogenic response. *J Cell Biol* 2003; **161**: 249-255 [PMID: 12719469 DOI: 10.1083/jcb.200208039]

87 **Suzuki M**, Mimuro H, Kiga K, Fukumatsu M, Ishijima N, Morikawa H, Nagai S, Koyasu S, Gilman RH, Kersulyte D, Berg DE, Sasakawa C. Helicobacter pylori CagA phosphorylation-independent function in epithelial proliferation and inflammation. *Cell Host Microbe* 2009; **5**: 23-34 [PMID: 19154985 DOI: 10.1016/j.chom.2008.11.010]

88 **DiDonato JA**, Mercurio F, Karin M. NF-κB and the link between inflammation and cancer. *Immunol Rev* 2012; **246**: 379-400 [PMID: 22435567 DOI: 10.1111/j.1600-065X.2012.01099.x]

89 **Hatakeyama M**. Structure and function of Helicobacter pylori CagA, the first-identified bacterial protein involved in human cancer. *Proc Jpn Acad Ser B Phys Biol Sci* 2017; **93**: 196-219 [PMID: 28413197 DOI: 10.2183/pjab.93.013]

90 **Ren S**, Higashi H, Lu H, Azuma T, Hatakeyama M. Structural basis and functional consequence of Helicobacter pylori CagA multimerization in cells. *J Biol Chem* 2006; **281**: 32344-32352 [PMID: 16954210 DOI: 10.1074/jbc.M606172200]

91 **Lu HS**, Saito Y, Umeda M, Murata-Kamiya N, Zhang HM, Higashi H, Hatakeyama M. Structural and functional diversity in the PAR1b/MARK2-binding region of Helicobacter pylori CagA. *Cancer Sci* 2008; **99**: 2004-2011 [PMID: 19016760 DOI: 10.1111/j.1349-7006.2008.00950.x]

92 **Saadat I**, Higashi H, Obuse C, Umeda M, Murata-Kamiya N, Saito Y, Lu H, Ohnishi N, Azuma T, Suzuki A, Ohno S, Hatakeyama M. Helicobacter pylori CagA targets PAR1/MARK kinase to disrupt epithelial cell polarity. *Nature* 2007; **447**: 330-333 [PMID: 17507984 DOI: 10.1038/nature05765]

93 **Umeda M**, Murata-Kamiya N, Saito Y, Ohba Y, Takahashi M, Hatakeyama M. Helicobacter pylori CagA causes mitotic impairment and induces chromosomal instability. *J Biol Chem* 2009; **284**: 22166-22172 [PMID: 19546211 DOI: 10.1074/jbc.M109.035766]

94 **Bakhoum SF**, Cantley LC. The Multifaceted Role of Chromosomal Instability in Cancer and Its Microenvironment. *Cell* 2018; **174**: 1347-1360 [PMID: 30193109 DOI: 10.1016/j.cell.2018.08.027]

95 **Kurashima Y**, Murata-Kamiya N, Kikuchi K, Higashi H, Azuma T, Kondo S, Hatakeyama M. Deregulation of beta-catenin signal by Helicobacter pylori CagA requires the CagA-multimerization sequence. *Int J Cancer* 2008; **122**: 823-831 [PMID: 17960618 DOI: 10.1002/ijc.23190]

96 **Tian X**, Liu Z, Niu B, Zhang J, Tan TK, Lee SR, Zhao Y, Harris DC, Zheng G. E-cadherin/β-catenin complex and the epithelial barrier. *J Biomed Biotechnol* 2011; **2011**: 567305 [PMID: 22007144 DOI: 10.1155/2011/567305]

97 **Carneiro P**, Fernandes MS, Figueiredo J, Caldeira J, Carvalho J, Pinheiro H, Leite M, Melo S, Oliveira P, Simões-Correia J, Oliveira MJ, Carneiro F, Figueiredo C, Paredes J, Oliveira C, Seruca R. E-cadherin dysfunction in gastric cancer--cellular consequences, clinical applications and open questions. *FEBS Lett* 2012; **586**: 2981-2989 [PMID: 22841718 DOI: 10.1016/j.febslet.2012.07.045]

98 **Murata-Kamiya N**, Kurashima Y, Teishikata Y, Yamahashi Y, Saito Y, Higashi H, Aburatani H, Akiyama T, Peek RM Jr, Azuma T, Hatakeyama M. Helicobacter pylori CagA interacts with E-cadherin and deregulates the beta-catenin signal that promotes intestinal transdifferentiation in gastric epithelial cells. *Oncogene* 2007; **26**: 4617-4626 [PMID: 17237808 DOI: 10.1038/sj.onc.1210251]

99 **Zhang X**, Li C, Chen D, He X, Zhao Y, Bao L, Wang Q, Zhou J, Xie Y. H. pylori CagA activates the NLRP3 inflammasome to promote gastric cancer cell migration and invasion. *Inflamm Res* 2022; **71**: 141-155 [PMID: 34854954 DOI: 10.1007/s00011-021-01522-6]

100 **Buti L**, Spooner E, Van der Veen AG, Rappuoli R, Covacci A, Ploegh HL. Helicobacter pylori cytotoxin-associated gene A (CagA) subverts the apoptosis-stimulating protein of p53 (ASPP2) tumor suppressor pathway of the host. *Proc Natl Acad Sci U S A* 2011; **108**: 9238-9243 [PMID: 21562218 DOI: 10.1073/pnas.1106200108]

101 **Wei J**, Noto JM, Zaika E, Romero-Gallo J, Piazuelo MB, Schneider B, El-Rifai W, Correa P, Peek RM, Zaika AI. Bacterial CagA protein induces degradation of p53 protein in a p14ARF-dependent manner. *Gut* 2015; **64**: 1040-1048 [PMID: 25080447 DOI: 10.1136/gutjnl-2014-307295]

102 **Tsang YH**, Lamb A, Romero-Gallo J, Huang B, Ito K, Peek RM Jr, Ito Y, Chen LF. Helicobacter pylori CagA targets gastric tumor suppressor RUNX3 for proteasome-mediated degradation. *Oncogene* 2010; **29**: 5643-5650 [PMID: 20676134 DOI: 10.1038/onc.2010.304]

103 **Bagnoli F**, Buti L, Tompkins L, Covacci A, Amieva MR. Helicobacter pylori CagA induces a transition from polarized to

invasive phenotypes in MDCK cells. *Proc Natl Acad Sci U S A* 2005; **102**: 16339-16344 [PMID: 16258069 DOI: 10.1073/pnas.0502598102]

104 **Ribatti D**, Tamma R, Annese T. Epithelial-Mesenchymal Transition in Cancer: A Historical Overview. *Transl Oncol* 2020; **13**: 100773 [PMID: 32334405 DOI: 10.1016/j.tranon.2020.100773]

105 **Polyak K**, Weinberg RA. Transitions between epithelial and mesenchymal states: acquisition of malignant and stem cell traits. *Nat Rev Cancer* 2009; **9**: 265-273 [PMID: 19262571 DOI: 10.1038/nrc2620]

106 **Yin Y**, Grabowska AM, Clarke PA, Whelband E, Robinson K, Argent RH, Tobias A, Kumari R, Atherton JC, Watson SA. Helicobacter pylori potentiates epithelial:mesenchymal transition in gastric cancer: links to soluble HB-EGF, gastrin and matrix metalloproteinase-7. *Gut* 2010; **59**: 1037-1045 [PMID: 20584780 DOI: 10.1136/gut.2009.199794]

107 **Lee DG**, Kim HS, Lee YS, Kim S, Cha SY, Ota I, Kim NH, Cha YH, Yang DH, Lee Y, Park GJ, Yook JI, Lee YC. Helicobacter pylori CagA promotes Snail-mediated epithelial-mesenchymal transition by reducing GSK-3 activity. *Nat Commun* 2014; **5**: 4423 [PMID: 25055241 DOI: 10.1038/ncomms5423]

108 **Li N**, Feng Y, Hu Y, He C, Xie C, Ouyang Y, Artim SC, Huang D, Zhu Y, Luo Z, Ge Z, Lu N. Helicobacter pylori CagA promotes epithelial mesenchymal transition in gastric carcinogenesis *via* triggering oncogenic YAP pathway. *J Exp Clin Cancer Res* 2018; **37**: 280 [PMID: 30466467 DOI: 10.1186/s13046-018-0962-5]

109 **Kinoshita-Daitoku R**, Kiga K, Miyakoshi M, Otsubo R, Ogura Y, Sanada T, Bo Z, Phuoc TV, Okano T, Iida T, Yokomori R, Kuroda E, Hirukawa S, Tanaka M, Sood A, Subsomwong P, Ashida H, Binh TT, Nguyen LT, Van KV, Ho DQD, Nakai K, Suzuki T, Yamaoka Y, Hayashi T, Mimuro H. A bacterial small RNA regulates the adaptation of Helicobacter pylori to the host environment. *Nat Commun* 2021; **12**: 2085 [PMID: 33837194 DOI: 10.1038/s41467-021-22317-7]

110 **Skinner GR**. Transformation of primary hamster embryo fibroblasts by type 2 simplex virus: evidence for a "hit and run" mechanism. *Br J Exp Pathol* 1976; **57**: 361-376 [PMID: 183803]

111 **Matsumoto Y**, Marusawa H, Kinoshita K, Endo Y, Kou T, Morisawa T, Azuma T, Okazaki IM, Honjo T, Chiba T. Helicobacter pylori infection triggers aberrant expression of activation-induced cytidine deaminase in gastric epithelium. *Nat Med* 2007; **13**: 470-476 [PMID: 17401375 DOI: 10.1038/nm1566]

112 **Muramatsu M**, Kinoshita K, Fagarasan S, Yamada S, Shinkai Y, Honjo T. Class switch recombination and hypermutation require activation-induced cytidine deaminase (AID), a potential RNA editing enzyme. *Cell* 2000; **102**: 553-563 [PMID: 11007474 DOI: 10.1016/s0092-8674(00)00078-7]

113 **Chaturvedi R**, Asim M, Romero-Gallo J, Barry DP, Hoge S, de Sablet T, Delgado AG, Wroblewski LE, Piazuelo MB, Yan F, Israel DA, Casero RA Jr, Correa P, Gobert AP, Polk DB, Peek RM Jr, Wilson KT. Spermine oxidase mediates the gastric cancer risk associated with Helicobacter pylori CagA. *Gastroenterology* 2011; **141**: 1696-708.e1 [PMID: 21839041 DOI: 10.1053/j.gastro.2011.07.045]

114 **Hanada K**, Uchida T, Tsukamoto Y, Watada M, Yamaguchi N, Yamamoto K, Shiota S, Moriyama M, Graham DY, Yamaoka Y. Helicobacter pylori infection introduces DNA double-strand breaks in host cells. *Infect Immun* 2014; **82**: 4182-4189 [PMID: 25069978 DOI: 10.1128/IAI.02368-14]

115 **Hartung ML**, Gruber DC, Koch KN, Grüter L, Rehrauer H, Tegtmeyer N, Backert S, Müller A. H. pylori-Induced DNA Strand Breaks Are Introduced by Nucleotide Excision Repair Endonucleases and Promote NF-κB Target Gene Expression. *Cell Rep* 2015; **13**: 70-79 [PMID: 26411687 DOI: 10.1016/j.celrep.2015.08.074]

116 **Imai S**, Ooki T, Murata-Kamiya N, Komura D, Tahmina K, Wu W, Takahashi-Kanemitsu A, Knight CT, Kunita A, Suzuki N, Del Valle AA, Tsuboi M, Hata M, Hayakawa Y, Ohnishi N, Ueda K, Fukayama M, Ushiku T, Ishikawa S, Hatakeyama M. Helicobacter pylori CagA elicits BRCAness to induce genome instability that may underlie bacterial gastric carcinogenesis. *Cell Host Microbe* 2021; **29**: 941-958.e10 [PMID: 33989515 DOI: 10.1016/j.chom.2021.04.006]

World Journal of Clinical Oncology

Submit a Manuscript: https://www.f6publishing.com

World J Clin Oncol 2022 November 24; 13(11): 880-895

DOI: 10.5306/wjco.v13.i11.880

ISSN 2218-4333 (online)

ORIGINAL ARTICLE

Basic Study

Folate receptor-targeted near-infrared photodynamic therapy for folate receptor-overexpressing tumors

Winn Aung, Atsushi B Tsuji, Kenjiro Hanaoka, Tatsuya Higashi

Specialty type: Oncology

Provenance and peer review: Unsolicited article; Externally peer reviewed.

Peer-review model: Single blind

Peer-review report's scientific quality classification

Grade A (Excellent): 0
Grade B (Very good): B, B
Grade C (Good): 0
Grade D (Fair): 0
Grade E (Poor): 0

P-Reviewer: Jabbarpour Z, Iran; Janmohammadi P, Iran

Received: August 3, 2022
Peer-review started: August 3, 2022
First decision: August 29, 2022
Revised: September 12, 2022
Accepted: October 18, 2022
Article in press: October 18, 2022
Published online: November 24, 2022

Winn Aung, Atsushi B Tsuji, Tatsuya Higashi, Department of Molecular Imaging and Theranostics, Institute for Quantum Medical Science, National Institutes for Quantum and Radiological Science and Technology, Chiba 263-8555, Japan

Kenjiro Hanaoka, Faculty of Pharmacy and Graduate School of Pharmaceutical Sciences, Keio University, Tokyo 105-8512, Japan

Corresponding author: Winn Aung, MBBS, PhD, Senior Researcher, Department of Molecular Imaging and Theranostics, Institute for Quantum Medical Science, National Institutes for Quantum and Radiological Science and Technology, 4-9-1 Anagawa, Inage-ku, Chiba 263-8555, Japan. winn.aung@qst.go.jp

Abstract

BACKGROUND

Photodynamic therapy (PDT) is a minimally invasive form of cancer therapy, and the development of a novel photosensitizer (PS) with optimal properties is important for enhancing PDT efficacy. Folate receptor (FR) membrane protein is frequently overexpressed in 40% of human cancer and a good candidate for tumor-specific targeting. Specific active targeting of PS to FR can be achieved by conjugation with the folate moiety. A folate-linked, near-infrared (NIR)-sensitive probe, folate-Si-rhodamine-1 (FolateSiR-1), was previously developed and is expected to be applicable to NIR-PDT.

AIM

To investigate the therapeutic efficacy of NIR-PDT induced by FolateSiR-1, a FR-targeted PS, in preclinical cancer models.

METHODS

FolateSiR-1 was developed by conjugating a folate moiety to the Si-rhodamine derivative through a negatively charged tripeptide linker. FR expression in the designated cell lines was examined by western blotting (WB). The selective binding of FolateSiR-1 to FR was confirmed in FR overexpressing KB cells (FR+) and tumors by fluorescence microscopy and *in vivo* fluorescence imaging. Low FR expressing OVCAR-3 and A4 cell lines were used as negative controls (FR-). The NIR light (635 ± 3 nm)-induced phototoxic effect of FolateSiR-1 was evaluated by cell viability imaging assays. The time-dependent distribution of FolateSiR-1 and its specific accumulation in KB tumors was determined using *in vivo* longitudinal fluorescence imaging. The PDT effect of FolateSiR-1 was evaluated in KB tumor-

bearing mice divided into four experimental groups: (1) FolateSiR-1 (100 μmol/L) alone; (2) FolateSiR-1 (100 μmol/L) followed by NIR irradiation (50 J/cm^2); (3) NIR irradiation (50 J/cm^2) alone; and (4) no treatment. Tumor volume measurement and immunohistochemical (IHC) and histological examinations of the tumors were performed to analyze the effect of PDT.

RESULTS

High FR expression was observed in the KB cells by WB, but not in the OVCAR-3 and A4 cells. Substantial FR-specific binding of FolateSiR-1 was observed by *in vitro* and *in vivo* fluorescence imaging. Cell viability imaging assays showed that NIR-PDT induced cell death in KB cells. *In vivo* longitudinal fluorescence imaging showed rapid peak accumulation of FolateSiR-1 in the KB tumors 2 h after injection. *In vivo* PDT conducted at this time point caused tumor growth delay. The relative tumor volumes in the PDT group were significantly reduced compared to those in the other groups [5.81 ± 1.74 (NIR-PDT) *vs* 12.24 ± 2.48 (Folate-SiR-1), *vs* 11.84 ± 3.67 (IR), *vs* 12.98 ± 2.78 (Untreated), at Day 16, $P < 0.05$]. IHC analysis revealed reduced proliferation marker Ki-67-positive cells in the PDT treated tumors, and hematoxylin-eosin staining revealed features of necrotic- and apoptotic cell death.

CONCLUSION

FolateSiR-1 has potential for use in PDT, and FR-targeted NIR-PDT may open a new effective strategy for the treatment of FR-overexpressing tumors.

Key Words: Photodynamic therapy; Near-infrared; Photosensitizer; Folate receptor; Fluorescence; Cancer

Core Tip: Photodynamic therapy (PDT) is a minimally invasive cancer therapy and photosensitizers (PS) with optimal properties are crucial for enhancing the efficacy of PDT. We evaluated the therapeutic efficacy of a folate receptor (FR)-targeted, near-infrared (NIR)-sensitive PS (FolateSiR-1). FolateSiR-1 showed FR specificity *in vitro* and *in vivo* and functions as a tumor-damaging PS by inducing necrosis, apoptosis, and cell growth inhibition upon activation with NIR light. Our findings suggest that FolateSiR-1 is effective in FR-targeted NIR-PDT with low side effects and has potential for presenting new and effective treatment options for FR-overexpressing tumors.

Citation: Aung W, Tsuji AB, Hanaoka K, Higashi T. Folate receptor-targeted near-infrared photodynamic therapy for folate receptor-overexpressing tumors. *World J Clin Oncol* 2022; 13(11): 880-895
URL: https://www.wjgnet.com/2218-4333/full/v13/i11/880.htm
DOI: https://dx.doi.org/10.5306/wjco.v13.i11.880

INTRODUCTION

Cancer incidence and mortality is continually growing worldwide. GLOBOCAN 2020 estimated that there were 19.3 million new cancer cases and almost 10 million cancer deaths in 2020 and the global cancer burden is expected to reach 28.4 million cases in 2040[1]. Molecular-targeted approaches with various therapeutic modalities are expected to provide effective cancer diagnosis and treatment.

Photodynamic therapy (PDT) is one of the emerging options to combat various cancer types along with other conventional therapies such as surgery, chemotherapy, radiation therapy, and immunotherapy[2]. It is approved for the clinical treatment of several tumor types and certain non-malignant diseases as a minimally invasive therapy[3]. Although the precise mechanisms of tumor cell death by photodamage are not yet fully understood, they involve necrosis, apoptosis, tumor blood vessel damage, and nonspecific activation of the immune response against tumor cells[4]. Cell death through PDT generally occurs through a combination of these mechanisms, and no single pathway leads to cell death[5]. Photodynamic therapy involves the administration of a light-sensitive photosensitizer (PS) followed by the irradiation of targeted tumors with light corresponding to the specific absorbance wavelength of the PS[3]. Light activated PS accumulated in the cancer tissue leads to the local generation of reactive oxygen species (ROS), such as highly reactive singlet oxygen and/or radicals, which kill tumor cells through necrosis and cause tumor regression[6,7]. However, off-target toxicities and PS metabolic problems were encountered in clinical trials, and therefore, only a few PSs have been approved for anti-cancer therapies[8]. The tumor selectivity of the PS improves tumor localization in PDT, enhances tumor destruction, and reduces the side effects due to off-target localization[9].

Moreover, effective targeting reduces the required PS dose which additionally limits side effects. Tumor-localizing properties are generally dependent on the passive enhanced permeability and retention effect[10]. More effective active targeting is expected and achieved by diverse approaches such as the conjugation of receptor ligands, antibodies, carrier proteins, carbohydrates, and loading into targeted nanoparticles[11-14].

The first-generation of PSs were hematoporphyrin derivatives, and the first PS to be clinically used for cancer therapy was porfimer sodium (Photofrin®)[4]. Its poor tissue selectivity, low light absorption, and weak tissue penetration of emission demanded the development of second-generation PSs, porphyrinoids, and non-porphyrin compounds[15]. Moreover, third-generation PSs were developed by conjugating carrier biomolecules, such as receptor ligands or antibodies, to the second-generation PSs to selectively target tumors[4]. Nevertheless, the number of new clinically approved PSs remains low, and researchers are developing new improved PSs.

Folate receptor (FR) membrane protein is frequently overexpressed in 40% of human cancer types, including ovary, breast, head and neck, endometrium, lung, bladder, pancreatic, colon, and kidney cancer, whereas its expression is restricted to normal tissues[16]. It binds to extracellular folate with very high affinity and can physically deliver folate into the cell through endocytosis[17]. Therefore, FR is a good candidate for tumor-specific PS targeting[9,18]. Specific active targeting of PS to FR present on the cancer cell surface can be achieved by conjugation with the folate moiety[19]. Several studies have shown that some PSs conjugated with folic acid *via* appropriate linkers increase tumor uptake and enhance the efficacy of PDT. For instance, conjugation of folic acid to *meta*-tetra(hydroxyphenyl)chlorin (*m*-THPC)-like PS[20] and chlorin-based PS pheophorbide-a[21] has been reported. In addition, various materials such as polymers, nanomaterials, polysaccharides and cyclodextrins have been explored to overcome the shortcoming of PSs *via* tissue-specific delivery[22]. For example, folate-conjugated micelles containing temoporfin[23] and polydopamine nanoparticles conjugated with folic acid[24] showed potential for therapeutic applications. Kim *et al*[22] showed that ROS-sensitive and FR-targeted nanophotosensitizer conjugates are promising candidates for PDT of cervical cancer. Kato *et al*[25,26] reported that folate-porphyrin-lipid nanoparticles induced the selective destruction of lung cancer and malignant pleural mesothelioma in a preclinical model based on FR targeting. Baydoun *et al*[27] proved the efficacy of a new PS (pyropheophorbide a-polyethylene glycol-folic acid) on human ovarian cancer cells. Quilbe *et al*[28] developed a new PS targeting FR, protected by patent (WO2019 016397-A1) and evaluated its PDT efficacy on a mouse model of pancreatic cancer. These latest state-of-the-art studies encourage the use of folate-mediated PSs in tumor-targeted photodynamic therapy. In an alternative approach called photoimmunotherapy (PIT), PSs conjugated with monoclonal antibodies that have high affinity to tumor specific antigens instead of using receptor ligands have also investigated[29,30].

PS targeting was developed or improved by conjugating fluorophores to tumor-seeking molecules [31]. We previously developed a folate-linked near-infrared (NIR)-sensitive probe, folate-Si-rhodamine-1 (FolateSiR-1, Abs_{max}/Em_{max} = 652/674 nm, and fluorescence quantum yield of 7.6%) using folate glutamate as a tumor-seeking agent, a negatively charged peptide linker, and rhodamine derivative, 2,5-diCOOH SiR650, as a photoactive component (Figure 1A)[32]. Folate receptor α contains a folate-binding pocket[33]. The folate pteroate moiety is buried inside the receptor, whereas its glutamate moiety is solvent-exposed and protrudes from the pocket, which allows its conjugation to the fluorophore without adversely affecting FRα binding[33]. We chose to conjugate the linker to the folate glutamate moiety, as this allowed high affinity- and highly selective binding of FolateSiR-1 probe to FR [34]. One of the main drawbacks of currently approved PDTs is the insufficient penetration of light during treatment. This may be overcome by using NIR absorbing PSs[32] and appropriate NIR light sources because red and infrared light penetrate tissue more deeply than other visible light[3]. The photophysical properties of FolateSiR-1 and the wavelength of our laser system (635 ± 3 nm) used in this study resolved this issue. Fluorophores emitting NIR light in the phototherapeutic window (650-900 nm) are most suitable due to high tissue penetration and low autofluorescence, which results in a low background signal[35]. FolateSiR-1 exhibited very low background fluorescence and showed a high ratio of tumor-to-background fluorescent intensity[32].

In this study, we evaluated the *in vitro* and *in vivo* tumor specific targeting- and photodynamic activity of FolateSiR-1 using high-FR-expressing-KB cells (FR+) and low-FR-expressing-OVCAR-3 cells (Low FR). We revealed the potential of FolateSiR-1 as a candidate for use in the PDT of cancer by assessing its phototoxic cell death and antitumor effects. In addition, the cell death mode induced by FolateSiR-1-based PDT was investigated.

MATERIALS AND METHODS

Cell lines and culture

The human oral epidermoid carcinoma cell line, KB (a Hela subline), and human epithelial ovarian cancer cell line, OVCAR-3, were purchased from the American Type Culture Collection (ATCC) (Manassas, VA, United States). The KB cells were cultured in Eagles's minimum essential medium (EMEM) (Wako Pure Chemical Corp., Osaka, Japan) supplemented with 10% fetal bovine serum (FBS)

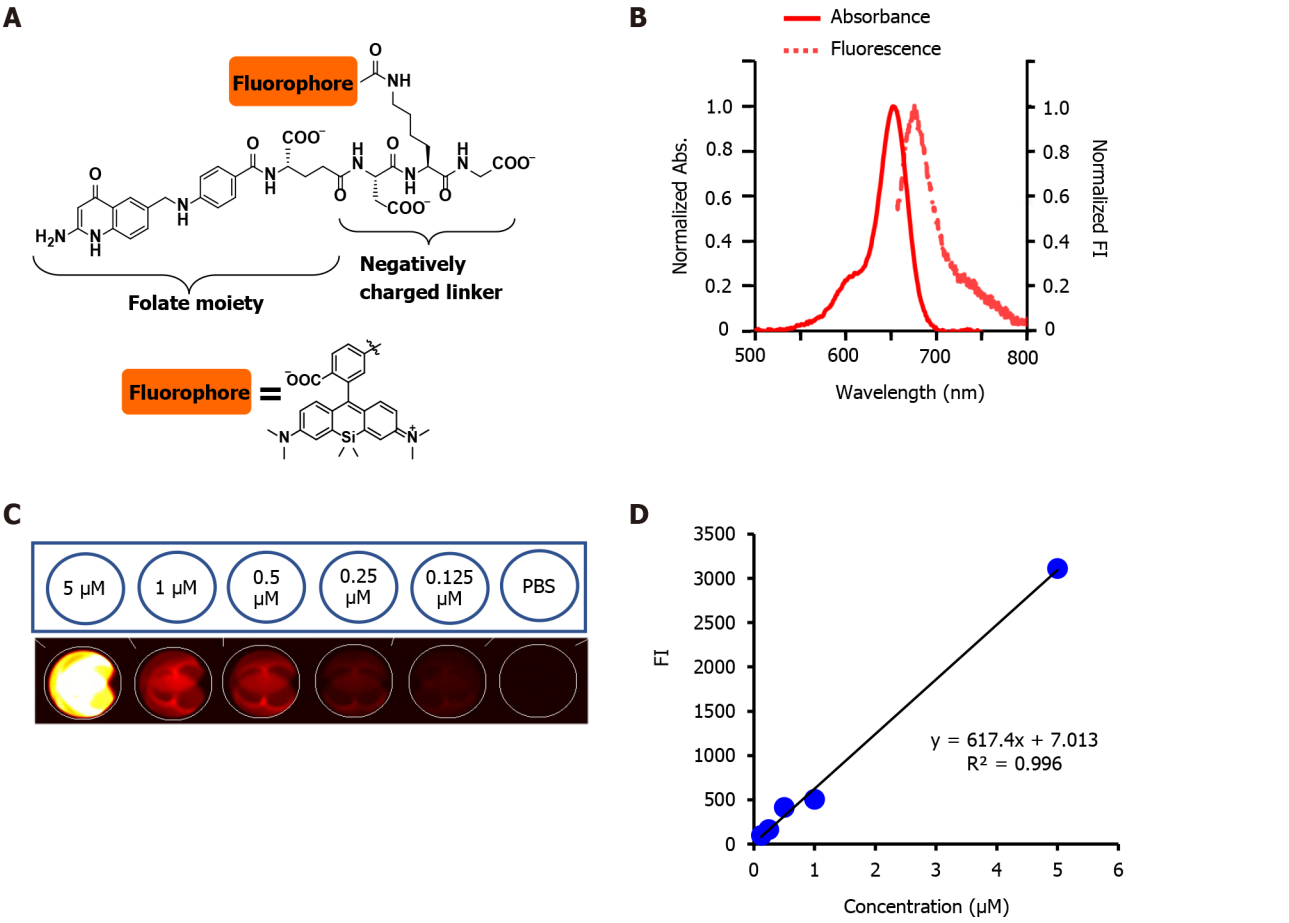

Figure 1 Folate-Si-rhodamine-1 characteristcs. A: Molecular design and chemical structure of folate-Si-rhodamine-1 (FolateSiR-1); B: Absorption and emission spectra of 1 μmol/L FolateSiR-1 in 100 mmol/L sodium phosphate buffer (pH 7.4) containing 0.1% DMSO: maximum absorption = 652 nm; maximum emission = 674 nm; C: Fluorescence images of FolateSiR-1 at a concentration of 5, 1, 0.5, 0.25, and 0.125 μmol/L in a 96-well plate captured using the VISQUE fluorescence imaging system; D: FolateSiR-1 concentration *vs* fluorescence signal intensity. Abs: Absorbance; FI: Fluorescence signal intensity; μM: μmol/L.

(Gibco, Life Technologies Japan Ltd., Tokyo, Japan), 100 U/mL penicillin-G sodium, and 100 μg/mL streptomycin sulfate (Wako) at 37 ˚C in a humidified incubator containing 5% CO_2. The A4 cell line is an immortalized mouse fibroblast cell line established from mouse 3T3 cells and transfected with human epidermal growth factor receptor 2-expression vector. The OVCAR-3 cells and A4 cells were similarly cultured in RPMI 1640 medium (Wako) supplemented with 10% FBS (Gibco), 100 U/mL penicillin-G sodium, and 100 μg/mL streptomycin sulfate (Wako).

FolateSiR-1 synthesis

FolateSiR-1 was designed and synthesized using folate glutamate as a tumor-seeking agent, a negatively charged peptide linker, and a rhodamine derivative, 2,5-diCOOH SiR650, as a photoactive component according to a previously described method[32]. Fluorescence spectroscopic analyses of FolateSiR-1 was conducted with a Hitachi F7000 spectrophotometer (Tokyo, Japan) using 2.5 nm excitation and emission slit widths and 700 V photomultiplier voltage. Different FolateSiR-1 concentrations (5, 1, 0.5, 0.25, 0.125 μmol/L) were prepared in 100 μL in a Nunc™ flat-bottom microplate (96 well, Black) (Thermo Fisher Scientific, Roskilde, Denmark). The fluorescence signal intensity (Fl) was determined using a VISQUE InVivo Smart fluorescence imaging and analysis system (Vieworks Co., Ltd, Gyeonggi, Korea) equipped with HyperRed light filter set (Ex/Em = 630-680/690-740 nm).

Animal and tumor model

Ethics Committee-approved animal studies were conducted in accordance with the institutional guidelines of the Animal Care and Use of Committee of National Institutes for Quantum and Radiological Science and Technology. The animal protocol was designed to minimize pain or discomfort to the animals. Four-week-old male BALB/cAJcl-nu/nu mice were obtained from CLEA (Shizuoka, Japan), kept in an air-conditioned facility (23 °C) with an artificial 12 h light-dark cycle, 50% humidity, and provided autofluorescence-free food and water *ad libitum* for one week prior to experimentation. Development of tumor models involved subcutaneous inoculation of early passage cells (5×10^6 KB cells/site, 1×10^7 OVCAR-3 cells/site, or 5×10^6 A4 cells/site, all in 100 μL medium) into both femoral

regions of nude mice. Mice were anesthetized with isoflurane during the experimental procedure. All animals were euthanized by cervical dislocation under anesthesia (inhalation of isoflurane) for tumor tissue collection.

Western blot analysis

Folate receptor expression in designated cells was examined by western blotting (WB). First, whole-cell lysate was prepared using radioimmunoprecipitation assay buffer (Wako) containing protease inhibitor cocktail (P8340; Sigma-Aldrich, St. Louis, MO, United States). Total protein concentration was determined using a NanoDrop One spectrophotometer (Thermo Fisher Scientific, Wilmington, DE, United States). Next, 50 μg of cell lysate protein samples were separated using 4%-20% polyacrylamide gel (ATTO Corporation, Tokyo, Japan) and transferred onto an Immobilon-P membrane (Millipore, Billerica, MA, United States). Mouse monoclonal antibody anti-FR of human origin (E-11) (Santa Cruz Biotechnology, Santa Cruz, CA, United States) (1:200 dilution) and goat polyclonal anti-human actin antibody (Santa Cruz Biotechnology) (1:500 dilution) were used as primary antibodies. Horseradish peroxidase (HRP)-linked anti-mouse IgG antibody (GE Healthcare, Little Chalfont, United Kingdom) (1:1000 dilution) and HRP-linked anti-goat IgG antibody (Santa Cruz Biotechnology) (1:1000 dilution) were used as secondary antibodies. The Enhanced Chemiluminescence Plus detection system (GE Healthcare) was used to visualize the immunoreactive bands.

Fluorescence microscopy

KB cells (1×10^5 cells/well) were seeded onto an EZVIEW glass bottom culture plate (24 well, black; IWAKI, Shizuoka, Japan) in complete EMEM medium (1 mL) and incubated for 24 h at 37 °C. The media was removed and each well was washed with PBS, subsequently, fresh medium was added with or without FolateSiR-1 (2.5 μmol/L in 0.5% DMSO) and incubated overnight at 37 ˚C. The medium was discarded, cells were washed with phenol red free EMEM α medium (Wako) two times, and each well was refilled with the same medium. The OVCAR-3 cells (5×10^5 cells/well) and A4 cells (1×10^5 cells/well) were prepared using RPMI 1640, and the cells were observed using a Keyence BZ-X700 fluorescence microscope (Keyence Japan Co, Ltd, Osaka, Japan) with an Ex/Em 590-650/665-732 nm filter for FolateSiR-1. The same exposure time was consistently used. Phase-contrast images were also captured.

Cell viability imaging

KB cells (1.5×10^5 cells/well) were seeded onto a EZVIEW glass bottom culture plate (24 well, black; IWAKI) in complete EMEM medium overnight at 37 °C. Spent medium was replaced with fresh medium with or without FolateSiR-1 (2.5 μmol/L in 0.5% DMSO) and the KB cells were incubated overnight. Next, the medium was discarded, cells were washed with phenol red free medium (Wako), and subsequently irradiated with NIR light from an infrared diode laser system (Laser Create Co., Tokyo, Japan) at 635 ± 3 nm and a power density of 10 J/cm^2 (0.1 W/cm^2 for 100 s). The distance between the sample and light source was set to 3 cm, and the light power was adjusted to 0.1 W/cm^2. The irradiation dose was measured using a Starlite thermal laser power sensor and optical power meter (OPHIR Japan, Saitama, Japan). After irradiation, each well was refilled with the same medium and incubated at 37 °C. Two hours later, two color staining assays were conducted using the ReadyProbes™ cell viability imaging kit (Thermo Fisher Scientific K.K, Tokyo, Japan) according to manufacturer's instructions. Nuclei of the viable cells and dead cells were stained with NucBlue® Live reagent and NucGreen® Dead reagent, respectively. Cell images were acquired with a Keyence BZ-X700 microscope (Keyence Japan Co, Ltd) with filter sets for NucBlue® (Ex/Em = 360/460 nm), NucGreen® (Ex/Em = 475/509 nm), and FolateSiR-1 (red, Ex/Em = 590-650/665-732 nm). Image acquisitions were conducted using similar exposure times.

Mice NIR fluorescence imaging

Intravenous injection of FolateSiR-1 (100 μmol/L in 100 μL saline and 10% DMSO) into the tail vein of tumor-bearing mice was followed by anesthetization and acquisition of fluorescent and white light images at the dorsal position. Pre-injection- and post-injection time points (5 min, 10 min, 15 min, 20 min, 30 min, 45 min, and 1 h, 2 h, 3 h, 4 h, 4.5 h, 5 h, 6 h, 24 h, and 48 h) were designated for longitudinal imaging. *In vivo* NIR fluorescence imaging was conducted using the VISQUE imaging system (Vieworks Co., Ltd,) equipped with HyperRed light filter (Ex/Em = 630-680/690-740 nm) using constant imaging parameters (exposure time: 100 ms, binning: 1 × 1, light intensity: high, mode: low gain). Tumor FI was acquired by subtracting nearby background FI using Clevue software (Vieworks). Two mice with OVCAR-3 and KB tumors in their left and right femoral regions, respectively, were imaged to confirm FR-specific binding. Similarly to the other control samples, KB tumor-bearing mice that did or did not receive the FolateSiR-1 injection were imaged together, and the A4 (low FR) tumor-bearing mouse was imaged after PS injection.

In vivo tumor PDT

Subcutaneous tumor lengths peaked at approximately 6-10 mm nine days after xenografting. These

mice were randomly assigned to one of the four groups (n = 5 in each group), and treatment was conducted using the designated schedule. FolateSiR-1 (100 μmol/L) was initially administered intravenously. After 2 h, the tumor was exposed to NIR light from a Diode Laser system (Laser Create Co.) at 635 ± 3 nm and 50 J/cm^2 (0.25 W/cm^2 for 200 s). The distance between the tumor and NIR light source was set to 3 cm. Whole body of the mouse, except for the tumor area, was shielded from the light using aluminum foil. Group 1 received PS injection, group 2 received PS injection followed by light irradiation at 2 h post-injection, group 3 was only irradiated, and group 4 received no treatment. Tumors sizes of all mice (n = 8 for each) were measured twice a week over 16 d using calipers, and volumes were calculated according to the formula: volume (mm^3) = [length (mm)] × [width (mm)]^2 × 0.5. The relative tumor volume was calculated based on the ratio of the volume on the indicated day and the starting volume prior to the treatment. Mice were weighed twice a week, while the skin condition of the light exposed area, and general conditions of the mice were monitored daily.

Immunohistochemical- and histological analysis

Twenty-four h after irradiation, a mouse from each group was sacrificed. The tumors were excised, fixed in 4% paraformaldehyde, embedded in paraffin, and cut into 5 μm-slices. Serial tissue sections were rehydrated and subjected to antigen retrieval for immunohistochemical (IHC) analysis. The sections were then stained for Ki-67 cell proliferation marker[36] using anti-human Ki-67 polyclonal antibody (Dako Denmark, Glostrup, Denmark) (1:200 dilution) as previously described[37]. Mouse monoclonal anti-FR antibody of human origin (E-11) (Santa Cruz Biotechnology) (1:200 dilution) was used to investigate tumor FR expression. Serial sections were stained with hematoxylin and eosin (H&E) dye to examine histopathological changes. Slides were examined with an Olympus BX43 microscope (Tokyo, Japan).

Statistical analysis

The quantitative results are presented as the mean ± SD. Relative tumor volume differences between groups were determined using ANOVA (two-factor with replication; Excel, Microsoft, Redmond, WA, United States), followed by Tukey's test. P values < 0.05 were considered statistically significant.

RESULTS

FolateSiR-1 conjugate characteristics

FolateSiR-1 probe (molecular weight 1232.78, Figure 1A) was developed from a Si-rhodamine derivative containing a carboxy group at the benzene moiety coupled to a folate ligand moiety through a negatively charged tripeptide[32]. FolateSiR-1 is expected to possess high affinity to FR with a tumor-seeking character of folate glutamate[38]. Rhodamine derivative 2,5-diCOOH SiR650 serves as a photoactive component. Maximum absorption and emission wavelengths of 1 μmol/L FolateSiR-1 in 100 mmol/L sodium phosphate buffer at pH 7.4 were 652 nm and 674 nm, respectively (Figure 1B)[32]. FolateSiR-1 fluorescence emission was most clearly visualized with HyperRed light filter (Ex/Em = 630-680/690-740 nm) using the VISQUE imaging system (Figure 1C). The quantitative evaluation of FI revealed that the linear correlation coefficient between fluorescence and FolateSiR-1 concentration was 0.996 (Figure 1D).

Folate receptor expression and FolateSiR-1 accumulation in cultured cells

High FR expression was observed in the KB cells by WB, but not in the OVCAR-3 and A4 cells (Figure 2A). Likewise, FolateSiR-1 accumulated in the KB cells at the cell membrane and their intracellular localization indicated substantial specific binding of FolateSiR-1 to FR and its internalization using fluorescence microscopy. However, this was not seen in almost any of the OVCAR-3 and A4 cells (Figure 2B). All three cell lines incubated in medium without FolateSiR-1 showed no fluorescence activity (data not shown).

Folate receptor-specific binding of FolateSiR-1 in in vivo tumors

Using the VISQUE imaging system 2 h after injecting FolateSiR-1 into tumor-bearing mice, the KB tumors inoculated in the right femoral regions showed high FI, while the OVCAR-3 tumors inoculated in the left femoral regions showed no FI (Figure 2C). Next, the KB tumor of the mouse that was administered FolateSiR-1 exhibited FI, but the negative control tumor of the mouse with no FolateSiR-1 injection did not (Figure 2D). Moreover, a mouse bearing A4 (low FR) tumor showed no FI (Figure 2E). After imaging, IHC examination of tumor tissue sections showed high FR expression in the KB tumor (Figure 2F). These results suggest that there was specific binding of FolateSiR-1 to FR in the tumors.

Phototoxic cell death induced by FolateSiR-1 mediated PDT

Immediate cell death induced by NIR-PDT was detected based on green colored cells by fluorescence microscopy, resulting from the staining with the NucGreen® Dead reagent, whereas viable cell nuclei

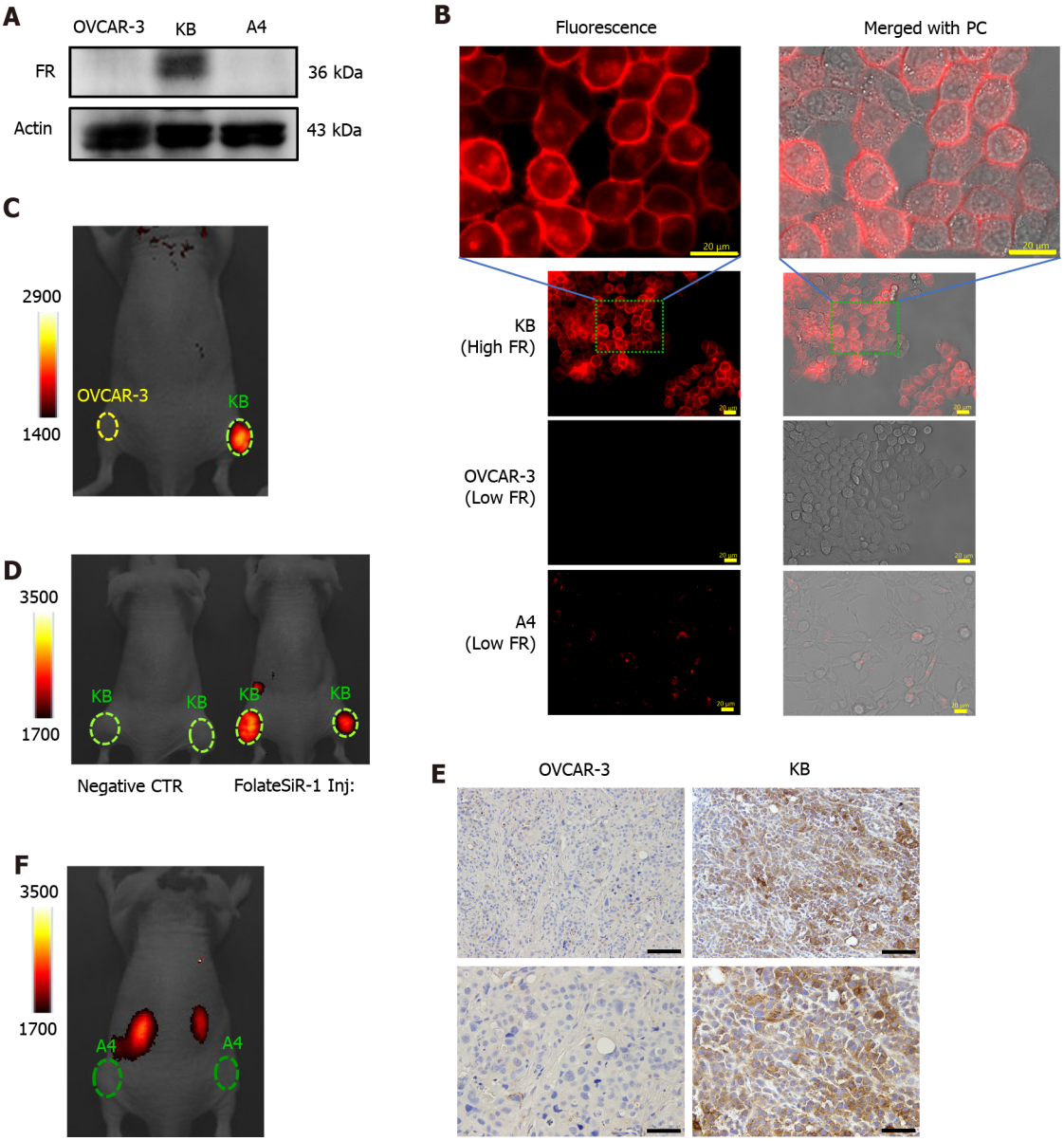

Figure 2 Folate receptor expression in designated cell lines and folate receptor-specific binding of folate-Si-rhodamine-1 in tumor *in vivo*. A: Folate receptor (FR) expression in cell lines OVCAR-3, KB, and A4 examined by western blotting; B: Cell lines were incubated with or without folate-Si-rhodamine-1 (FolateSiR-1) for 24 h and examined under a fluorescent microscope. FolateSiR-1 fluorescence was detected using the appropriate filters (Ex/Em 590-650/665-732 nm). The uppermost images are magnifications of the indicated portion of the lower image showing KB cells (scale bar = 20 μm, 40 × magnification, and 120 × magnification for the upper most image); C: Near-infrared (NIR) fluorescence image of a representative mouse bearing subcutaneous KB (right) and OVCAR-3 (left) tumors at 2 h after receiving the FolateSiR-1 injection: KB tumor (FR+) showed high fluorescence signal intensity (FI), and OVCAR-3 tumor (low FR) did not; D: NIR fluorescence image of mice bearing KB tumors: the right mouse received the FolateSiR-1 injection showed FI, while the left mouse did not (negative control tumor) show no FI; E: NIR fluorescence image of a mouse bearing A4 (low FR) tumor showed no FI; F: Immunohistochemical analysis of tumor tissue sections for FR expression: KB tumor (right column), OVCAR-3 tumor (left column). Scale bar = 100 μm, 20 × magnification for upper panel, and scale bar = 50 μm, 40 × magnification, for lower panel. FR: Folate receptor; Ex: Excitation; Em: Emission; FI: Fluorescence signal intensity; FolateSiR-1: Folate-Si-rhodamine-1; PC: Phase-contrast; NIR: Near-infrared; CTR: Control.

were stained blue with NucBlue® Live reagent (Figure 3). No noticeable phototoxic cell death was observed with FolateSiR-1 treatment alone, light treatment alone, or no treatment (Figure 3).

In vivo FolateSiR-1 biodistribution in tumorbearing mice

Time-dependent distribution of FolateSiR-1 and its specific accumulation in the tumors was determined based on serial images of a representative mouse following FolateSiR-1 injection (Figure 4A). The quantified FI in the tumor rapidly increased, peaking approximately 2 h after injection, and almost disappearing over 24 h (Figure 4B). Moreover, in another experiment, decreased tumor FI was observed in the right tumor that received PDT after 30 min compared with that of the non-irradiated left tumor (Figure 5A). Although there was a time-dependent decrease of FI due to normal washout of the PS from the tumor, the degree of FI reduction in the tumor treated with PDT was greater than in the untreated

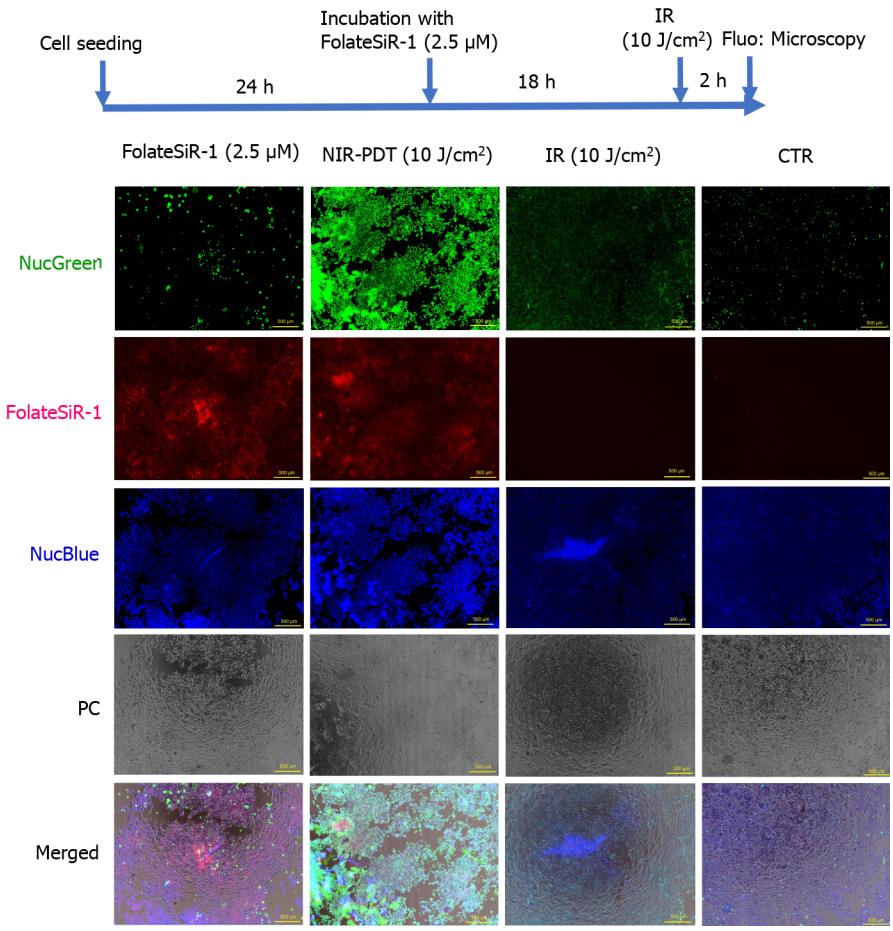

Figure 3 *In vitro* phototoxicity of folate-Si-rhodamine-1 after laser irradiation. The cells were stained using the reagents from the Cell viability imaging kit at 2 h after near-infrared photodynamic therapy (NIR-PDT). The nuclei of dead cells were stained with NucGreen® Dead reagent (green), while the viable cell nuclei were stained with NucBlue® Live reagent (blue). Rapid cell death-induced by PDT (10 J/cm^2) and abundant dead cells were clearly noted. (scale bar = 500 μm, 10 × magnification). NIR-PDT: Near-infrared photodynamic therapy; IR: Laser irradiation; CTR: Control; NucGreen: NucGreen® Dead reagent; NucBlue: NucBlue® Live reagent; PC: Phase-contrast; μM: μmol/L.

tumor. Therefore, the percentage decrease of tumor FI was higher in the PDT-induced tumors (Figure 5B). Mice were euthanized shortly after *in vivo* imaging, with tumors and other organs removed and analyzed by the VISQUE imaging system. *Ex vivo* NIR images showed higher FI in tumor tissues compared with major organs, and higher FI in the right tumor compared with that of the left tumor. Meanwhile, FI from organs including the liver and kidney was barely visible (Figure 5C). *Ex vivo* results showed similar trends in data as that in *in vivo* imaging data.

In vivo PDT efficacy of FolateSiR-1 on tumor size

The tumor-bearing mice were treated according to the scheme shown in Figure 6. Statistically significant tumor growth inhibition was observed after NIR-PDT treatment *vs* FolateSiR-1 treatment alone, NIR irradiation alone, and no treatment ($P < 0.05$, Figure 7A). No significant differences were observed amongst other groups. There was no significant body weight loss, skin damage, or abnormal general conditions in these mice (Figure 7B). Relatively decreased sizes of PDT-treated tumors were observed *ex vivo* 16 d after treatment compared with that in the other groups (Figure 7C).

Evaluation of tumor tissue response to PDT by IHC and histopathology

Proliferative factor Ki67 nuclear staining in the control tumor cells was observed by IHC analysis. In contrast, the tumor tissues treated with PDT showed weak staining and markedly reduced numbers of Ki-67-positive cells, suggesting that PDT inhibited tumor growth (Figure 8). Furthermore, PDT treated tumors showed rapid extensive damage with necrotic- and apoptotic cell death at the irradiated tumor site as indicated by H&E staining. PDT treated tumor cells showed some features of necrosis and apoptosis such as nuclear fading due to DNA degradation (karyolysis), anuclear necrotic cells with a glossier homogenous appearance, nuclear chromatin condensation (pyknosis), and nuclear fragmentation (karyorrhexis). No conspicuous damage was found in the tumors of the other control groups receiving FolateSiR-1 alone, irradiation alone, or no treatment (Figure 9).

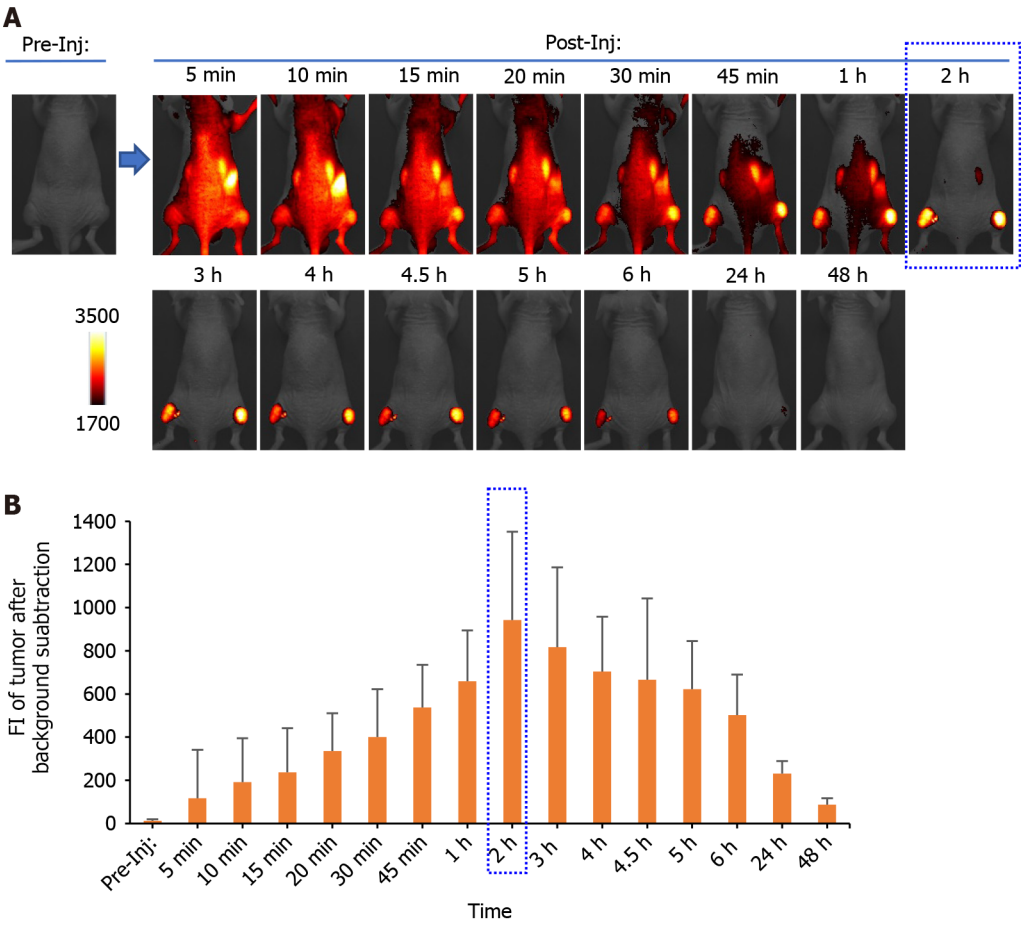

Figure 4 *In vivo* longitudinal near-infrared fluorescence imaging of folate-Si-rhodamine-1 in a KB tumor-bearing representative mouse. A: Imaging was conducted before and after folate-Si-rhodamine-1 (FolateSiR-1) injection. The indicated time points after injection are at 5 min, 10 min, 15 min, 20 min, 30 min, 45 min, 1 h, 2 h, 3 h, 4 h, 4.5 h, 5 h, 6 h, 24 h, and 48 h. Time-dependent FolateSiR-1 distribution and its specific tumor accumulation is shown in serial images; B: Quantitative fluorescent signal intensity analysis of the tumors. Data are presented as the mean ± SD (n = 4). NIR: Near-infrared; FI: Fluorescent signal intensity; Pre-Inj: Pre-injection; Post-Inj: Post-injection.

DISCUSSION

FolateSiR-1 significantly accumulated in the FR-expressing KB tumors, but not in the FR-negative tumors and normal organs. This PS was activated by NIR light to evoke cytotoxic effects on cells and tumors, resulting in PDT induced necrosis and apoptosis. Our findings suggest that FolateSiR-1 has potential for application in the PDT of FR-expressing tumors.

High FR expression was observed in the KB cells, but not in the OVCAR-3 and A4 cells (Figure 2A). Furthermore, fluorescence microscopy revealed that KB cells incubated with FolateSiR-1 showed strong FI which contrasted with that of the other two cell lines (Figure 2B). These results encouraged us to use KB cells as a representative FR-expressing xenograft tumor in a mouse model. Stronger FI was observed in KB tumors, compared to OVCAR-3 tumors, A4 tumors, and other sites throughout the body, which was attributed to the presence of FolateSiR-1 (Figures 2C-E). Furthermore, strongly positive FR staining was observed in KB tumor cells, whereas it was almost entirely absent in OVCAR-3 cells based on IHC (Figure 2F). These findings and *ex vivo* images of normal tissues (Figure 5C) indicate that FolateSiR-1 binds FR with high specificity in FR-overexpressing cells and tumors.

In this study, FolateSiR-1 accumulation peaked at 2 h after injection in KB tumors, followed by its disappearance over the next 24 h based on quantification of serial fluorescence images. The rapid peak accumulation of FolateSiR-1 in tumors may be a more convenient clinical setting of PDT than the number of days required for PIT using an antibody as a PS carrier. Furthermore, rapid tumor contrast enhancement within a few hours after PS injection could be advantageous for real-time cancer detection in the intraoperative setting. Moreover, irradiation delivered at a shorter interval when PS is still present in the blood vessels results in a superior tumor response which causes marked vascular damage[39]. *In vivo* time-dependent images (Figure 4) and *ex vivo* images of tissues (Figure 5C) showed that FolateSiR-1 was cleared relatively quickly from normal tissues, including the main excretory organs (liver and kidney), indicating that the phototoxic side effects were minimized.

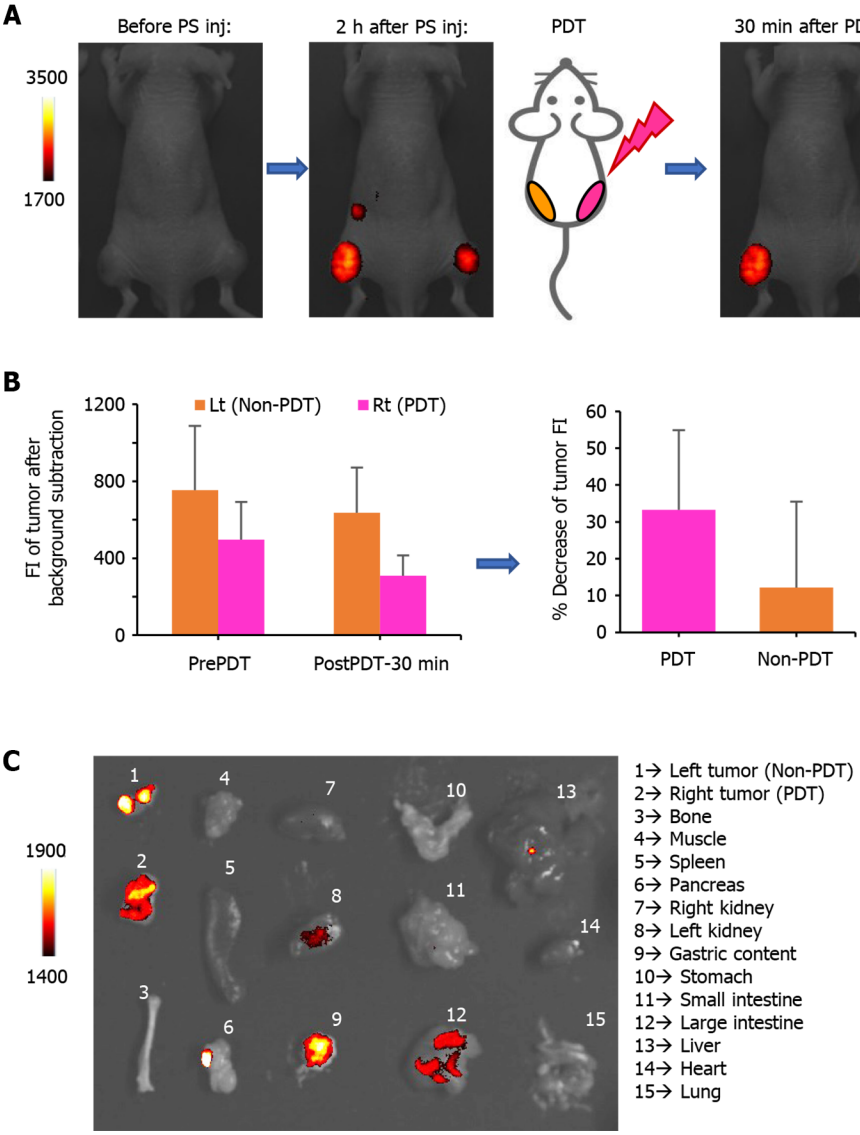

Figure 5 *In vivo* and *ex vivo* images before and after photodynamic therapy. A: Near-infrared fluorescence images of representative tumor bearing mice: before photosensitizer (PS) (FolateSiR-1) injection (left), 2 h after PS injection (center), and 30 min after photodynamic therapy (PDT) (right). The right tumor received PDT while the left tumor did not. Fluorescent signal intensity (FI) of the right tumor decreased immediately after PDT, and the extent of FI reduction is larger than that of the left tumor; B: Bar graph showing the FI of the tumor before- and 30 min after PDT. Data are presented as the mean ± SD (n = 4); C: *Ex vivo* fluorescence images captured 30 min after PDT. NIR: Near-infrared; Lt: Left; Rt: Right; PS inj: photosensitizer injection; PDT: Photodynamic therapy; Non-PDT: Without PDT; FI: Fluorescent signal intensity.

KB cells showed extensive bright fluorescence signals, whereas there was no obvious PS binding or uptake in the negative control cells indicating that FolateSiR-1 was selectively localized in KB cells (Figure 2B). Fluorescent signals were mainly observed at the plasma membrane of KB cells and in some cytoplasmic component sites. The cellular response to photodamage primarily depends on PS localization and PDT dose[40-42]. Photosensitizer localization and activation inside tumor tissues generates ROS which can directly kill malignant tumor cells[4]. Mitochondria-localized PS induces apoptotic cell death within a certain threshold of oxidative stress[6,43]. Necrosis is more often observed if the cell membrane is the site of action for the PS[44]. Mild oxidative damage by PS localized in the plasma membrane causes apoptosis, but severe damage leads to the loss of plasma membrane integrity and causes necrotic cell death[6,41,45]. Meanwhile, PSs targeting the endoplasmic reticulum, Golgi membranes, and lysosomes mediates necrosis[43]. Moreover, high PDT doses (dependent on the amount of PS and the irradiation dose) inactivate essential enzymes and other components of the apoptotic cascade resulting in increased cellular damage leading to necrosis rather than apoptosis[40, 46]. The merged fluorescence- and phase-contrast images showed strong FolateSiR-1 fluorescence intensity in the KB cell membrane and the cytoplasm, but not in the nucleus (Figure 2B). This finding suggests that FolateSiR-1 promotes necrosis and is a suitable probe for PDT. The probe alone did not penetrate the nuclear membrane and therefore did not cause genetic damage.

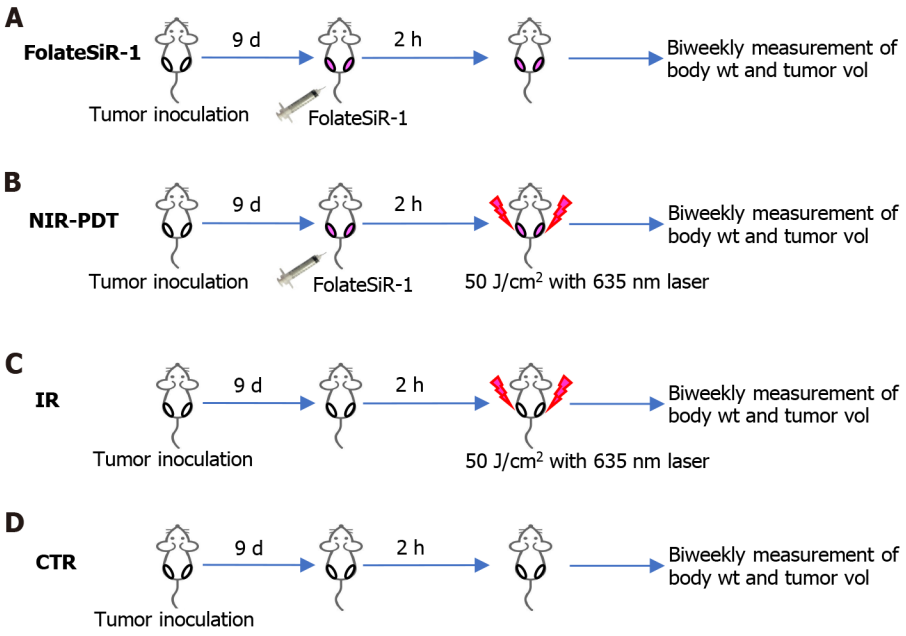

Figure 6 Experimental treatment scheme. Tumor bearing mice were assigned to four groups: A: folate-Si-rhodamine-1 injection alone; B: Near-infrared (NIR) photodynamic therapy (50 J/cm^2); C: NIR irradiation alone (50 J/cm^2); and D: no treatment. FolateSiR-1: Folate-Si-rhodamine-1; NIR-PDT: Near-infrared photodynamic therapy; IR: Laser irradiation; CTR: Control; wt: Weight; vol: Volume.

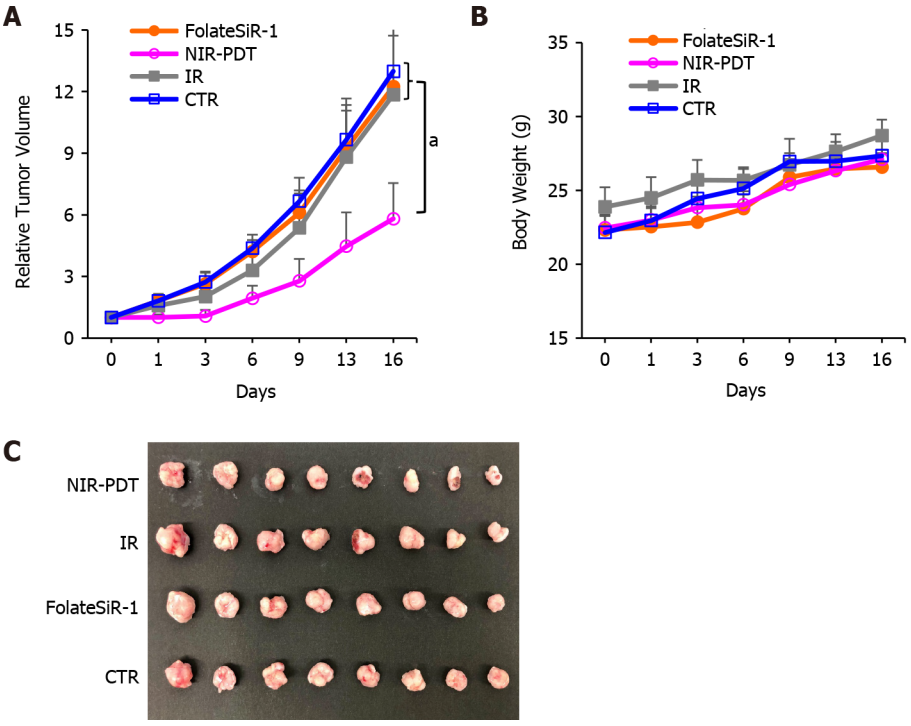

Figure 7 Phototherapeutic effects of photodynamic therapy on KB xenografts and body weight in mice. A: Tumor volume change is expressed as the relative tumor volume (volume on the indicated day/starting volume prior to the treatment. Tumors-treated by near-infrared photodynamic therapy (NIR-PDT) (50 J/cm^2), irradiation alone (50 J/cm^2), folate-Si-rhodamine-1 alone, and no treatment are shown in pink (○), gray (■), orange (●), and blue (□), respectively. Tumors-treated by NIR-PDT show significantly delayed growth compared to those of other groups. Values represent the mean ± SD (n = 8), $^aP < 0.05$ NIR-PDT *vs* other groups; B: Average body weight did not differ significantly among the four groups of mice; C: Images of *ex vivo* tumors excised 16 d after treatment. FolateSiR-1: Folate-Si-rhodamine-1; NIR-PDT: Near-infrared photodynamic therapy; IR: Laser irradiation; CTR: Control.

Our NIR-PDT regimen delivered a single dose of NIR light (50 J/cm^2) to KB tumors after intravenous administration of FolateSiR-1 (100 μg). The growth rate of tumors receiving PDT was significantly suppressed even with this single irradiation compared with the control groups (Figure 7). Complete tumor remission was not achieved with a single irradiation, however, partial remission for three days and delayed relapse was noted after PDT. Therefore, NIR-PDT using FolateSiR-1 is expected to be as

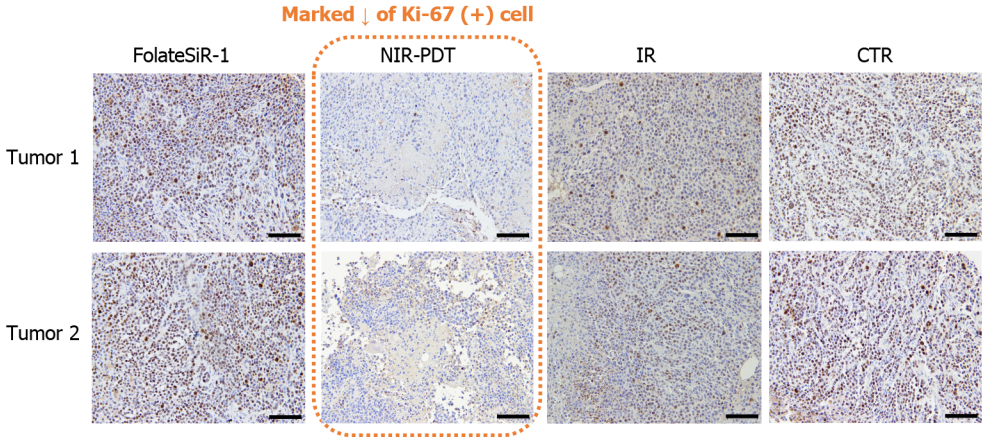

Figure 8 Tumor immunohistochemical staining of Ki-67 at 24 h after near-infrared photodynamic therapy. The weak staining and marked reduction of Ki-67-positive cells were detected in tumors treated with near-infrared photodynamic therapy (scale bar = 100 μm, 20 × magnification). FolateSiR-1: Folate-Si-rhodamine-1; NIR-PDT: Near-infrared photodynamic therapy; IR: Laser irradiation; CTR: Control.

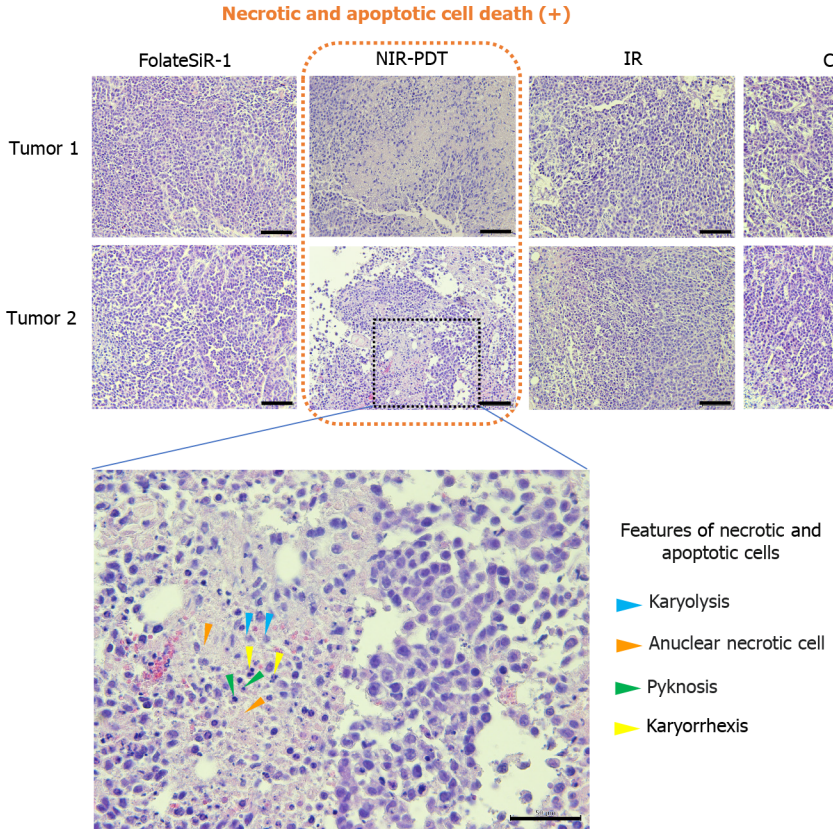

Figure 9 Histological examination of the destructive effects of near-infrared photodynamic therapy in tumor tissues 24 h after near-infrared photodynamic therapy. Tumors are stained with hematoxylin and eosin. The left lowermost image is a magnification of the indicated portion of the upper image. Some features of necrotic and apoptotic cells are shown with arrowheads: nuclear fading due to DNA loss, karyolysis (blue), anuclear necrotic cells with a glossier homogenous appearance (orange), nuclear chromatin condensation, pyknosis (green), nuclear fragmentation, and karyorrhexis (yellow). (Scale bar = 100 μm, 20 × magnification for upper two rows, and scale bar = 50 μm, 40 × magnification for lower row). FolateSiR-1: folate-Si-rhodamine-1; NIR-PDT: Near-infrared photodynamic therapy; IR: laser irradiation; CTR: control.

effective as other currently tested PDTs and PITs, because more precise treatment regimens can be easily designed by adjusting PS and irradiation doses, and repeating the treatment to improve the therapeutic efficacy and potentially achieving complete pathological remission. An extended study aiming to optimize the treatment will be performed in the future.

Photobleaching is the light-mediated destruction of PS. Linear correlation between protoporphyrin IX photobleaching and necrosis was used as a predictive tool of the PDT response in the rat ovarian cancer model[47]. Our limited mice experiments showed a tendency for FI reduction in tumors immediately

after PDT (Figure 5A and B), and this was probably due to some PS photobleaching and necrosis of cancer cells. An extended study is required to confirm this association.

Rapid phototoxic cell death-induced by NIR-PDT (10 J/cm^2) and abundant dead cells stained green with NucGreen® Dead reagent were clearly observed in viability imaging assays (Figure 3). In contrast, neither FolateSiR-1 alone nor irradiation alone induced noticeable cell death, suggesting that FolateSiR-1 is an effective PS with high phototoxicity and low dark toxicity.

Nuclear staining of the proliferative factor Ki67 in tumor cells using IHC indicating that these cells were actively proliferating at 24 h post-PDT. Meanwhile, tumors treated with PDT (50 J/cm^2) showed weak staining and a marked decrease in Ki-67 positive cells, suggesting that FolateSiR-1 mediated PDT inhibited cell proliferation in tumors (Figure 8). Therefore, some cells stop proliferating, but do not immediately undergo necrosis or apoptosis. In addition, tumors irradiated with targeted PDT exhibited rapid and extensive damage with a phenotype of necrosis and apoptotic cell death at the irradiated site as indicated by H&E staining. Some cells displayed necrotic cell death features such as nuclear fading (karyolysis) and anuclear necrotic cells, while other cells showed apoptotic cell death features such as chromatin condensation of the nucleus (pyknosis) and nuclear fragmentation (karyorrhexis). No distinct damage was found in the tumors of the other control groups (Figure 9). These results were consistent with that of tumor growth and revealed the presumptive mechanism of the effects of PDT.

The main mechanism of tumor destruction by PDT is the direct damage to cells[45], however, there are other indirect mechanisms such as damage to tumor blood vessels and nonspecific activation of the immune response against tumor cells[42,48]. As these mechanisms were not addressed in this study, additional research on this topic is required. Furthermore, only one FR-overexpressing cell line-derived subcutaneous tumor was used. The nature of the xenografted-tumor microenvironment does not reflect all of the characteristics of human cancer tissue. Not all tumors express high FR levels in a clinical setting. These drawbacks may limit the wide use of FR-targeted NIR-PDT. Nevertheless, further research may elucidate these limitations. The fascinating features of FolateSiR-1, including selectivity for tumor cells, membranous and subcellular localization, and cytotoxicity in combination with NIR irradiation, prompted the development of an alternative PS for NIR-PDT. The results of this study indicate that FR-targeted NIR-PDT using this PS may have potential for application in the treatment of FR-overexpressing tumors. Moreover, specific binding of FolateSiR-1 to FRs and emission of near-infrared light may be useful for decision making in various settings including patient screening for treatment selection, theranostic applications such as image-guided cancer detection and PDT, or in combination with other treatments.

CONCLUSION

FolateSiR-1 displayed FR-specificity *in vitro* and *in vivo* and functioned as a potential PS when irradiated with NIR light, causing cellular tumor damage by provoking the cumulative effect of necrosis, apoptosis, and cell proliferation-inhibition. These findings suggest that FolateSiR-1 may be effectively utilized in PDT with low side effects, and FR-targeted NIR-PDT can potentially provide new effective strategies for the treatment of FR-overexpressing tumors.

ARTICLE HIGHLIGHTS

Research background

Photodynamic therapy (PDT) is one of the emerging options to combat cancer and it requires photosensitizer (PS) and corresponding light irradiation. The tumor selectivity of the photosensitizer improves tumor localization in PDT, enhances tumor destruction, and reduces side effects due to off-target localization. Folate receptor (FR) membrane protein is frequently overexpressed in human cancer and specific active targeting of PS to FR can be achieved by conjugation with the folate moiety.

Research motivation

We previously developed a folate-linked, near-infrared (NIR)-sensitive probe folate-Si-rhodamine-1 (FolateSiR-1). The feasibility of NIR-PDT using FolateSiR-1 and appropriate light irradiation had not been determined and reqired elucidation.

Research objectives

The aim of this study was to evaluate the photodynamic therapeutic efficacy of FolateSiR-1 in a preclinical cancer model and determine the cell death mode induced by FolateSiR-1-based PDT.

Research methods

FolateSiR-1 was synthesized by conjugating a folate moiety to the Si-rhodamine derivative through a

negatively charged tripeptide linker. Utilizing FR-overexpressing cell line KB and low FR-expressing cell lines OVCAR-3 and A4, selective binding of FolateSiR-1 to FR was evaluated by fluorescence microscopy. Cell viability imaging assays was exploited to assess the phototoxic effect of FolateSiR-1. *In vivo* longitudinal fluorescence imaging was conducted to examine the time-dependent biodistribution of FolateSiR-1 and its specific accumulation in KB tumors. To evaluate PDT efficacy of FolateSiR-1, KB tumor-bearing mice were divided into four groups: (1) FolateSiR-1 alone; (2) FolateSiR-1 followed by NIR irradiation; (3) NIR irradiation alone; and (4) no treatment. Tumor volume measurement, as well as immunohistochemical (IHC) and histological examinations of tumors were performed to determine the effect of PDT.

Research results

FR-specific binding of FolateSiR-1 was observed by fluorescence microscopy and *in vivo* fluorescence imaging. Cell viability imaging assays indicated that NIR-PDT induced cell death. *In vivo* longitudinal fluorescence imaging showed rapid peak accumulation of FolateSiR-1 in KB tumors 2 h after injection. The tumor volumes in the PDT group were significantly reduced compared to the other groups ($P < 0.05$). IHC analysis revealed reduced numbers of proliferation marker Ki-67-positive cells in PDT treated tumors, and hematoxylin-eosin staining revealed features of necrotic- and apoptotic cell death.

Research conclusions

FolateSiR-1 may be effectively utilized in PDT with low side effects, and the FR-targeted NIR-PDT can potentially reveal new strategies for the treatment of FR-overexpressing tumors.

Research perspectives

The fascinating features of FolateSiR-1, including specificity to FR, cytotoxicity in combination with NIR irradiation and relatively fast clearance implying low toxicity, prompted the development of an alternative PS for NIR-PDT. The therapeutic effect was significant after a single dose of irradiation and may be optimized to achieve patient-specific clinical effects. Moreover, fluorescence emission from FolateSiR-1 may be used for real time cancer detection and patient screening for treatment selection. Further research may elucidate these additional details of these processes.

ACKNOWLEDGEMENTS

We thank Aya Sugyo for help with the animal experiments and Tsuneo Saga for providing the A4 cell.

FOOTNOTES

Author contributions: Aung W designed the study, conducted most of the experiments, analyzed the data, and wrote the manuscript; Hanaoka K, designed, synthesized, and provided the folate-Si-rhodamine-1; Tsuji AB and Higashi T coordinated the research and contributed to manuscript preparation; all authors critically reviewed and approved the final version of the article.

Supported by a Grant-in-Aid for Scientific Research (C) from the Japan Society for the Promotion of Science, No. 21K07740 (to Aung W).

Institutional animal care and use committee statement: This study was reviewed and approved by the Institutional Review Board of National Institute for Quantum and Radiological Science and Technology, No. 13-1022-9.

Conflict-of-interest statement: All the authors report no relevant conflicts of interest for this article.

Data sharing statement: All relevant data were presented in the manuscript. Further information is available from the corresponding author.

ARRIVE guidelines statement: The authors have read the ARRIVE guidelines, and the manuscript was prepared and revised according to the ARRIVE guidelines.

Country/Territory of origin: Japan

ORCID number: Winn Aung 0000-0002-0896-7158; Atsushi B Tsuji 0000-0003-2726-288X; Kenjiro Hanaoka 0000-0003-0797-4038; Tatsuya Higashi 0000-0002-8338-4737.

S-Editor: Gong ZM
L-Editor: A
P-Editor: Wu RR

REFERENCES

1 **Sung H**, Ferlay J, Siegel RL, Laversanne M, Soerjomataram I, Jemal A, Bray F. Global Cancer Statistics 2020: GLOBOCAN Estimates of Incidence and Mortality Worldwide for 36 Cancers in 185 Countries. *CA Cancer J Clin* 2021; **71**: 209-249 [PMID: 33538338 DOI: 10.3322/caac.21660]
2 **Algorri JF**, Ochoa M, Roldán-Varona P, Rodríguez-Cobo L, López-Higuera JM. Photodynamic Therapy: A Compendium of Latest Reviews. *Cancers (Basel)* 2021; **13** [PMID: 34503255 DOI: 10.3390/cancers13174447]
3 **Agostinis P**, Berg K, Cengel KA, Foster TH, Girotti AW, Gollnick SO, Hahn SM, Hamblin MR, Juzeniene A, Kessel D, Korbelik M, Moan J, Mroz P, Nowis D, Piette J, Wilson BC, Golab J. Photodynamic therapy of cancer: an update. *CA Cancer J Clin* 2011; **61**: 250-281 [PMID: 21617154 DOI: 10.3322/caac.20114]
4 **van Straten D**, Mashayekhi V, de Bruijn HS, Oliveira S, Robinson DJ. Oncologic Photodynamic Therapy: Basic Principles, Current Clinical Status and Future Directions. *Cancers (Basel)* 2017; **9** [PMID: 28218708 DOI: 10.3390/cancers9020019]
5 **Mroz P**, Yaroslavsky A, Kharkwal GB, Hamblin MR. Cell death pathways in photodynamic therapy of cancer. *Cancers (Basel)* 2011; **3**: 2516-2539 [PMID: 23914299 DOI: 10.3390/cancers3022516]
6 **Agostinis P**, Buytaert E, Breyssens H, Hendrickx N. Regulatory pathways in photodynamic therapy induced apoptosis. *Photochem Photobiol Sci* 2004; **3**: 721-729 [PMID: 15295626 DOI: 10.1039/b315237e]
7 **Hamblin MR**, Abrahamse H. Factors Affecting Photodynamic Therapy and Anti-Tumor Immune Response. *Anticancer Agents Med Chem* 2021; **21**: 123-136 [PMID: 32188394 DOI: 10.2174/1871520620666200318101037]
8 **Abrahamse H**, Hamblin MR. New photosensitizers for photodynamic therapy. *Biochem J* 2016; **473**: 347-364 [PMID: 26862179 DOI: 10.1042/BJ20150942]
9 **Bugaj AM**. Targeted photodynamic therapy--a promising strategy of tumor treatment. *Photochem Photobiol Sci* 2011; **10**: 1097-1109 [PMID: 21547329 DOI: 10.1039/c0pp00147c]
10 **Shirasu N**, Nam SO, Kuroki M. Tumor-targeted photodynamic therapy. *Anticancer Res* 2013; **33**: 2823-2831 [PMID: 23780966]
11 **Sibani SA**, McCarron PA, Woolfson AD, Donnelly RF. Photosensitiser delivery for photodynamic therapy. Part 2: systemic carrier platforms. *Expert Opin Drug Deliv* 2008; **5**: 1241-1254 [PMID: 18976134 DOI: 10.1517/17425240802444673]
12 **Debele TA**, Peng S, Tsai HC. Drug Carrier for Photodynamic Cancer Therapy. *Int J Mol Sci* 2015; **16**: 22094-22136 [PMID: 26389879 DOI: 10.3390/ijms160922094]
13 **Kaščáková S**, Hofland LJ, De Bruijn HS, Ye Y, Achilefu S, van der Wansem K, van der Ploeg-van den Heuvel A, van Koetsveld PM, Brugts MP, van der Lelij AJ, Sterenborg HJ, Ten Hagen TL, Robinson DJ, van Hagen MP. Somatostatin analogues for receptor targeted photodynamic therapy. *PLoS One* 2014; **9**: e104448 [PMID: 25111655 DOI: 10.1371/journal.pone.0104448]
14 **St Denis TG**, Hamblin MR. Synthesis, bioanalysis and biodistribution of photosensitizer conjugates for photodynamic therapy. *Bioanalysis* 2013; **5**: 1099-1114 [PMID: 23641699 DOI: 10.4155/bio.13.37]
15 **Ormond AB**, Freeman HS. Dye Sensitizers for Photodynamic Therapy. *Materials (Basel)* 2013; **6**: 817-840 [PMID: 28809342 DOI: 10.3390/ma6030817]
16 **Shen J**, Hu Y, Putt KS, Singhal S, Han H, Visscher DW, Murphy LM, Low PS. Assessment of folate receptor alpha and beta expression in selection of lung and pancreatic cancer patients for receptor targeted therapies. *Oncotarget* 2018; **9**: 4485-4495 [PMID: 29435118 DOI: 10.18632/oncotarget.23321]
17 **Vlahov IR**, Leamon CP. Engineering folate-drug conjugates to target cancer: from chemistry to clinic. *Bioconjug Chem* 2012; **23**: 1357-1369 [PMID: 22667324 DOI: 10.1021/bc2005522]
18 **Li PX**, Mu JH, Xiao HL, Li DH. Antitumor effect of photodynamic therapy with a novel targeted photosensitizer on cervical carcinoma. *Oncol Rep* 2015; **33**: 125-132 [PMID: 25376180 DOI: 10.3892/or.2014.3593]
19 **Stallivieri A**, Colombeau L, Jetpisbayeva G, Moussaron A, Myrzakhmetov B, Arnoux P, Acherar S, Vanderesse R, Frochot C. Folic acid conjugates with photosensitizers for cancer targeting in photodynamic therapy: Synthesis and photophysical properties. *Bioorg Med Chem* 2017; **25**: 1-10 [PMID: 27769669 DOI: 10.1016/j.bmc.2016.10.004]
20 **Gravier J**, Schneider R, Frochot C, Bastogne T, Schmitt F, Didelon J, Guillemin F, Barberi-Heyob M. Improvement of meta-tetra(hydroxyphenyl)chlorin-like photosensitizer selectivity with folate-based targeted delivery. synthesis and in vivo delivery studies. *J Med Chem* 2008; **51**: 3867-3877 [PMID: 18553957 DOI: 10.1021/jm800125a]
21 **Wang J**, Liu Q, Zhang Y, Shi H, Liu H, Guo W, Ma Y, Huang W, Hong Z. Folic Acid-Conjugated Pyropheophorbide a as the Photosensitizer Tested for In Vivo Targeted Photodynamic Therapy. *J Pharm Sci* 2017; **106**: 1482-1489 [PMID: 28263847 DOI: 10.1016/j.xphs.2017.02.019]
22 **Kim H**, Kim MW, Jeong YI, Yang HS. Redox-Sensitive and Folate-Receptor-Mediated Targeting of Cervical Cancer Cells for Photodynamic Therapy Using Nanophotosensitizers Composed of Chlorin e6-Conjugated β-Cyclodextrin *via* Diselenide Linkage. *Cells* 2021; **10** [PMID: 34571839 DOI: 10.3390/cells10092190]
23 **Syu WJ**, Yu HP, Hsu CY, Rajan YC, Hsu YH, Chang YC, Hsieh WY, Wang CH, Lai PS. Improved photodynamic cancer treatment by folate-conjugated polymeric micelles in a KB xenografted animal model. *Small* 2012; **8**: 2060-2069 [PMID:

22508664 DOI: 10.1002/smll.201102695]
24 **Li H**, Jin Z, Cho S, Jeon MJ, Nguyen VD, Park JO, Park S. Folate-receptor-targeted NIR-sensitive polydopamine nanoparticles for chemo-photothermal cancer therapy. *Nanotechnology* 2017; **28**: 425101 [PMID: 28944765 DOI: 10.1088/1361-6528/aa8477]
25 **Kato T**, Jin CS, Ujiie H, Lee D, Fujino K, Wada H, Hu HP, Weersink RA, Chen J, Kaji M, Kaga K, Matsui Y, Wilson BC, Zheng G, Yasufuku K. Nanoparticle targeted folate receptor 1-enhanced photodynamic therapy for lung cancer. *Lung Cancer* 2017; **113**: 59-68 [PMID: 29110850 DOI: 10.1016/j.lungcan.2017.09.002]
26 **Kato T**, Jin CS, Lee D, Ujiie H, Fujino K, Hu HP, Wada H, Wu L, Chen J, Weersink RA, Kanno H, Hatanaka Y, Hatanaka KC, Kaga K, Matsui Y, Matsuno Y, De Perrot M, Wilson BC, Zheng G, Yasufuku K. Preclinical investigation of folate receptor-targeted nanoparticles for photodynamic therapy of malignant pleural mesothelioma. *Int J Oncol* 2018; **53**: 2034-2046 [PMID: 30226590 DOI: 10.3892/ijo.2018.4555]
27 **Baydoun M**, Moralès O, Frochot C, Ludovic C, Leroux B, Thecua E, Ziane L, Grabarz A, Kumar A, de Schutter C, Collinet P, Azais H, Mordon S, Delhem N. Photodynamic Therapy Using a New Folate Receptor-Targeted Photosensitizer on Peritoneal Ovarian Cancer Cells Induces the Release of Extracellular Vesicles with Immunoactivating Properties. *J Clin Med* 2020; **9** [PMID: 32326210 DOI: 10.3390/jcm9041185]
28 **Quilbe A**, Moralès O, Baydoun M, Kumar A, Mustapha R, Murakami T, Leroux B, de Schutter C, Thecua E, Ziane L, Colombeau L, Frochot C, Mordon S, Delhem N. An Efficient Photodynamic Therapy Treatment for Human Pancreatic Adenocarcinoma. *J Clin Med* 2020; **9** [PMID: 31936786 DOI: 10.3390/jcm9010192]
29 **Mussini A**, Uriati E, Bianchini P, Diaspro A, Cavanna L, Abbruzzetti S, Viappiani C. Targeted photoimmunotherapy for cancer. *Biomol Concepts* 2022; **13**: 126-147 [PMID: 35304984 DOI: 10.1515/bmc-2022-0010]
30 **Aung W**, Tsuji AB, Sugyo A, Takashima H, Yasunaga M, Matsumura Y, Higashi T. Near-infrared photoimmunotherapy of pancreatic cancer using an indocyanine green-labeled anti-tissue factor antibody. *World J Gastroenterol* 2018; **24**: 5491-5504 [PMID: 30622378 DOI: 10.3748/wjg.v24.i48.5491]
31 **Olivo M**, Bhuvaneswari R, Lucky SS, Dendukuri N, Soo-Ping Thong P. Targeted Therapy of Cancer Using Photodynamic Therapy in Combination with Multi-faceted Anti-Tumor Modalities. *Pharmaceuticals (Basel)* 2010; **3**: 1507-1529 [PMID: 27713315 DOI: 10.3390/ph3051507]
32 **Numasawa K**, Hanaoka K, Saito N, Yamaguchi Y, Ikeno T, Echizen H, Yasunaga M, Komatsu T, Ueno T, Miura M, Nagano T, Urano Y. A Fluorescent Probe for Rapid, High-Contrast Visualization of Folate-Receptor-Expressing Tumors In Vivo. *Angew Chem Int Ed Engl* 2020; **59**: 6015-6020 [PMID: 31984590 DOI: 10.1002/anie.201914826]
33 **Chen C**, Ke J, Zhou XE, Yi W, Brunzelle JS, Li J, Yong EL, Xu HE, Melcher K. Structural basis for molecular recognition of folic acid by folate receptors. *Nature* 2013; **500**: 486-489 [PMID: 23851396 DOI: 10.1038/nature12327]
34 **Silva EF**, Schaberle FA, Monteiro CJ, Dąbrowski JM, Arnaut LG. The challenging combination of intense fluorescence and high singlet oxygen quantum yield in photostable chlorins--a contribution to theranostics. *Photochem Photobiol Sci* 2013; **12**: 1187-1192 [PMID: 23584281 DOI: 10.1039/c3pp25419d]
35 **Weissleder R**, Ntziachristos V. Shedding light onto live molecular targets. *Nat Med* 2003; **9**: 123-128 [PMID: 12514725 DOI: 10.1038/nm0103-123]
36 **Scholzen T**, Gerdes J. The Ki-67 protein: from the known and the unknown. *J Cell Physiol* 2000; **182**: 311-322 [PMID: 10653597 DOI: 10.1002/(SICI)1097-4652(200003)182:3<311::AID-JCP1>3.0.CO;2-9]
37 **Sudo H**, Tsuji AB, Sugyo A, Ogawa Y, Sagara M, Saga T. ZDHHC8 knockdown enhances radiosensitivity and suppresses tumor growth in a mesothelioma mouse model. *Cancer Sci* 2012; **103**: 203-209 [PMID: 22017350 DOI: 10.1111/j.1349-7006.2011.02126.x]
38 **Low PS**, Kularatne SA. Folate-targeted therapeutic and imaging agents for cancer. *Curr Opin Chem Biol* 2009; **13**: 256-262 [PMID: 19419901 DOI: 10.1016/j.cbpa.2009.03.022]
39 **Chen B**, Roskams T, de Witte PA. Antivascular tumor eradication by hypericin-mediated photodynamic therapy. *Photochem Photobiol* 2002; **76**: 509-513 [PMID: 12462645 DOI: 10.1562/0031-8655(2002)076<0509:atebhm>2.0.co;2]
40 **Lavie G**, Kaplinsky C, Toren A, Aizman I, Meruelo D, Mazur Y, Mandel M. A photodynamic pathway to apoptosis and necrosis induced by dimethyl tetrahydroxyhelianthrone and hypericin in leukaemic cells: possible relevance to photodynamic therapy. *Br J Cancer* 1999; **79**: 423-432 [PMID: 10027308 DOI: 10.1038/sj.bjc.6690066]
41 **Buytaert E**, Dewaele M, Agostinis P. Molecular effectors of multiple cell death pathways initiated by photodynamic therapy. *Biochim Biophys Acta* 2007; **1776**: 86-107 [PMID: 17693025 DOI: 10.1016/j.bbcan.2007.07.001]
42 **Piette J**, Volanti C, Vantieghem A, Matroule JY, Habraken Y, Agostinis P. Cell death and growth arrest in response to photodynamic therapy with membrane-bound photosensitizers. *Biochem Pharmacol* 2003; **66**: 1651-1659 [PMID: 14555246 DOI: 10.1016/s0006-2952(03)00539-2]
43 **Benov L**. Photodynamic therapy: current status and future directions. *Med Princ Pract* 2015; **24** Suppl 1: 14-28 [PMID: 24820409 DOI: 10.1159/000362416]
44 **Hsieh YJ**, Wu CC, Chang CJ, Yu JS. Subcellular localization of Photofrin determines the death phenotype of human epidermoid carcinoma A431 cells triggered by photodynamic therapy: when plasma membranes are the main targets. *J Cell Physiol* 2003; **194**: 363-375 [PMID: 12548556 DOI: 10.1002/jcp.10273]
45 **Oleinick NL**, Morris RL, Belichenko I. The role of apoptosis in response to photodynamic therapy: what, where, why, and how. *Photochem Photobiol Sci* 2002; **1**: 1-21 [PMID: 12659143 DOI: 10.1039/b108586g]
46 **Castano AP**, Demidova TN, Hamblin MR. Mechanisms in photodynamic therapy: part two-cellular signaling, cell metabolism and modes of cell death. *Photodiagnosis Photodyn Ther* 2005; **2**: 1-23 [PMID: 25048553 DOI: 10.1016/S1572-1000(05)00030-X]
47 **Ascencio M**, Collinet P, Farine MO, Mordon S. Protoporphyrin IX fluorescence photobleaching is a useful tool to predict the response of rat ovarian cancer following hexaminolevulinate photodynamic therapy. *Lasers Surg Med* 2008; **40**: 332-341 [PMID: 18563777 DOI: 10.1002/lsm.20629]
48 **Juarranz A**, Jaén P, Sanz-Rodríguez F, Cuevas J, González S. Photodynamic therapy of cancer. Basic principles and applications. *Clin Transl Oncol* 2008; **10**: 148-154 [PMID: 18321817 DOI: 10.1007/s12094-008-0172-2]

World Journal of Clinical Oncology

Submit a Manuscript: https://www.f6publishing.com

World J Clin Oncol 2022 November 24; 13(11): 896-906

DOI: 10.5306/wjco.v13.i11.896

ISSN 2218-4333 (online)

ORIGINAL ARTICLE

Retrospective Cohort Study

Is it possible to adopt the same oncological approach in urgent surgery for colon cancer?

Bruno Yuki Yoshida, Raphael L C Araujo, José Francisco M Farah, Alberto Goldenberg

Specialty type: Oncology

Provenance and peer review: Invited article; Externally peer reviewed.

Peer-review model: Single blind

Peer-review report's scientific quality classification

Grade A (Excellent): 0
Grade B (Very good): 0
Grade C (Good): C, C
Grade D (Fair): 0
Grade E (Poor): 0

P-Reviewer: Chen SY, China; Liu Z, China

Received: June 30, 2022
Peer-review started: June 30, 2022
First decision: August 1, 2022
Revised: August 16, 2022
Accepted: October 27, 2022
Article in press: October 27, 2022
Published online: November 24, 2022

Bruno Yuki Yoshida, Raphael L C Araujo, José Francisco M Farah, Alberto Goldenberg, Department of Surgery, Federal University of Sao Paulo, Sao Paulo 04024-002, Sao Paulo, Brazil

Bruno Yuki Yoshida, José Francisco M Farah, Department of General and Oncological Surgery, Sao Paulo State Employee Hospital, Sao Paulo 04029-000, Sao Paulo, Brazil

Corresponding author: Raphael L C Araujo, MD, PhD, Adjunct Professor, Surgical Oncologist, Department of Surgery, Federal University of Sao Paulo, Rua Napoleao de Barros, 715, Second Floor Vila Clementino, Sao Paulo 04024-002, Sao Paulo, Brazil. raphaellcaraujo@gmail.com

Abstract

BACKGROUND

Locoregional complications may occur in up to 30% of patients with colon cancer. As they are frequent events in the natural history of this disease, there should be a concern in offering an oncologically adequate surgical treatment to these patients.

AIM

To compare the oncological radicality of surgery for colon cancer between urgent and elective cases.

METHODS

One-hundred and eighty-nine consecutive patients with non-metastatic colon adenocarcinoma were studied over two years in a single institution, who underwent surgical resection as the first therapeutic approach, with 123 elective and 66 urgent cases. The assessment of oncological radicality was performed by analyzing the extension of the longitudinal margins of resection, the number of resected lymph nodes, and the percentage of surgeries with 12 or more resected lymph nodes. Other clinicopathological variables were compared between the two groups in terms of sex, age, tumor location, type of urgency, surgical access, staging, compromised lymph nodes rate, differentiation grade, angiolymphatic and perineural invasion, and early mortality.

RESULTS

There was no difference between the elective and urgency group concerning the longitudinal margin of resection (average of 6.1 in elective *vs* 7.3 cm in urgency, $P = 0.144$), number of resected lymph nodes (average of 17.7 in elective *vs* 16.6 in urgency, $P = 0.355$) and percentage of surgeries with 12 or more resected lymph

nodes (75.6% in elective *vs* 77.3% in urgency, $P = 0.798$). It was observed that the percentage of patients aged 80 and over was higher in the urgency group (13.0% in elective *vs* 25.8% in urgency, $P = 0.028$), and the early mortality was 4.9% in elective *vs* 15.2% in urgency ($P = 0.016$, OR: 3.48, 95%CI: 1.21–10.06). Tumor location ($P = 0.004$), surgery performed ($P = 0.016$) and surgical access ($P < 0.001$) were also different between the two groups. There was no difference in other clinicopathological variables studied.

CONCLUSION
Oncological radicality of colon cancer surgery may be achieved in both emergency and elective procedures.

Key Words: Colorectal cancer; Intestinal obstruction; Intestinal perforation; Surgical oncology; Lymph node excision

Core Tip: The oncological radicality was compared between patients undergoing elective and urgent surgery for colon cancer. A total of 189 patients with nonmetastatic colorectal cancer who underwent surgical resection as the first therapeutic approach were included over two years in a single institution. The analysis of the oncological principles of the surgery, including the longitudinal margins of resection and the number of resected lymph nodes, revealed no statistical difference between elective and urgent surgeries. Therefore, the oncological principles of colorectal surgery should be followed in urgency as well as in elective cases.

Citation: Yoshida BY, Araujo RLC, Farah JFM, Goldenberg A. Is it possible to adopt the same oncological approach in urgent surgery for colon cancer? *World J Clin Oncol* 2022; 13(11): 896-906
URL: https://www.wjgnet.com/2218-4333/full/v13/i11/896.htm
DOI: https://dx.doi.org/10.5306/wjco.v13.i11.896

INTRODUCTION

Colorectal cancer (CRC) is a leading cause of cancer worldwide, representing 1 148 515 new cases a year [1]. Although many signs of progress in early detection and systemic treatment have been achieved, surgical resection remains the only curative-intent treatment for localized colon cancer[2]. Therefore, the basic principles of surgery should be oncologically adequate[3]. Considering the inherent difficulty of urgent cases, mostly presenting with obstruction or bleeding, and surgical morbidity, the achievement of good oncological outcomes seems to be challenging. Thus, this study aimed to compare oncological radicality and surgical outcomes between patients who underwent colectomy for colon cancer in urgent or elective procedures.

MATERIALS AND METHODS

One hundred and eighty-nine consecutive patients with non-metastatic colon adenocarcinoma who underwent surgery with curative intent as the first therapeutic approach were selected, with or without colostomy, operated using urgent (66) or elective (123) procedures, from May 2016 to April 2018. All cases were operated at the General and Oncological Surgery Service of Hospital do Servidor Público Estadual de São Paulo (HSPE/SP), Brazil. The project was approved by the Universidade Federal de São Paulo Ethics Committee (CEP/UNIFESP: 0498/2019; approval decision: 3460953). The selected patients were divided into two groups: Urgency and Elective. Those admitted to the Emergency Room with a locoregional complication of colon cancer, whether obstruction or perforation, requiring a prompt surgical approach, were classified as "Urgency". In this study, no patient required urgent surgery for incoercible bleeding. Conversely, those who, despite the admission to the hospital *via* the Emergency Room, had their initial emergency controlled, making it possible to perform complete staging, preoperative examinations and assessments, and colon preparation according to the institution's routine, were classified as Electives, along with the cases scheduled on an outpatient basis. This study excluded patients with rectal cancer, metastatic disease, diagnosed before or during surgery, those who underwent other therapeutic interventions before surgical resection (colonic prosthesis, derivative surgery, neoadjuvant), histological types other than adenocarcinoma, as well as patients with

insufficient medical record data. Clinicopathological variables were selected to compare the "elective" and "urgency" groups. Histopathological analysis was performed by the Pathology Service of Hospital do Servidor Público Estadual, and no slide review was necessary to carry out in this study. All variables were collected by the chief researcher, retrospectively, through reviewing electronic medical records. The clinicopathological variables evaluated were longitudinal margin (cm), number of resected lymph nodes, percentage of surgeries with 12 or more resected lymph nodes, sex, age (years), tumor location, surgery performed, type of urgency, access route used, staging according to the AJCC UICC 8th edition (2017), rate of compromised lymph nodes, degree of differentiation, angiolymphatic and perineural invasion, and early mortality (up to 30 days). The oncological radicality for colectomies was assessed by the minimal longitudinal margin of resection of 5 cm and the harvesting of at least 12 lymph nodes (representing proximal ligature of colic vessels). Inferential analysis was performed using the R program version 3.5.2 R Core Team (2016). Pearson's Chi-square test or Fisher's exact test was applied when comparing groups for categorical variables. For numerical variables, the *t* test or Mann-Whitney test was applied in independent samples, and the Shapiro-Wilk test was used to determine the normality of numerical variables. In all conclusions obtained through inferential analyzes, an alpha significance level of 5% ($P < 0.05$) was used.

RESULTS

Of the 189 patients, 66 (34.9%) were in the urgency group and 123 in the elective group (65.1%). There was no difference between the two groups in terms of distribution by sex ($P = 0.632$). Higher mean age was observed in the urgency group (71.8 years) *vs* 68.1 years in the elective group, $P = 0.031$), with 25.8% of patients aged 80 years or older in the urgency group, against 130% in the elective group ($P = 0.028$). Regarding the type of urgency that led to surgery in the emergency room, 47 (71.2%) were due to obstruction and 19 (28.8%) to perforation, with no patient being operated on for bleeding. These general characteristics are summarized in Table 1. Urgency group had a higher early mortality (up to 30 d) than the elective group (15.2% *vs* 4.9%, $P = 0.016$, OR: 3.48, 95%CI: 1.21-10.06) and there was no difference in the interval for starting systemic chemotherapy when indicated (average of 75.2 *vs* 71.8 d, $P = 0.535$). There was a difference between the two groups directly related to the location of the tumor (Table 2). In both groups, there was a predominance of location in the sigmoid, followed by the ascending colon. The surgical access also differed between the two groups, with a higher frequency of surgeries performed by laparoscopy in the elective group (43.1%) *vs* 0% in urgency group ($P < 0.001$).

Pathological characteristics are summarized in Table 3. It was observed that there was no statistical difference between the groups concerning the T and N classification, staging, degree of differentiation, and presence of angiolymphatic and perineural invasion. It was noted that, in both groups, more than 80% of patients had advanced stages (II or III). The rate of compromised lymph nodes was also found to be similar between the two groups (8.1% *vs* 7.9%, $P = 0.785$). Regarding the variables referring to the oncological principles for colon cancer surgery, there was also no statistically significant difference in the urgency group when compared to the elective group (Table 4). The stratified analysis by the location of the tumor is summarized in Table 5. Tumors located in the cecum, ascending colon, and transversus (3 cases) were considered to be in the right colon; and those located at the splenic, descending colon, sigmoid, and transversus (2 cases) as in the left colon. Four cases of transverse tumors (2 in the elective group and 2 in the urgency group) were excluded from this stratification as they underwent transversectomy, and it was not able to assign them to the right or left colon. There was a difference in the longitudinal margin in the analysis of the left colon (4.8 in the elective *vs* 7.6 cm in urgency, $P = 0.003$), with all other variables being similar between the groups. Early mortality was analyzed (up to 30 d) in patients who underwent emergency surgery. It was observed that the mean age was significantly higher in patients who died (84.0 *vs* 69.6 years, $P < 0.001$, 95%CI: 7.2-21.6). Of the 10 patients who died, 8 (80.0%) were 80 years old or older, in contrast to the 56 patients who survived, in which only 9 (16.1%) were in this age group ($P < 0.001$). There was no statistically significant difference regarding early mortality between the two groups, as shown in Table 6.

DISCUSSION

One of the criteria for achieving oncological radicality involves the extension of the longitudinal margin of the colon, which must be 5 cm to 7 cm[4,5]. Regarding the radial margin, block resection of adjacent structures should be performed in case of direct invasion, given their tumoral involvement by contiguity[2,6]. Another oncological preconized principle is the complete resection of the main vascular pedicles with the corresponding lymphadenectomy[7]. The number of resected lymph nodes directly influences the prognosis of the patient with colon cancer[8,9], considering that at least 12 lymph nodes must be resected and evaluated for lymphadenectomy to be oncologically adequate[3]. A situation inherent to colon cancer is the presence of possible locoregional complications that lead to the need for urgent surgery[10], which can occur in up to 30% of cases[11]. Intestinal obstruction is the most common

Table 1 General characteristics of the patients

	Elective	Urgency	*P* value
Total	123 (65.1%)	66 (34.9%)	
Sex			0.632[a]
Male	51 (41.5%)	25 (37.9%)	
Female	72 (58.5%	41 (62.1%)	
Age (yr)			
mean ± SD	68.1 ± 11.1	71.8 ± 11.5	0.031[b]
< 80	107 (87.0%)	49 (74.2%)	0.028[a]
≥ 80	16 (13.0%)	17 (25.8%)	
Type of urgency			
Obstruction		47 (71.2%)	
Perforation		19 (28.8%)	

[a]Qui-square of Pearson test.
[b]*t* test for independent samples.

Table 2 Clinical and surgical characteristics

	Elective	Urgency	*P* value	OR and 95%CI
Location			0.004[c]	
Cecum/Ascendent	44 (35.8%)	18 (27.3%)		
Transverse	4 (3.3%)	5 (7.6%)		
Splenic Angle	0	4 (6.1%)		
Descendent	6 (4.9%)	9 (13.6%)		
Sigmoid	69 (56.1%)	30 (45.5%)		
Surgery1			0.016[c]	
Right colectomy	45 (36.6%)	20 (30.3%)		
Transversectomy	2 (1.6%)	2 (3.0%)		
Left colectomy	6 (4.9%)	11 (16.7%)		
Retosigmoidectomy	66 (53.7%)	27 (40.9%)		
Total colectomy	4 (3.3%)	6 (9.1%)		
Surgical access			< 0.001[a]	
Open	70 (56.9%)	66 (100%)		
Videolaparoscopy	53 (43.1%)	0		
Early mortality	6 (4.9%)	10 (15.2%)	0.016[a]	OR: 3.48, 95%CI: 1.21-10.06

[1]With or without enterostomy.
[a]Qui-square of Pearson's test.
[b]*t* test for independent samples.
[c]Exact Fisher's test.
[d]Mean and standard deviation.

locoregional complication, followed by intestinal perforation[12]. Incoercible bleeding is a less frequent cause of urgent indication for colon cancer because, in most cases, bleeding stops or reduces, either spontaneously or through endoscopic or hemodynamic therapies, allowing the elective surgery to be performed[13,14]. In the face of an emergency, whether perforation or obstruction, surgical resection should be proposed as the first therapeutic approach, provided that patients are in clinical conditions

Table 3 Pathological characteristics of the tumors

	Elective	Urgency	*P* value
T			0.278[c]
Tis	2 (1.6%)	0	
T1	6 (4.9%)	0	
T2	16 (13.0%)	6 (9.1%)	
T3	88 (71.5%)	54 (81.8%)	
T4	11 (8.9%)	6 (9.1%)	
N			0.943[a]
N0	76 (61.8%)	42 (63.6%)	
N1	32 (26.0%)	17 (25.8%)	
N2	15 (12.2%)	7 (10.6%)	
Staging			0.199[c]
0	2 (1.6%)	0	
I	20 (16.3%)	5 (7.6%)	
II	54 (43.9%)	37 (56.1%)	
III	47 (38.2%)	24 (36.4%)	
Differentiation grade			0.938[c]
Well	7 (6.0%)	3 (5.0%)	
Moderate	101 (87.1%)	52 (86.7%)	
Poor	8 (6.9%)	5 (8.3%)	
Compromised lymph nodes rated	8.1% ± 16.7	7.9% ± 17.1	0.785[c]
Angiolymphatic invasion	44 (36.4%)	21 (31.8%)	0.533[a]
Perineural invasion	19 (16.4%)	7 (11.1%)	0.339[a]
ALI + PNI	16 (13.0%)	5 (7.6%)	0.257[a]

[a]Qui-square of Pearson's test.
[b]*t* test for independent samples.
[c]Exact Fisher's test.
[d]Mean and SD.
[e]Mann Whitney test.
ALI: Angiolymphatic invasion; PNI: Perineural invasion.

for this purpose[15,16].

In emergency surgeries, however, it is observed that the oncological principles described above cannot always be contemplated, considering that locoregional complications can lead to abdominal sepsis, and patients may be complicated with pre-existing underlying diseases[17]. Thus, the surgeon must choose a less aggressive procedure to save the patient's life, avoiding any complications associated with more extensive surgeries[18]. In contrast, it is known that, despite the urgency, many patients are still able to undergo surgery with all the necessary oncological radical approaches.[19] As it is a frequent situation in the natural history of colon cancer, it is essential to be concerned regarding the oncological principles also in urgent surgeries. Teixeira *et al*[19] and Enciu *et al*[20] showed that it was possible to follow the oncological principles for colon cancer surgery even in emergency cases. In both studies there was no control group and, therefore, did not allow inferential analyzes to be carried out related to elective cases. Weixler *et al*[21] studied clinical and pathological data of patients with colorectal cancer who underwent emergency surgery, and included elective patients as a control group. In their study, , 747 patients were selected over 24 years, with 663 (88.8%) elective and 84 (11.2%) urgent cases. The percentage of patients who underwent emergency surgery was lower than that reported in other studies (about 30%), and the period of capturing patients was longer than most studies in this field[12,19,20]. The study showed that there was a statistically significant difference in relation to the percentage of surgeries with 12 or more resected lymph nodes ($P = 0.016$) and the presence of compromised margins ($P = 0.014$), showing a difference in the pattern of elective and urgent surgery. Despite these differences,

Table 4 Variables referring to oncological principles for colon cancer surgery

	Elective	Urgency	*P* value
Longitudinal margin (cm)			0.144[a]
mean ± SD	6.1 ± 4.7	7.3 ± 5.6	
Median	5.0	6.5	
Q1 e Q3	3.0 e 8.0	3.1 e 10.0	
Number of resected lymph nodes			0.355[a]
mean ± SD	17.7 ± 8.7	16.6 ± 8.3	
Median	16.0	14.0	
Q1 e Q3	12.0 e 22.0	12.0 e 20.0	
≥ 12 resected lymph nodes	93 (75.6%)	51 (77.3%)	0.798[b]

[a]Mann Whitney test.
[b]Qui-square of Pearson's test.
Q1: Quartil 1; Q3: Quartil 3.

Table 5 Variables referring to oncological principles for colon cancer surgery according to tumor location

	Right			Left		
	Elective	Urgency	*P* value	Elective	Urgency	*P* value
Total	45 (69.2%)	20 (30.8%)		76 (63.3%)	44 (36.7%)	
Longitudinal margin (cm)[1]	7.0 (5.0 - 10.0)	6.5 (2.8 - 10.3)	0.270[a]	4.0 (2.0 - 5.9)	6.5 (4.0 - 9.3)	0.002[a]
Number of resected lymph nodes[1]	19.0 (13.0 - 23.0)	19.5 (13.0 - 26.3)	0.446[a]	15.0 (11.0 - 19.3)	13.0 (11.0 - 17.3)	0.223[a]
≥12 resected lymph nodes	35 (77.8%)	19 (95.0%)	0.151[b]	56 (73.7%)	31 (70.5%)	0.832[c]

[1]p25 - p75.
[a]Mann Whitney test.
[b]Exact Fisher's test.
[c]Qui-square of Pearson's test.

the study demonstrated that the overall and disease-free survivals were not affected by emergency surgery[21].

Data available in the literature, therefore, are not able to show whether the emergency surgery for colon cancer is being performed with the same technical standard as the elective ones. The strength of the present study is based on the collected data from emergency and elective patients, in the same period of over two years in a single institution, which allowed the homogenization of the group of surgeons and pathologists. Elective patients constituted the ideal control group for the analysis of oncological radicality in the emergency surgery, which is the object of this investigation. In the hospital where the study was carried out, the same service is offered for elective and emergency oncological surgeries. Thus, in both situations, surgeons are duly qualified for coloncancer surgeries, ensuring the technical standard approach. It is known that the surgeon's experience and the volume of surgery at the institution have an impact on the short- and long-term prognosis of patients with colon cancer[22]. Although some patients underwent therapeutic interventions before surgical resection, such as colonic prosthesis or derivative surgery, they represented a small number of patients and there was a difficulty in allocating them between the elective and urgency groups. Thus, they were excluded from this study population. In the two main variables of the study, longitudinal margin and the number of resected lymph nodes, there was no statistically significant difference between the two groups. Thus, it was observed that, even in an emergency, it is feasible to perform an oncologically adequate surgery. Also, the percentage of surgeries with 12 or more resected lymph nodes was also similar between the groups, showing the same technical pattern of oncological radicality in urgency and elective approaches. The percentage values observed in this study are compatible with previous literature data[19,20]. The analysis of demographic characteristics revealed a statistically significant difference related to age. It was observed that urgency patients were older than elective ones. This data can be explained by the fact that elderly patients receive fewer screening tests for colon cancer, which increases the chance of presenting with symptomatic or complicated lesions. In addition, this hypothesis confirmation is not

Table 6 Analysis of early mortality (up to 30 d) after urgent surgery for colon cancer

	Early mortality	Survivals	*P* value	OR and 95%CI
Total	10 (15.2%)	56 (84.8%)		
Sex			0.076[a]	
Male	1 (10.0%)	24 (42.9%)		
Female	9 (90.0%)	32 (57.1%)		
Age (yr)				
mean and SD	84.0 ± 8.7	69.6 ± 10.7	< 0.001[b]	95%CI: 7.2-21.6
< 80	2 (20.0%)	47 (83.9%)	< 0.001[a]	
≥ 80	8 (80.0%)	9 (16.1%)		OR: 20.89, 95%CI: 3.79-115.00
Type of urgency			0.156[a]	
Obstruction	5 (50.0%)	41 (73.2%)		
Perforation	5 (50.0%)	15 (26.8%)		
Location			0.245[a]	
Cecum/Ascendent	2 (20.0%)	16 (28.6%)		
Transverse	2 (20.0%)	3 (5.4%)		
Splenic Angle	1 (10.0%)	3 (5.4%)		
Descendent	0	9 (16.1%)		
Sigmoid	5 (50.0%)	25 (44.6%)		
Surgery			0.059[a]	
Right colectomy	2 (20.0%)	18 (32.1%)		
Transversectomy	2 (20.0%)	0		
Left colectomy	1 (10.0%)	10 (17.9%)		
Retosigmoidectomy	5 (50.0%)	22 (39.3%)		
Total colectomy	0	6 (10.7%)		
T			0.407[a]	
T2	1 (10.0%)	5 (8.9%)		
T3	7 (70.0%)	47 (83.9%)		
T4	2 (20.0%)	4 (7.4%)		
N			0.100[a]	
N0	9 (90.0%)	33 (58.9%)		
N1	0	17 (30.4%)		
N2	1 (10.0%)	6 (10.7%)		
Staging			0.118[a]	
I	1 (10.0%)	4 (7.1%)		
II	8 (80.0%)	29 (51.8%)		
III	1 (10.0%)	23 (41.1%)		
Differentiation grade			> 0.999[a]	
Well	0	3 (5.4%)		
Moderate	9 (90.0%)	43 (76.8%)		
Poor	1 (10.0%)	4 (7.1%)		
Compromised lymph nodes rate	5.0% ± 15.8	8.4% ± 17.4	0.147[c]	
Angiolymphatic invasion	2 (20.0%)	19 (33.9%)	0.483[a]	

Perineural invasion	1 (10.0%)	6 (10.7%)	> 0.999[a]
ALI + PNI	1 (10.0%)	4 (7.1%)	0.573[a]
Margin (cm)1	5.3 (1.6-8.5)	7.0 (3.9-10.0)	0.400[c]
Number of resected lymph nodes1	12.5 (11.3-17.5)	14.0 (12.0-20.3)	0.306[c]
≥ 12 resected lymph nodes	7 (70.0%)	44 (78.6%)	0.683[a]

[1]p25-p75.
[a]Exact Fisher's test.
[b]*t* test for independent samples.
[c]Mann Whitney test.
Q1: Quartil 1, Q3: Quartil 3.

within the scope of this study. As for the type of urgency, it was observed that the prevalence of perforation (28.8%) was slightly higher than that reported in most of the literature, which is around 20% [11,12], yet similar distributions have also been demonstrated[23].

The early mortality rate was found about three times higher in urgency than in elective (15.2% *vs* 4.9%) cases. Morris *et al*[24] conducted an extensive population study in England, involving 160 920 individuals undergoing surgical resection for colorectal cancer, and also found a difference in early mortality with a similar proportion (14.9% *vs* 5.8%). Other studies have reported early emergency mortality rates ranging from 8.3%–34.0%, that is, it can be said that the mortality observed in this study is within the expected range according to previous literature data[19-22]. In the present study, when analyzing the clinicopathological characteristics between emergency patients who died and those who survived, a statistically significant difference was observed in relation to age. The percentage of the elderly was highest among those who died, of whom 80% were aged 80 years or over. Different from reports in the literature[25], there was no difference in pathological characteristics between those who died and survived, revealing those factors intrinsic to the patient would be more important than tumor staging for the outcome of early mortality. There was a statistically significant difference related to the resection approach employed, and it was observed that 43.1% of the elective surgeries were performed by laparoscopy, while all urgent surgeries were opened. The laparoscopic approaches in the urgency group were less expected based on their indissociable indications for urgency procedures (70.2% of bowel obstruction, and 28.8% of bowel perforation), and in older patients, possibly with more comorbidities. Nevertheless, the results suggest that even for patients in these unfavorable scenarios, patients of the urgency group obtained similar oncological outcomes concerning margin and node status to patients who underwent elective procedures. Laparoscopy was offered in the elective group, as much as possible, based on the current evidence in the literature that supports the oncological safety of minimally invasive colorectal surgery[26-28]. Thus, all patients regardless of their surgical approaches were used, in order not to exclude a certain group of patients or surgeons based on their practice. Ghazi *et al*[25] demonstrated the presence of more advanced tumors in the emergency room, with a higher rate of more advanced staging, greater angiolymphatic and perineural invasion, and a higher rate of compromised lymph nodes. However, our study did not reveal any significant difference between the elective and urgency groups in terms of staging, degree of differentiation, angiolymphatic invasion, perineural invasion and compromised lymph node rate. It is noteworthy that the present study revealed a low rate of early stages even in the elective group, which may be one of the reasons for not having observed this difference. Regarding the location of the tumor, some studies show a worse prognosis in the right colon compared to the left colon[29]. Furthermore, the extent of lymphadenectomy for colon cancer is still an object of study in the literature[30], most of which refer to the right colon, where there is a greater difficulty in standardizing the lymphadenectomy[9]. As there was a statistically significant difference between groups in terms of the location of the tumor in this study, this could bias the results regarding the oncological principles of surgery. However, in the analysis stratified by location, it was observed that, on the right, there was no difference between groups in relation to longitudinal margins, number of lymph nodes resected, or percentage of surgeries with 12 or more lymph nodes resected. On the left, lymphadenectomy was also similar between the groups, but there was a difference concerning the longitudinal margins, being lower in the elective group. The assessment of possible causes for this difference is out of the scope of this study.

Like any retrospective study, this study has limitations regarding the impact of inferential analyzes. In terms of long-term survival analyses, the study's limitations are associated with the immeasurable biases as seen in all retrospective studies, particularly those addressing oncologic outcomes. Selection bias based on several nonobjective criteria could have contributed to some of the differences between the two study groups. Because detailed data on systemic treatment, radiotherapy, or their toxicity were not reasonably available to analyze, they were not addressed in this study. However, for the investigation of oncological approach in urgency compared to elective surgeries, this is a useful and applicable model. The allocation to the elective or emergency group takes into account the patient's

clinical presentation, but not possible *via* any type of randomization. In 30-d mortality, our sample presented a small number of deceased patients to perform an adequate multivariate analysis. Thus, only univariate analysis was presented, and confounding bias cannot be excluded. In summary, we do believe that this study provides subsidies to recommend the oncologically adequate surgery to be performed even in an emergency for most patients. However, it also suggests that a more specific assessment of patients aged over 80 years is appropriate, especially due to the observed mortality. It should be noted that this conduct should be reserved for surgeons with experience in oncology surgery for colon cancer, as well as institutions with a high volume of this disease, as occurred in this study.

CONCLUSION

It is possible to achieve the oncological radicality of colon cancer surgery in both emergency and elective procedures.

ARTICLE HIGHLIGHTS

Research background

Locoregional complications of colon cancer may occur in up to 30% of patients. Many of these patients will need a surgical resection in an urgent scenario. Because of the patient's clinical deterioration, the oncological principles of surgery may be jeopardized.

Research motivation

We intended to determine whether the same oncological principles and surgical outcomes can be achieved in both urgent and elective colon cancer surgery.

Research objectives

This study aims to compare the oncological radicality of urgent surgery for colon cancer in comparison to elective cases.

Research methods

A total of 189 consecutive patients with colon cancer who underwent surgical resection as the first therapeutic approach were selected over two years in a single institution. The institution where the study was performed has a high volume of colorectal cancer patients (over 100 cases per year) and there are experienced surgeons in both elective and urgent situations. Patients were assigned to two groups: elective (123) and urgency (66). Clinicopathological variables were analyzed and compared retrospectively, including the longitudinal margin of resection and the number of harvested lymph nodes, between the two groups.

Research results

There was no significant difference between the two groups concerning the longitudinal margins of resection and the number of resected lymph nodes. A higher percentage of patients aged 80 and over was observed in the urgency group (25.8% *vs*. 13.0% in elective group, $P = 0.028$). Early mortality was higher in the urgency group (15.2% *vs* 4.9%), as expected according to previous studies.

Research conclusions

The oncological principles of colon cancer surgery can be adopted in urgency as well as in elective cases.

Research perspectives

Further studies are necessary to elucidate which patients should undergo classical oncological resection in urgency, especially in patients aged 80 and over, due to the higher early mortality in urgent approaches for this population. Intermediate interventions in urgent cases, such as derivative surgery or colonic prosthesis, require further studies as an alternative approach in high-risk patients.

FOOTNOTES

Author contributions: Yoshida BY, Farah JFM, and Goldenberg A contributed to the study conception, data preparation, data interpretation, and writing; Araujo RLC contributed to the data preparation, data interpretation, and critical writing of the paper.

Institutional review board statement: This study was performed with the permission of the institutional review board

according to the institutional policy for protected health information.

Conflict-of-interest statement: The authors certify that there is no conflict of interest related to the manuscript.

Data sharing statement: Regarding the manuscript entitled: "Is it possible to achieve the same oncological approach in urgent surgery for colon cancer?", the original anonymous dataset is available on request from the corresponding author.

STROBE statement: The authors have read the STROBE Statement – checklist of items, and the manuscript was prepared and revised according to the STROBE Statement – checklist of items.

Country/Territory of origin: Brazil

ORCID number: Bruno Yuki Yoshida 0000-0003-4742-804X; Raphael L C Araujo 0000-0002-7834-5944; José Francisco M Farah 0000-0003-2391-633X; Alberto Goldenberg 0000-0003-1218-4890.

Corresponding Author's Membership in Professional Societies: International Hepato-Pancreato-Biliary Association; The Society of the Alimentary Tract; American Hepato-Pancreato-Biliary Association.

S-Editor: Xing YX
L-Editor: Ma JY-MedE A
P-Editor: Xing YX

REFERENCES

1 **Sung H**, Ferlay J, Siegel RL, Laversanne M, Soerjomataram I, Jemal A, Bray F. Global Cancer Statistics 2020: GLOBOCAN Estimates of Incidence and Mortality Worldwide for 36 Cancers in 185 Countries. *CA Cancer J Clin* 2021; **71**: 209-249 [PMID: 33538338 DOI: 10.3322/caac.21660]
2 **Vogel JD**, Eskicioglu C, Weiser MR, Feingold DL, Steele SR. The American Society of Colon and Rectal Surgeons Clinical Practice Guidelines for the Treatment of Colon Cancer. *Dis Colon Rectum* 2017; **60**: 999-1017 [PMID: 28891842 DOI: 10.1097/DCR.0000000000000926]
3 **Benson AB**, Venook AP, Al-Hawary MM, Arain MA, Chen YJ, Ciombor KK, Cohen S, Cooper HS, Deming D, Farkas L, Garrido-Laguna I, Grem JL, Gunn A, Hecht JR, Hoffe S, Hubbard J, Hunt S, Johung KL, Kirilcuk N, Krishnamurthi S, Messersmith WA, Meyerhardt J, Miller ED, Mulcahy MF, Nurkin S, Overman MJ, Parikh A, Patel H, Pedersen K, Saltz L, Schneider C, Shibata D, Skibber JM, Sofocleous CT, Stoffel EM, Stotsky-Himelfarb E, Willett CG, Gregory KM, Gurski LA. Colon Cancer, Version 2.2021, NCCN Clinical Practice Guidelines in Oncology. *J Natl Compr Canc Netw* 2021; **19**: 329-359 [PMID: 33724754 DOI: 10.6004/jnccn.2021.0012]
4 **Hashiguchi Y**, Hase K, Ueno H, Mochizuki H, Shinto E, Yamamoto J. Optimal margins and lymphadenectomy in colonic cancer surgery. *Br J Surg* 2011; **98**: 1171-1178 [PMID: 21560120 DOI: 10.1002/bjs.7518]
5 **Rørvig S**, Schlesinger N, Mårtensson NL, Engel S, Engel U, Holck S. Is the longitudinal margin of carcinoma-bearing colon resections a neglected parameter? *Clin Colorectal Cancer* 2014; **13**: 68-72 [PMID: 24503112 DOI: 10.1016/j.clcc.2013.11.007]
6 **Eveno C**, Lefevre JH, Svrcek M, Bennis M, Chafai N, Tiret E, Parc Y. Oncologic results after multivisceral resection of clinical T4 tumors. *Surgery* 2014; **156**: 669-675 [PMID: 24953279 DOI: 10.1016/j.surg.2014.03.040]
7 **Chang GJ**, Rodriguez-Bigas MA, Skibber JM, Moyer VA. Lymph node evaluation and survival after curative resection of colon cancer: systematic review. *J Natl Cancer Inst* 2007; **99**: 433-441 [PMID: 17374833 DOI: 10.1093/jnci/djk092]
8 **Le Voyer TE**, Sigurdson ER, Hanlon AL, Mayer RJ, Macdonald JS, Catalano PJ, Haller DG. Colon cancer survival is associated with increasing number of lymph nodes analyzed: a secondary survey of intergroup trial INT-0089. *J Clin Oncol* 2003; **21**: 2912-2919 [PMID: 12885809 DOI: 10.1200/JCO.2003.05.062]
9 **Bertelsen CA**, Neuenschwander AU, Jansen JE, Tenma JR, Wilhelmsen M, Kirkegaard-Klitbo A, Iversen ER, Bols B, Ingeholm P, Rasmussen LA, Jepsen LV, Born PW, Kristensen B, Kleif J. 5-year outcome after complete mesocolic excision for right-sided colon cancer: a population-based cohort study. *Lancet Oncol* 2019; **20**: 1556-1565 [PMID: 31526695 DOI: 10.1016/S1470-2045(19)30485-1]
10 **Wong SKC**, Jalaludin BB, Morgan MJ, Berthelsen AS, Morgan A, Gatenby AH, Fulham SB. Tumor pathology and long-term survival in emergency colorectal cancer. *Dis Colon Rectum* 2008; **51**: 223-230 [PMID: 18097722 DOI: 10.1007/s10350-007-9094-2]
11 **Pisano M**, Zorcolo L, Merli C, Cimbanassi S, Poiasina E, Ceresoli M, Agresta F, Allievi N, Bellanova G, Coccolini F, Coy C, Fugazzola P, Martinez CA, Montori G, Paolillo C, Penachim TJ, Pereira B, Reis T, Restivo A, Rezende-Neto J, Sartelli M, Valentino M, Abu-Zidan FM, Ashkenazi I, Bala M, Chiara O, De' Angelis N, Deidda S, De Simone B, Di Saverio S, Finotti E, Kenji I, Moore E, Wexner S, Biffl W, Coimbra R, Guttadauro A, Leppäniemi A, Maier R, Magnone S, Mefire

AC, Peitzmann A, Sakakushev B, Sugrue M, Viale P, Weber D, Kashuk J, Fraga GP, Kluger I, Catena F, Ansaloni L. 2017 WSES guidelines on colon and rectal cancer emergencies: obstruction and perforation. *World J Emerg Surg* 2018; **13**: 36 [PMID: 30123315 DOI: 10.1186/s13017-018-0192-3]

12 **Alvarez JA**, Baldonedo RF, Bear IG, Truán N, Pire G, Alvarez P. Presentation, treatment, and multivariate analysis of risk factors for obstructive and perforative colorectal carcinoma. *Am J Surg* 2005; **190**: 376-382 [PMID: 16105522 DOI: 10.1016/j.amjsurg.2005.01.045]

13 **Koh DC**, Luchtefeld MA, Kim DG, Knox MF, Fedeson BC, Vanerp JS, Mustert BR. Efficacy of transarterial embolization as definitive treatment in lower gastrointestinal bleeding. *Colorectal Dis* 2009; **11**: 53-59 [PMID: 18462224 DOI: 10.1111/j.1463-1318.2008.01536.x]

14 **Green BT**, Rockey DC, Portwood G, Tarnasky PR, Guarisco S, Branch MS, Leung J, Jowell P. Urgent colonoscopy for evaluation and management of acute lower gastrointestinal hemorrhage: a randomized controlled trial. *Am J Gastroenterol* 2005; **100**: 2395-2402 [PMID: 16279891 DOI: 10.1111/j.1572-0241.2005.00306.x]

15 **Daniels M**, Merkel S, Agaimy A, Hohenberger W. Treatment of perforated colon carcinomas-outcomes of radical surgery. *Int J Colorectal Dis* 2015; **30**: 1505-1513 [PMID: 26248792 DOI: 10.1007/s00384-015-2336-1]

16 **Webster PJ**, Aldoori J, Burke DA. Optimal management of malignant left-sided large bowel obstruction: do international guidelines agree? *World J Emerg Surg* 2019; **14**: 23 [PMID: 31139245 DOI: 10.1186/s13017-019-0242-5]

17 **Zielinski MD**, Merchea A, Heller SF, You YN. Emergency management of perforated colon cancers: how aggressive should we be? *J Gastrointest Surg* 2011; **15**: 2232-2238 [PMID: 21913040 DOI: 10.1007/s11605-011-1674-8]

18 **Person B**, Dorfman T, Bahouth H, Osman A, Assalia A, Kluger Y. Abbreviated emergency laparotomy in the non-trauma setting. *World J Emerg Surg* 2009; **4**: 41 [PMID: 19925649 DOI: 10.1186/1749-7922-4-41]

19 **Teixeira F**, Akaishi EH, Ushinohama AZ, Dutra TC, Netto SD, Utiyama EM, Bernini CO, Rasslan S. Can we respect the principles of oncologic resection in an emergency surgery to treat colon cancer? *World J Emerg Surg* 2015; **10**: 5 [PMID: 26191078 DOI: 10.1186/1749-7922-10-5]

20 **Enciu O**, Calu V, Angelescu M, Nădrăgea MA, Miron A. Emergency Surgery and Oncologic Resection for Complicated Colon Cancer: What Can We Expect? *Chirurgia (Bucur)* 2019; **114**: 200-206 [PMID: 31060652 DOI: 10.21614/chirurgia.114.2.200]

21 **Weixler B**, Warschkow R, Ramser M, Droeser R, von Holzen U, Oertli D, Kettelhack C. Urgent surgery after emergency presentation for colorectal cancer has no impact on overall and disease-free survival: a propensity score analysis. *BMC Cancer* 2016; **16**: 208 [PMID: 26968526 DOI: 10.1186/s12885-016-2239-8]

22 **Archampong D**, Borowski D, Wille-Jørgensen P, Iversen LH. Workload and surgeon´s specialty for outcome after colorectal cancer surgery. *Cochrane Database Syst Rev* 2012; **14**: CD005391 [PMID: 22419309 DOI: 10.1002/14651858.CD005391.pub3]

23 **Chen TM**, Huang YT, Wang GC. Outcome of colon cancer initially presenting as colon perforation and obstruction. *World J Surg Oncol* 2017; **15**: 164 [PMID: 28841901 DOI: 10.1186/s12957-017-1228-y]

24 **Morris EJA**, Taylor EF, Thomas JD, Quirke P, Finan PJ, Coleman MP, Rachet B, Forman D. Thirty-day postoperative mortality after colorectal cancer surgery in England. *Gut* 2011; **60**: 806-813 [PMID: 21486939 DOI: 10.1136/gut.2010.232181]

25 **Ghazi S**, Berg E, Lindblom A, Lindforss U; Low-Risk Colorectal Cancer Study Group. Clinicopathological analysis of colorectal cancer: a comparison between emergency and elective surgical cases. *World J Surg Oncol* 2013; **11**: 133 [PMID: 23758762 DOI: 10.1186/1477-7819-11-133]

26 **Clinical Outcomes of Surgical Therapy Study Group**; Nelson H, Sargent DJ, Wieand HS, Fleshman J, Anvari M, Stryker SJ, Beart RW Jr, Hellinger M, Flanagan R Jr, Peters W, Ota D. A comparison of laparoscopically assisted and open colectomy for colon cancer. *N Engl J Med* 2004; **350**: 2050-2059 [PMID: 15141043 DOI: 10.1056/NEJMoa032651]

27 **Fleshman J**, Sargent DJ, Green E, Anvari M, Stryker SJ, Beart RW Jr, Hellinger M, Flanagan R Jr, Peters W, Nelson H; Clinical Outcomes of Surgical Therapy Study Group. Laparoscopic colectomy for cancer is not inferior to open surgery based on 5-year data from the COST Study Group trial. *Ann Surg* 2007; **246**: 655-662 [PMID: 17893502 DOI: 10.1097/SLA.0b013e318155a762]

28 **Bonjer HJ**, Hop WC, Nelson H, Sargent DJ, Lacy AM, Castells A, Guillou PJ, Thorpe H, Brown J, Delgado S, Kuhrij E, Haglind E, Påhlman L; Transatlantic Laparoscopically Assisted vs Open Colectomy Trials Study Group. Laparoscopically assisted vs open colectomy for colon cancer: a meta-analysis. *Arch Surg* 2007; **142**: 298-303 [PMID: 17372057 DOI: 10.1001/archsurg.142.3.298]

29 **Ghazi S**, Lindforss U, Lindberg G, Berg E, Lindblom A, Papadogiannakis N; Low-Risk Colorectal Cancer Study Group. Analysis of colorectal cancer morphology in relation to sex, age, location, and family history. *J Gastroenterol* 2012; **47**: 619-634 [PMID: 22249212 DOI: 10.1007/s00535-011-0520-9]

30 **Bertelsen CA**, Neuenschwander AU, Jansen JE, Wilhelmsen M, Kirkegaard-Klitbo A, Tenma JR, Bols B, Ingeholm P, Rasmussen LA, Jepsen LV, Iversen ER, Kristensen B, Gögenur I; Danish Colorectal Cancer Group. Disease-free survival after complete mesocolic excision compared with conventional colon cancer surgery: a retrospective, population-based study. *Lancet Oncol* 2015; **16**: 161-168 [PMID: 25555421 DOI: 10.1016/S1470-2045(14)71168-4]

World Journal of Clinical Oncology

Submit a Manuscript: https://www.f6publishing.com

World J Clin Oncol 2022 November 24; 13(11): 907-917

DOI: 10.5306/wjco.v13.i11.907

ISSN 2218-4333 (online)

ORIGINAL ARTICLE

Retrospective Cohort Study

Epidemiologic risk factors for patients admitted with chronic pancreatitis and pancreatic ductal adenocarcinoma in the United States

Daniel Lew, Fatima Kamal, Khiem Phan, Karamvir Randhawa, Sam Cornwell, Ayrton I Bangolo, Simcha Weissman, Stephen J Pandol

Specialty type: Oncology

Provenance and peer review: Unsolicited article; Externally peer reviewed.

Peer-review model: Single blind

Peer-review report's scientific quality classification

Grade A (Excellent): 0
Grade B (Very good): 0
Grade C (Good): C, C
Grade D (Fair): D, D
Grade E (Poor): 0

P-Reviewer: Kalayarasan R, India; Tan CL, China; Zhao CF, China

Received: July 28, 2022
Peer-review started: July 28, 2022
First decision: September 5, 2022
Revised: September 8, 2022
Accepted: November 6, 2022
Article in press: November 6, 2022
Published online: November 24, 2022

Daniel Lew, Stephen J Pandol, Department of Gastroenterology, Cedars-Sinai Medical Center, Los Angeles, CA 90048, United States

Fatima Kamal, Khiem Phan, Karamvir Randhawa, Sam Cornwell, Ayrton I Bangolo, Simcha Weissman, Department of Internal Medicine, Hackensack Meridian Health/Palisades Medical Center, North Bergen, NJ 07047, United States

Corresponding author: Ayrton I Bangolo, MBBS, MD, Doctor, Department of Internal Medicine, Hackensack Meridian Health/Palisades Medical Center, 7600 River Road, North Bergen, NJ 07047, United States. ayrtonbangolo@yahoo.com

Abstract

BACKGROUND

Epidemiological studies of chronic pancreatitis (CP) and its association with pancreatic ductal adenocarcinoma (PDAC) are limited. Understanding demographic and ethno-racial factors may help identify patients at the highest risk for CP and PDAC.

AIM

To evaluate the ethno-racial risk factors for CP and its association with PDAC. The secondary aim was to evaluate hospitalization outcomes in patients admitted with CP and PDAC.

METHODS

This retrospective cohort study used the 2016 and 2017 National Inpatient Sample databases. Patients included in the study had ICD-10 codes for CP and PDAC. The ethnic, socioeconomic, and racial backgrounds of patients with CP and PDAC were analyzed.

RESULTS

Hospital admissions for CP was 29 *per* 100000, and 2890 (0.78%) had PDAC. Blacks [adjusted odds ratio (aOR) 1.13], men (aOR 1.35), age 40 to 59 (aOR 2.60), and being overweight (aOR 1.34) were significantly associated with CP (all with $P < 0.01$). In patients with CP, Whites (aOR 1.23), higher income, older age (aOR 1.05), and being overweight (aOR 2.40) were all significantly associated with

PDAC (all with $P < 0.01$). Men (aOR 1.81) and Asians (aOR 15.19) had significantly increased mortality ($P < 0.05$). Hispanics had significantly increased hospital length of stay (aOR 5.24) ($P < 0.05$).

CONCLUSION

Based on this large, nationwide analysis, black men between 40-59 years old and overweight are at significantly increased risk for admission with CP. White men older than 40 years old and overweight with higher income were found to have significant associations with CP and PDAC. This discrepancy may reflect underlying differences in healthcare access and utilization among different socioeconomic and ethno-racial groups.

Key Words: Chronic pancreatitis; Pancreatic cancer; Ethno-racial; Risk factors; Hospitalization outcomes; Adult

Core Tip: What is known chronic pancreatitis (CP) and pancreatic ductal adenocarcinoma (PDAC) rates are rising. Pancreatitis admissions costed 133 million dollars, and accounted for the 3rd leading cause of hospital admissions. There is lack of data identifying those at highest risk for admissions with CP and PDAC. What we found Black men between 40-59 years old and overweight are at significantly increased risk for admission with CP. White men with higher income were found to have significantly increased risk for admissions with CP and PDAC. Asians/Pacific Islanders had the highest risk for mortality from CP and PDAC.

Citation: Lew D, Kamal F, Phan K, Randhawa K, Cornwell S, Bangolo AI, Weissman S, Pandol SJ. Epidemiologic risk factors for patients admitted with chronic pancreatitis and pancreatic ductal adenocarcinoma in the United States. *World J Clin Oncol* 2022; 13(11): 907-917
URL: https://www.wjgnet.com/2218-4333/full/v13/i11/907.htm
DOI: https://dx.doi.org/10.5306/wjco.v13.i11.907

INTRODUCTION

The overall incidence of chronic pancreatitis (CP) is increasing worldwide, and accounts for significant healthcare utilization and costs. In the United States, CP hospital admissions costed 133 million dollars, and pancreatitis accounted for the 3rd leading cause of hospital admissions among gastrointestinal diseases in 2015[1]. The most common reason for CP-related admission is abdominal pain, but other complications can develop including pancreatic ductal adenocarcinoma (PDAC). PDAC is currently the fourth leading cause of cancer-related deaths in the United States and is projected to become the second leading cause by 2030[2]. CP is the major risk factor for developing PDAC[3-5].

There have been few epidemiological studies available for CP[6-14], and fewer studies for CP and PDAC[3,15-18]. Ethnic and socioeconomic factors including insurance status, median income, type and hospital factors are lacking.

Herein, we utilize hospital discharges from a large nationwide database to examine the demographic, ethno-racial, socioeconomic, and hospital factors associated with hospitalizations for CP and its association with PDAC. We also sought to determine the association between ethnicity/race on hospitalization outcomes in patients admitted with CP and PDAC.

MATERIALS AND METHODS

Data source

This retrospective cohort study utilized the 2016 and 2017 National Inpatient Sample (NIS) databases. The NIS is a database of inpatient stays derived from billing data based upon discharge abstracts. As such, it contains de-identified clinical and nonclinical elements at both the patient and hospital level. The NIS 2016 database contains data from 7.1 million hospital stays in 4575 hospitals in 47 states, while the 2017 database contains data from 7.1 million hospital stays in 4584 hospitals in 48 states. Using the combination of the NIS 2016 and 2017 databases allowed for inclusion of a greater total number of cases/patients.

Study population

Patients included in the study carried a primary diagnosis of CP based on ICD-10 codes (K86.0, K86.1, K90.3). The demographics and ethnic/racial profiles of those with CP were compared to the general population and examined for any associations. Subsequently, all patients with CP were then evaluated for PDAC based on ICD-10 diagnostic codes C25.0-C25.9. The demographic and ethnic/racial profiles of those with only CP were compared to the ethnic/racial profiles of those who also had PDAC and were examined for any associations. Finally, we analyzed the associations between ethnicity/race and hospitalization outcomes in patients admitted for PDAC.

Inclusion and exclusion criteria are shown in Figure 1. Institutional Review Board approval was not required for this study as it was performed using de-identified and nationally available data.

Census data

The estimated national population during 2016-2017 was obtained from the United States Census Bureau (www.census.gov).

Study variables

Patient demographics included age, gender, race, median household income, primary expected payer, hospital bed size, hospital teaching status, hospital region, and urban location. Burden of comorbidities was assessed using the Charlson comorbidity index.

Study outcomes

The primary outcomes were the ethno-racial factors associated with CP hospital admissions as compared to the general population and the ethno-racial factors associated between CP and PDAC. Secondary outcomes were the associations between ethnicity/race and hospitalization outcomes (mortality, hospital length of stay (LOS), expenses), in patients admitted with CP and PDAC.

Statistical analysis

Statistical analyses were performed using STATA, version 16.0 (StataCorp., College Station, Texas, United States). Weighting of patient-level observations was implemented. Univariate analysis was initially performed to calculate unadjusted odds ratio and determine confounders significantly associated with the outcomes. Multivariate regression analysis was used to adjust for potential confounders. Multivariate regression model was then built by including all confounders that were found to be significant by univariate analysis, to calculate an adjusted odds ratio (aOR). Logistic regression was used for binary outcomes and linear regression was used for continuous outcomes. Proportions were compared using Fisher's exact test, and continuous variables were compared using Student's *t*-test. All *P*-values were two-sided, with 0.05 as the threshold for statistical significance. Calculated rates of hospital admissions *per* 100000 population was performed using the United States Census Bureau national population estimates.

RESULTS

CP cohort

In our sample (NIS 2016-2017) of 14.2 million admissions, 371275 (2.6%) adult patients were found to have a diagnosis of CP. The mean age was 57.72 years, and most patients were white (64.82%) men (55.76%). Medicare was the primary payer insurance (40.2%). The majority of admissions were in teaching hospitals (69.54%). Additional patient and hospital characteristics are presented in Table 1. Overall hospitalization rate for 2016 and 2017 was 29 *per* 100000 (95%CI: 57.9-58.2).

On multivariate regressions analysis, men (aOR 1.35), Blacks (aOR 1.13), age between 40 and 59 years old (aOR 2.60), and body mass index (BMI) between 25 and 29.9 (aOR 1.34) were at higher risk of developing CP as compared to the general population ($P < 0.01$). On the contrary, women (aOR 0.65), Hispanics (aOR 0.63) or Asian/Pacific Islanders (aOR 0.50) and those above 80 years old (aOR 0.46) had a significantly decreased likelihood of having CP as compared to the general population (all with $P < 0.01$) (Table 2).

PDAC and CP cohort

Of the 371275 adult patients admitted with a primary diagnosis of CP, 2890 (0.78%) also had PDAC. Patients with PDAC and CP were significantly older ($P < 0.05$), White ($P < 0.01$), had Medicare as the primary insurance ($P < 0.01$), were from a higher income population ($P < 0.01$), were admitted to teaching hospitals ($P < 0.01$), and had a higher burden of comorbidities ($P < 0.01$) (Table 3). Overall hospitalization rate for 2016 and 2017 was 0.45 *per* 100000 (95%CI: 0.44-0.47).

On multivariate regressions analysis, older age (greater than 40 years old) (aOR 1.05), and BMI between 25 and 29.9 (aOR 2.40) had a higher risk of developing PDAC in patients with CP (all with $P < 0.01$). On the contrary, women (aOR 0.77), Blacks (aOR 0.77) and Hispanics (aOR 0.66) were associated

Table 1 Demographics, ethno-racial, socioeconomic, and hospital factors for patients hospitalized with chronic pancreatitis

Variable	*n* = 371275
Race	
White	64.82%
Black	22.35%
Hispanic	8.4%
Asian or Pacific Islander	1.31%
Native American	0.87%
Other	2.25%
Gender	
Women	44.24%
Men	55.76%
Age	
Mean age, years	52.72
Age 18-39 yr	21.63%
Age 40-59 yr	49.84%
Age 60-79 yr	24.26%
Age > 80 yr	4.28%
Insurance provider	
Medicare	40.2%
Medicaid	30.28%
Private	22.53%
Uninsured	6.99%
Charlson comorbidity index	
0	24.09%
1	25.97%
2	17.37%
3 or more	32.58%
Median income in patient zip code	
$1–$38999	36.17%
$39000–$47999	26.11%
$48000–$62999	21.78%
$63000	15.94%
Hospital region	
Northwest	17.54%
Midwest	24.63%
South	40.23%
West	17.6%
Hospital location	
Rural	8.29%
Urban	91.71%
Hospital size	
Small	19%

Medium	28.34%
Large	52.65%
Type of hospital	
Teaching	69.54%
Non-teaching	30.46%

Table 2 Multivariate regressions analysis for demographic, socioeconomic, and hospital factors associated with hospitalizations secondary to chronic pancreatitis

Classification		*P* value
Age	aOR 0.98	< 0.01
Age 18-39 yr	Reference	
Age 40-59 yr	aOR 2.60	< 0.01
Age 60-79 yr	aOR 0.96	0.37
Age > 80 yr	aOR 0.46	< 0.01
BMI: 18-24.9	Reference	
BMI: 25-29.9	aOR 1.34	< 0.01
BMI: 30-39.9	aOR 0.62	< 0.01
Women	aOR 0.65	< 0.01
Whites	Reference	
Blacks	1.13	< 0.01
Hispanics	0.63	< 0.01
Asians/Pacific Islanders	0.50	< 0.01
Native Americans	1.05	0.31
Other	0.67	< 0.01

aOR: Adjusted odds ratio; BMI: Body mass index.

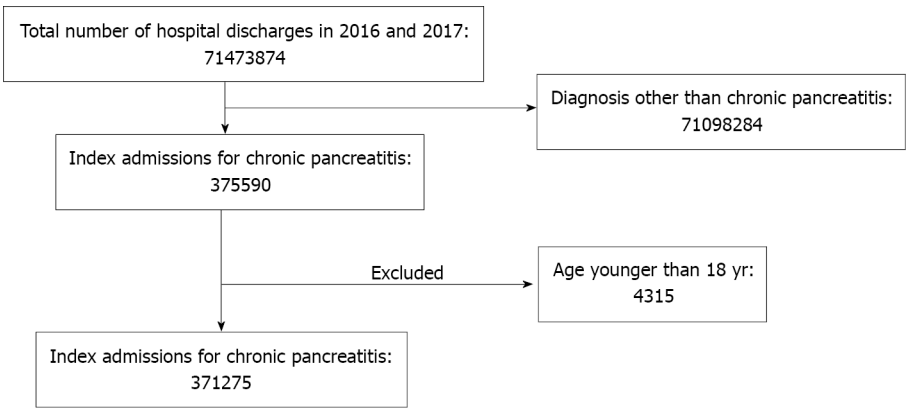

DOI: 10.5306/wjco.v13.i11.907

Figure 1 Flowchart for patient inclusion.

with a significantly decreased likelihood of PDAC in patients with CP (all with $P < 0.01$) (Table 4).

Hospitalization outcomes in PDAC and CP

Men (aOR 1.81) and Asians/Pacific Islanders (aOR 15.19) had the highest mortality among patients with PDAC and CP (all with $P < 0.05$). Hispanics had the highest hospital LOS (aOR 5.24), charges (adjusted

Table 3 Demographics, ethno-racial, socioeconomic, and hospital factors for patients hospitalized with chronic pancreatitis and pancreatic ductal adenocarcinoma

Variable	CP without PDAC (*n* = 368385)	CP with PDAC (*n* = 2890)	*P* value
Race			< 0.01
Whites	64.75%	74.22%	
Blacks	22.4%	16.76%	
Hispanics	8.43%	4.97%	
Asians or Pacific Islanders	1.31%	1.29%	
Native Americans	0.87%	0.37%	
Other	2.25%	2.39%	
Gender			
Women	44.27%	40.31%	0.07
Men	55.73%	59.69%	
Age			
Mean age, years	52.61	66.32	< 0.05
Age 18-39 yr	21.78%	19%	
Age 40-59 yr	50.02%	26.99%	
Age 60-79 yr	23.97%	60.03%	
Age > 80 yr	4.23%	11.07%	
Insurance provider			< 0.01
Medicare	40.04%	60.64%	
Medicaid	30.44%	10.73%	
Private	22.5%	26.48%	
Uninsured	7.03%	2.15%	
Charlson comorbidity index			< 0.01
0	24.28%	0	
1	26.17%	0	
2	17.35%	19.38%	
3 or more	32.2%	80.62%	
Median income in patient zip code			< 0.01
$1–$38999	36.24%	28.22%	
$39000–$47999	26.1%	26.81%	
$48000–$62999	21.78%	21.34%	
$63000	15.88%	23.63%	
Hospital region			0.68
Northwest	17.53%	19.38%	
Midwest	24.64%	23.53%	
South	40.25%	38.24%	
West	17.59%	18.86%	
Hospital location			< 0.01
Rural	8.34%	1.56%	
Urban	91.66%	98.44%	
Hospital size			< 0.01

Small	19.08%	8.65%	
Medium	28.43%	16.78%	
Large	52.48%	74.57%	
Type of hospital			
Teaching	69.41%	86.16%	< 0.01
Non-teaching	30.59%	13.84%	

CP: Chronic pancreatitis; PDAC: Pancreatic ductal adenocarcinoma.

Table 4 Multivariate regressions analysis for demographic, socioeconomic, and hospital factors associated with hospitalizations in patients with chronic pancreatitis and pancreatic ductal adenocarcinoma

Classification		*P* value
Age	aOR 1.05	< 0.01
Age 18-39 yr	Reference	
Age 40-59 yr	aOR 6.79	< 0.01
Age 60-79 yr	aOR 24.17	< 0.01
Age > 80 yr	aOR 21.02	< 0.01
BMI: 18-24.9	Reference	
BMI: 25-29.9	aOR 2.40	< 0.01
Female	aOR 0.77	< 0.01
White	Reference	
Black	aOR 0.77	< 0.05
Hispanic	aOR 0.66	< 0.05
Asian or Pacific Islander	aOR 0.69	0.36
Native American	aOR 0.68	0.60
Other	aOR 0.97	0.94

aOR: Adjusted odds ratio; BMI: Body mass index.

coefficient $87285), and costs (adjusted coefficient $15212) amongst patients with PDAC and CP (all with $P < 0.05$). Gender was not found to be a significant contributing factor for hospital expenses.

DISCUSSION

In this nationwide cohort study, we found black men who were overweight had a significantly increased likelihood of being admitted with CP. These findings are consistent with previous studies, most likely due to alcoholic CP, though our current study is not able to definitively elucidate the cause of CP[14]. Our hospitalization rates for CP is much higher compared to the study by Yang *et al*[13], which also used the NIS database from 1988-2004 and found an incident rate of 7.0-8.1 *per* 100000 population[13]. Similarly, population-based studies from Olmsted County, MN, United States found an incident rate of 4.05 *per* 100000 population from 1997-2006 and Allegheny County, PA, United States found incident rate of 7.75 *per* 100000 population[11,12]. Our findings of an increased incidence rate may reflect recent trends in increased hospitalizations with pancreatitis being the 3rd most common reason for hospitalization in 2015 among gastrointestinal diseases[1]. This is likely due in part to increased use of cross-sectional imaging for the evaluation of abdominal pain in adults[19]. Another possible explanation is that our findings may be more of a reflection of prevalence rate rather than incidence rate. In 2014, Lévy *et al*[20] summarized 11 studies and found a prevalence rate ranging up to 41.76 *per* 100000 population[20]. Additionally, patients with CP are reported to have good overall survival despite complications with reported 10-year survival rate of 70%[17]. Taken together, our increased hospitalization rate is likely due to increased diagnosis of CP and longevity of patients with CP.

Other novel demographic findings from our study include the findings that patients with CP-related admissions had predominantly Medicare insurance and were from lower median income families. Additionally, we found patients were more likely to be admitted to teaching hospitals in large urban centers, predominantly in the Southern part of the United States. A potential reason for this finding may correlate with the South having the highest prevalence of obesity at 30% and higher. Furthermore, non-Hispanic Blacks were found to have the highest prevalence of obesity[21]. Our hope is that future studies can use our findings to further evaluate the exact association of CP-related admissions in this high-risk population in an effort to improve patient outcomes and decrease healthcare expenditures. While our study is not able to elucidate the reason for admission, it is presumed that abdominal pain is most likely the cause given extensive findings from previous studies[14,22]. Given that it is well established that abdominal pain is chronic, persistent, and can lead to significant impairment in quality of life including high rates of unemployment as well as recurrent hospitalizations and healthcare expenditure, future research in this area is needed[23,24]. The findings from our study can be used in future studies to target those patients at higher risk for CP-related hospitalizations to improve patient outcomes and limit healthcare expenditures.

A potential complication of CP is the development of PDAC. In our study, we found that 0.78% (approximately 0.39%/year) of patients with CP also carried a diagnosis of PDAC and that these patients were predominantly White men who were overweight and of older age. Our findings are similar to the 2014 Danish nationwide study by Bang *et al*[3], which found a 4.26% rate over a 15-year period (approximately 0.28%/year) of PDAC in CP patients occurring predominantly in older men[3]. While there is moderate amount of literature for the ethno-racial factors for CP and PDAC separately, there is limited data regarding ethno-racial factors specifically in patients with CP and PDAC. Bracci *et al*[25] in 2009 found in a multicenter study that majority of patients with PDAC were White men who were older, however, they did not provide demographic data specifically for PDAC in CP patients[25]. In a meta-analysis published in 2010 containing 22 studies, Raimondi *et al*[15] found a 13 fold increased risk for PDAC in CP patients but did not evaluate the ethno-racial factors[15]. A more recent meta-analysis published in 2017 by Kirkegård *et al*[4] also found an increased risk for PDAC in CP patients but again did not evaluate the ethno-racial factors[4]. To our knowledge, our study is the first to evaluate ethno-racial factors in patients with CP and PDAC. A major caveat to our findings is that we cannot definitively evaluate PDAC development as a progression of CP. Thus, there could be cases where PDAC occurred first and CP developed afterwards. However, current literature suggests the overwhelming likelihood of this occurring is extremely low and may actually be misclassifications given the similarities between the two diseases[4]. An interesting finding from our study was that we found that Blacks had a higher risk for having CP, but this did not translate into having a higher association with CP and PDAC. A potential explanation could be due to discrepancies in healthcare utilization given that our data showed patients with CP and PDAC were significantly more likely to have higher median incomes, lower rates of being uninsured, and high rates of being admitted to large urban teaching hospitals when compared to CP patients alone. Racial disparities have been shown for PDAC in blacks. Khawja *et al*[26] conducted an evidence-based review of PDAC in blacks and found significantly worse outcomes compared to whites. A 2019 review also showed blacks had worse outcomes, but also lower referral rates to see oncology or a surgeon and lower rates of surgical resection and adjuvant chemoradiation[26,27]. Potential reasons for this discrepancy include suboptimal patient communication, greater mistrust of the medical field, and unmeasured differences in morbidity/functional status. Future studies should further evaluate the accuracy of this finding and to evaluate the exact cause of this discrepancy if one exists. Another interesting finding from our study is that we found Asians/Pacific Islanders had an aOR 15.19. This is in contrast to recent data from the American Cancer Society, which showed Blacks had the highest risk of mortality at 15.0/100000 compared to 8.1/100000 with Asians/Pacific Islanders[2]. A possible explanation is that our study evaluated patients with PDAC and CP rather than all PDAC patients, though it is beyond the scope of this study as to why Asians/Pacific Islanders had the highest mortality. Finally, we found that Hispanics had the highest LOS and hospital expenses. Future studies should further evaluate these findings in an effort to identify reasons for increased mortality among Asians/Pacific Islanders and increased LOS and hospital expenses among Hispanics, respectively, to improve patient outcomes and decreased healthcare expenditures.

Limitations of this study include it being limited solely to inpatient encounters. Therefore, our study may not represent a complete epidemiological study given its lack of outpatient encounters. As mentioned previously, there are limitations associated with using the NIS database. We are not able to identify individual patients and review each patients' charts, thus we are not able to identify the reason for CP-related admissions though current literature suggest most likely related to abdominal pain. Additionally, we are not able to determine if patients with CP progressed to PDAC or if PDAC occurred before CP, but again current literature suggests majority of patients develop PDAC after CP. Incidence of PDAC in CP is related to etiology of CP. Risk is significantly higher in hereditary pancreatitis than with alcohol related pancreatitis. As the etiology is not captured in the database it might introduce bias. Duration of CP could not be found, as longer history associated with increased risk. Findings may be applicable only to the population studied and cannot be generalized.

CONCLUSION

In conclusion, based on this large, nationwide analysis, there is an increased trend in hospitalization rates for CP, predominantly among black men between 40-59 years old who were overweight. In patients with CP, white men older than 40 years old who were overweight with higher income had a higher risk of PDAC. The observed disparity may be a consequence of the difference in healthcare access among different ethnic groups.

ARTICLE HIGHLIGHTS

Research background

Chronic pancreatitis (CP) and pancreatic ductal adenocarcinoma (PDAC) rates are rising. Pancreatitis admissions costed 133 million dollars, and accounted for the 3rd leading cause of hospital admissions. There is lack of data identifying those at highest risk for admissions with CP and PDAC.

Research motivation

The main motivation of this study was to establish racial risk factors and their associations with PDAC.

Research objectives

This study had the objective to examine the demographic, ethno-racial, socioeconomic, and hospital factors associated with hospitalizations for CP and its association with PDAC.

Research methods

This retrospective study used the 2016 and 2017 National Inpatient Sample databases. ICD-10 codes compatible with CP and PDAC were used in the study. The ethnic, socioeconomic, and racial backgrounds of patients with CP and PDAC were analyzed.

Research results

Hospital admissions for CP was 29 *per* 100000, and 2890 (0.78%) had PDAC. Blacks [adjusted odds ratio (aOR) 1.13], men (aOR 1.35), age 40 to 59 (aOR 2.60), and being overweight (aOR 1.34) were significantly associated with CP (all with $P < 0.01$). In patients with CP, Whites (aOR 1.23), higher income, older age (aOR 1.05), and being overweight (aOR 2.40) were all significantly associated with PDAC (all with $P < 0.01$). Men (aOR 1.81) and Asians (aOR 15.19) had significantly increased mortality ($P < 0.05$). Hispanics had significantly increased hospital length of stay (aOR 5.24) ($P < 0.05$).

Research conclusions

There is an increased trend in hospitalization rates for CP, predominantly among black men between 40-59 years old who were overweight. Wealthy white men above the age of 40 had a higher PDAC diagnosis.

Research perspectives

Black men between 40-59 years old and overweight are at significantly increased risk for admission with CP. White men with higher income were found to have significantly increased risk for admissions with CP and PDAC. Asians/Pacific Islanders had the highest risk for mortality from CP and PDAC.

FOOTNOTES

Author contributions: Lew D, Kamal F, Phan K, Randhawa K, Cornwell S, and Weissman S assisted with data acquisition, analyses, and manuscript preparation; Lew D drafted and critically revised the manuscript; Lew D, Weissman S, Bangolo AI, and Pandol SJ provided input regarding methodology; Pandol SJ critically revised the manuscript and provided direct supervision and guidance; Weissman S is the article guarantor; All authors agree to the final version of this manuscript.

Institutional review board statement: This retrospective cohort study utilized the 2016 and 2017 National Inpatient Sample (NIS) databases. The NIS is a database of inpatient stays derived from billing data based upon discharge abstracts. As such, it contains de-identified clinical and nonclinical elements at both the patient and hospital level. Making the need for an Institutional review board approval dispensable.

Informed consent statement: The National Inpatient Database was a public-use dataset, of which the informed consent was waived.

Conflict-of-interest statement: All the authors report no relevant conflicts of interest for this article.

Data sharing statement: This retrospective cohort study utilized the 2016 and 2017 National Inpatient Sample (NIS) databases. The NIS is a database of inpatient stays derived from billing data based upon discharge abstracts. As such, it contains de-identified clinical and nonclinical elements at both the patient and hospital level. The dataset is publicly available.

STROBE statement: The authors have read the STROBE Statement—checklist of items, and the manuscript was prepared and revised according to the STROBE Statement—checklist of items.

Country/Territory of origin: United States

ORCID number: Daniel Lew 0000-0001-8843-6447; Ayrton I Bangolo 0000-0002-2133-2480; Simcha Weissman 0000-0002-0796-6217.

S-Editor: Fan JR
L-Editor: A
P-Editor: Fan JR

REFERENCES

1 **Peery AF**, Crockett SD, Murphy CC, Lund JL, Dellon ES, Williams JL, Jensen ET, Shaheen NJ, Barritt AS, Lieber SR, Kochar B, Barnes EL, Fan YC, Pate V, Galanko J, Baron TH, Sandler RS. Burden and Cost of Gastrointestinal, Liver, and Pancreatic Diseases in the United States: Update 2018. *Gastroenterology* 2019; **156**: 254-272.e11 [PMID: 30315778 DOI: 10.1053/j.gastro.2018.08.063]
2 **Siegel RL**, Miller KD, Jemal A. Cancer statistics, 2019. *CA Cancer J Clin* 2019; **69**: 7-34 [PMID: 30620402 DOI: 10.3322/caac.21551]
3 **Bang UC**, Benfield T, Hyldstrup L, Bendtsen F, Beck Jensen JE. Mortality, cancer, and comorbidities associated with chronic pancreatitis: a Danish nationwide matched-cohort study. *Gastroenterology* 2014; **146**: 989-994 [PMID: 24389306 DOI: 10.1053/j.gastro.2013.12.033]
4 **Kirkegård J**, Mortensen FV, Cronin-Fenton D. Chronic Pancreatitis and Pancreatic Cancer Risk: A Systematic Review and Meta-analysis. *Am J Gastroenterol* 2017; **112**: 1366-1372 [PMID: 28762376 DOI: 10.1038/ajg.2017.218]
5 **Munigala S**, Kanwal F, Xian H, Agarwal B. New diagnosis of chronic pancreatitis: risk of missing an underlying pancreatic cancer. *Am J Gastroenterol* 2014; **109**: 1824-1830 [PMID: 25286967 DOI: 10.1038/ajg.2014.318]
6 **Díte P**, Starý K, Novotný I, Precechtelová M, Dolina J, Lata J, Zboril V. Incidence of chronic pancreatitis in the Czech Republic. *Eur J Gastroenterol Hepatol* 2001; **13**: 749-750 [PMID: 11434607 DOI: 10.1097/00042737-200106000-00024]
7 **Lankisch PG**, Assmus C, Maisonneuve P, Lowenfels AB. Epidemiology of pancreatic diseases in Lüneburg County. A study in a defined german population. *Pancreatology* 2002; **2**: 469-477 [PMID: 12378115 DOI: 10.1159/000064713]
8 **Lévy P**, Barthet M, Mollard BR, Amouretti M, Marion-Audibert AM, Dyard F. Estimation of the prevalence and incidence of chronic pancreatitis and its complications. *Gastroenterol Clin Biol* 2006; **30**: 838-844 [PMID: 16885867 DOI: 10.1016/s0399-8320(06)73330-9]
9 **Lin Y**, Tamakoshi A, Matsuno S, Takeda K, Hayakawa T, Kitagawa M, Naruse S, Kawamura T, Wakai K, Aoki R, Kojima M, Ohno Y. Nationwide epidemiological survey of chronic pancreatitis in Japan. *J Gastroenterol* 2000; **35**: 136-141 [PMID: 10680669 DOI: 10.1007/s005350050026]
10 **O'Sullivan JN**, Nobrega FT, Morlock CG, Brown AL Jr, Bartholomew LG. Acute and chronic pancreatitis in Rochester, Minnesota, 1940 to 1969. *Gastroenterology* 1972; **62**: 373-379 [PMID: 5011528]
11 **Yadav D**, Muddana V, O'Connell M. Hospitalizations for chronic pancreatitis in Allegheny County, Pennsylvania, USA. *Pancreatology* 2011; **11**: 546-552 [PMID: 22205468 DOI: 10.1159/000331498]
12 **Yadav D**, Timmons L, Benson JT, Dierkhising RA, Chari ST. Incidence, prevalence, and survival of chronic pancreatitis: a population-based study. *Am J Gastroenterol* 2011; **106**: 2192-2199 [PMID: 21946280 DOI: 10.1038/ajg.2011.328]
13 **Yang AL**, Vadhavkar S, Singh G, Omary MB. Epidemiology of alcohol-related liver and pancreatic disease in the United States. *Arch Intern Med* 2008; **168**: 649-656 [PMID: 18362258 DOI: 10.1001/archinte.168.6.649]
14 **Wilcox CM**, Sandhu BS, Singh V, Gelrud A, Abberbock JN, Sherman S, Cote GA, Al-Kaade S, Anderson MA, Gardner TB, Lewis MD, Forsmark CE, Guda NM, Romagnuolo J, Baillie J, Amann ST, Muniraj T, Tang G, Conwell DL, Banks PA, Brand RE, Slivka A, Whitcomb D, Yadav D. Racial Differences in the Clinical Profile, Causes, and Outcome of Chronic Pancreatitis. *Am J Gastroenterol* 2016; **111**: 1488-1496 [PMID: 27527745 DOI: 10.1038/ajg.2016.316]
15 **Raimondi S**, Lowenfels AB, Morselli-Labate AM, Maisonneuve P, Pezzilli R. Pancreatic cancer in chronic pancreatitis; aetiology, incidence, and early detection. *Best Pract Res Clin Gastroenterol* 2010; **24**: 349-358 [PMID: 20510834 DOI: 10.1016/j.bpg.2010.02.007]
16 **Shelton CA**, Umapathy C, Stello K, Yadav D, Whitcomb DC. Hereditary Pancreatitis in the United States: Survival and Rates of Pancreatic Cancer. *Am J Gastroenterol* 2018; **113**: 1376 [PMID: 30018304 DOI: 10.1038/s41395-018-0194-5]

17 **Lowenfels AB**, Maisonneuve P, Cavallini G, Ammann RW, Lankisch PG, Andersen JR, Dimagno EP, Andrén-Sandberg A, Domellöf L. Pancreatitis and the risk of pancreatic cancer. International Pancreatitis Study Group. *N Engl J Med* 1993; **328**: 1433-1437 [PMID: 8479461 DOI: 10.1056/NEJM199305203282001]

18 **Malka D**, Hammel P, Maire F, Rufat P, Madeira I, Pessione F, Lévy P, Ruszniewski P. Risk of pancreatic adenocarcinoma in chronic pancreatitis. *Gut* 2002; **51**: 849-852 [PMID: 12427788 DOI: 10.1136/gut.51.6.849]

19 **Wang RC**, Kornblith AE, Grupp-Phelan J, Smith-Bindman R, Kao LS, Fahimi J. Trends in Use of Diagnostic Imaging for Abdominal Pain in U.S. Emergency Departments. *AJR Am J Roentgenol* 2021; **216**: 200-208 [PMID: 33211574 DOI: 10.2214/AJR.19.22667]

20 **Lévy P**, Domínguez-Muñoz E, Imrie C, Löhr M, Maisonneuve P. Epidemiology of chronic pancreatitis: burden of the disease and consequences. *United European Gastroenterol J* 2014; **2**: 345-354 [PMID: 25360312 DOI: 10.1177/2050640614548208]

21 **CDC**. National Center for Health Statistics-Adult Obesity Prevalence Maps. [cited 10 July 2022]. Available from: https://www.cdc.gov/obesity/data/prevalence-maps.html

22 **Wilcox CM**, Yadav D, Ye T, Gardner TB, Gelrud A, Sandhu BS, Lewis MD, Al-Kaade S, Cote GA, Forsmark CE, Guda NM, Conwell DL, Banks PA, Muniraj T, Romagnuolo J, Brand RE, Slivka A, Sherman S, Wisniewski SR, Whitcomb DC, Anderson MA. Chronic pancreatitis pain pattern and severity are independent of abdominal imaging findings. *Clin Gastroenterol Hepatol* 2015; **13**: 552-60; quiz e28 [PMID: 25424572 DOI: 10.1016/j.cgh.2014.10.015]

23 **Mullady DK**, Yadav D, Amann ST, O'Connell MR, Barmada MM, Elta GH, Scheiman JM, Wamsteker EJ, Chey WD, Korneffel ML, Weinman BM, Slivka A, Sherman S, Hawes RH, Brand RE, Burton FR, Lewis MD, Gardner TB, Gelrud A, DiSario J, Baillie J, Banks PA, Whitcomb DC, Anderson MA; NAPS2 Consortium. Type of pain, pain-associated complications, quality of life, disability and resource utilisation in chronic pancreatitis: a prospective cohort study. *Gut* 2011; **60**: 77-84 [PMID: 21148579 DOI: 10.1136/gut.2010.213835]

24 **Pezzilli R**, Morselli-Labate AM, Frulloni L, Cavestro GM, Ferri B, Comparato G, Gullo L, Corinaldesi R. The quality of life in patients with chronic pancreatitis evaluated using the SF-12 questionnaire: a comparative study with the SF-36 questionnaire. *Dig Liver Dis* 2006; **38**: 109-115 [PMID: 16243011 DOI: 10.1016/j.dld.2005.09.015]

25 **Bracci PM**, Wang F, Hassan MM, Gupta S, Li D, Holly EA. Pancreatitis and pancreatic cancer in two large pooled case-control studies. *Cancer Causes Control* 2009; **20**: 1723-1731 [PMID: 19760029 DOI: 10.1007/s10552-009-9424-x]

26 **Khawja SN**, Mohammed S, Silberfein EJ, Musher BL, Fisher WE, Van Buren G 2nd. Pancreatic cancer disparities in African Americans. *Pancreas* 2015; **44**: 522-527 [PMID: 25872128 DOI: 10.1097/MPA.0000000000000323]

27 **Noel M**, Fiscella K. Disparities in Pancreatic Cancer Treatment and Outcomes. *Health Equity* 2019; **3**: 532-540 [PMID: 31663065 DOI: 10.1089/heq.2019.0057]

World Journal of Clinical Oncology

Submit a Manuscript: https://www.f6publishing.com

World J Clin Oncol 2022 November 24; 13(11): 918-928

DOI: 10.5306/wjco.v13.i11.918

ISSN 2218-4333 (online)

ORIGINAL ARTICLE

Retrospective Cohort Study

Efficacy of texture analysis of pre-operative magnetic resonance imaging in predicting microvascular invasion in hepatocellular carcinoma

Jordan Zheng Ting Sim, Terrence Chi Hong Hui, Tong Kuan Chuah, Hsien Min Low, Cher Heng Tan, Vishal G Shelat

Specialty type: Radiology, nuclear medicine and medical imaging

Provenance and peer review: Invited article; Externally peer reviewed.

Peer-review model: Single blind

Peer-review report's scientific quality classification

Grade A (Excellent): 0
Grade B (Very good): 0
Grade C (Good): C, C
Grade D (Fair): 0
Grade E (Poor): 0

P-Reviewer: Inmutto N, Thailand; Zimmitti G, Italy

Received: September 19, 2022
Peer-review started: September 19, 2022
First decision: October 13, 2022
Revised: October 13, 2022
Accepted: November 4, 2022
Article in press: November 4, 2022
Published online: November 24, 2022

Jordan Zheng Ting Sim, Terrence Chi Hong Hui, Hsien Min Low, Cher Heng Tan, Department of Diagnostic Radiology, Tan Tock Seng Hospital, Singapore 308433, Singapore

Tong Kuan Chuah, School of Engineering, Ngee Ann Polytechnic, Singapore 599489, Singapore

Cher Heng Tan, Vishal G Shelat, Lee Kong Chian School of Medicine, Nanyang Technological University, Singapore 308232, Singapore

Vishal G Shelat, Department of General Surgery, Tan Tock Seng Hospital, Singapore 308433, Singapore

Corresponding author: Jordan Zheng Ting Sim, MBBS, Doctor, Department of Diagnostic Radiology, Tan Tock Seng Hospital, 11 Jalan Tan Tock Seng, Tan Tock Seng Hospital, Singapore 308433, Singapore. jordansim92@gmail.com

Abstract

BACKGROUND

Presence of microvascular invasion (MVI) indicates poorer prognosis post-curative resection of hepatocellular carcinoma (HCC), with an increased chance of tumour recurrence. By present standards, MVI can only be diagnosed post-operatively on histopathology. Texture analysis potentially allows identification of patients who are considered 'high risk' through analysis of pre-operative magnetic resonance imaging (MRI) studies. This will allow for better patient selection, improved individualised therapy (such as extended surgical margins or adjuvant therapy) and pre-operative prognostication.

AIM

This study aims to evaluate the accuracy of texture analysis on pre-operative MRI in predicting MVI in HCC.

METHODS

Retrospective review of patients with new cases of HCC who underwent hepatectomy between 2007 and 2015 was performed. Exclusion criteria: No pre-operative MRI, significant movement artefacts, loss-to-follow-up, ruptured HCCs, previous hepatectomy and adjuvant therapy. Fifty patients were divided into MVI

(n = 15) and non-MVI (n = 35) groups based on tumour histology. Selected images of the tumour on post-contrast-enhanced T1-weighted MRI were analysed. Both qualitative (performed by radiologists) and quantitative data (performed by software) were obtained. Radiomics texture parameters were extracted based on the largest cross-sectional area of each tumor and analysed using MaZda software. Five separate methods were performed. Methods 1, 2 and 3 exclusively made use of features derived from arterial, portovenous and equilibrium phases respectively. Methods 4 and 5 made use of the comparatively significant features to attain optimal performance.

RESULTS

Method 5 achieved the highest accuracy of 87.8% with sensitivity of 73% and specificity of 94%.

CONCLUSION

Texture analysis of tumours on pre-operative MRI can predict presence of MVI in HCC with accuracies of up to 87.8% and can potentially impact clinical management.

Key Words: Carcinoma; Hepatocellular; Magnetic resonance imaging; Liver neoplasms; Retrospective studies; Margins of excision

Core Tip: This study demonstrates the utility of texture analysis on pre-operative magnetic resonance imaging to potentially impact clinical management in patients with surgically resectable hepatocellular carcinoma.

Citation: Sim JZT, Hui TCH, Chuah TK, Low HM, Tan CH, Shelat VG. Efficacy of texture analysis of pre-operative magnetic resonance imaging in predicting microvascular invasion in hepatocellular carcinoma. *World J Clin Oncol* 2022; 13(11): 918-928

URL: https://www.wjgnet.com/2218-4333/full/v13/i11/918.htm

DOI: https://dx.doi.org/10.5306/wjco.v13.i11.918

INTRODUCTION

Macrovascular invasion and microvascular invasion (MVI) are independent prognostic factors of hepatocellular carcinoma (HCC) recurrence after curative partial hepatectomy or liver transplantation[1-3]. Previous studies have shown MVI to shorten disease-free survival and overall survival post-liver transplantation and liver resection[4]. While presence of macrovascular invasion can often be determined definitively on pre-operative cross-sectional imaging, microvascular invasion in HCC is typically only diagnosed post-operatively on histopathology. Moreover, the lack of consensus definition and grading of MVI, coupled with inter/intra-observer variability, has resulted in great heterogeneity in evaluation of this histopathological feature[5]. Previous studies have shown that the incidence of MVI ranges between 15% and 57.1%[4]. Pre-operative diagnosis of microvascular invasion to identify patients who are considered 'high risk' will allow for better patient selection, improved individualised therapy (such as extended surgical margins or adjuvant therapy) and pre-operative prognostication.

Texture analysis (TA) is a branch of computer vision that analyses and objectifies imaging characteristics that may be imperceptible to the human eye. It can be applied to any cross-sectional imaging and has been proven to reflect underlying heterogeneity. This technique may provide quantitative data and insight into tumor biology and thus has the potential to be used to diagnose and prognosticate disease [6-9]. Several groups have attempted to identify MVI pre-operatively using clinical data and imaging scoring systems albeit with variable and sometimes conflicting results[10-12], limiting its translation into clinical practice. Moreover, the detection of MVI by using pre-operative biopsy has proven to be unreliable as it did not correlate well with post-operative pathology[13]. Recent studies have sought to use TA to predict MVI on MRI and have identified certain imaging and textural features (such as tumour entropy) that may be associated with bad tumour behaviour[14,15]. While TA continues to grow as an emerging technology, before it can be considered for widespread clinical implementation, we sought to validate and replicate those findings. In this study, we aim to evaluate the accuracy of texture analysis on pre-operative contrast-enhanced MRI to predict microvascular invasion in HCC.

MATERIALS AND METHODS

Study cohort

Institutional review board was obtained and the requirement to obtain written consent was waived. All patients who underwent hepatectomy between January 1, 2007 and December 31, 2015 were considered for study inclusion. Clinical and pathologic parameters were retrospectively reviewed on electronic medical records. Inclusion criteria included histologically proven HCC with pre-operative MRI (done with 1.5T), tumour size ≥ 1 cm, treatment-naïve HCC. Exclusion criteria included loss to follow-up, collision tumours, ruptured HCCs, previous hepatectomy and interval adjuvant therapy, such as transarterial chemoembolization or radiofrequency ablation. For texture analysis evaluation, additional imaging-specific exclusion criteria included 3 T MRI, outdated MRI protocols, and images degraded by motion artefacts.

A total of 129 hepatectomies were performed on 129 HCC patients within the study period. 79 patients were excluded from the study for the following reasons: absence of pre-operative MRI (n = 37), interval adjuvant therapy or prior hepatectomy (n = 18), loss to follow-up (n = 12), 3 T MRI (n = 6), ruptured HCC (n = 2), old MRI protocol (n = 2), collision tumour (n = 1), movement artefact (n = 1). A representative flowchart is shown in Figure 1.

The primary outcome measure was the presence of MVI based on histopathological findings. Clinical factors that were potentially associated with MVI were analysed: age, gender, aetiology, hepatitis B surface antigen (HBsAg), serum alpha-fetoprotein, albumin, bilirubin, alanine amino-transferase, aspartate amino-transferase, alkaline phosphatase, ɣ-glutamyltranspeptidase (GGT) and Child-Pugh score.

MRI technique

Magnetic resonance (MR) imaging studies were performed using 1.5 T scanners (Signa HDxt, GE Medical Systems, Milwaukee, WI, United States; Ingenia, Philips, Amsterdam, The Netherlands). The liver imaging protocol included the following sequences: Breath-hold gradient-echo T1-weighted [4.2 ms repetition time (TR)/2 ms echo time (TE), 40 cm field of view, 12° flip angle, 5 mm section thickness], free-breathing spin-echo T2-weighted (10000 ms TR/82.8 ms TE, 40 cm field of view, 90° flip angle, 6 mm section thickness), diffusion-weighted (6000 ms TR / 66.1 ms TE, 40 cm field of view, 90° flip angle, 5 mm section thickness, b = 1000 s/mm^2) and T1-weighted contrast-enhanced sequences performed in the arterial (20-second scanning delay), portal venous (70-second scanning delay), and equilibrium phases (180-second scanning delay). Of note, one of the cases had no useable equilibrium phase image. Gadobenate dimeglumine (n = 36; MultiHance, BRACCO Altana Pharma, Constance, Switzerland), gadoterate meglumine (n = 8; Dotarem, Guerbet Roissy, France) and gadoxetic acid (n = 6; Primovist, Bayer Schering Pharma AG, Berlin, Germany) were used as contrast material. All MR examinations utilised 10 cc of the respective contrast agents.

Qualitative analysis

The pre-operative MR images were first independently evaluated on the picture archiving communication system by two radiologists with 13 and five years of experience (Tan CH and Low HM). The reviewers were aware that the patients had HCC but were blinded to the diagnosis of MVI by pathologic examination. The images were evaluated for tumour size (mm), tumour multiplicity, T1 pre-contrast signal intensity, post-contrast enhancement pattern in all phases, T2 hyperintensity, restricted diffusion, visibility of vessels in post-contrast sequences, peri-tumoral features, presence of hypodense halo, definition of border between tumour and liver, tumour margin smoothness and LI-RADS score (see Table 1). The reviewers reviewed the images in consensus and assessed the imaging features subjectively, with a binary "Yes/No" output.

Image segmentation and texture analysis

T1W post-contrast sequences in the arterial, portal venous (PV) and equilibrium phases were exported as DICOM (digital imaging and communications in medicine) files. A polygonal region of interest (ROI) was manually drawn on the largest cross-sectional area of the tumour. The segmented images were checked visually by a researcher and vetted by a third radiologist. Discordant findings were verified by one of the two senior radiologists (Tan CH). A typical segmentation result is shown in Figure 2.

Texture analysis was performed using MaZda software (MaZda, Technical University of Lodz)[16]. The MaZda software automatically extracts and analyses 290 texture parameters including area, histogram-based, gradient based, co-occurrence matrix based, autoregressive model, run-length matrix-based and wavelet analysis.

Five distinct methods were evaluated in an attempt to optimise the accuracy of the binary classification (presence or absence of MVI). Support vector machine classifiers developed for each study were tested using either bootstrapping method (1000 runs of five randomly selected test samples at a time, thus obtaining the average accuracy) or leave-one-out method.

Table 1 Tumor features on magnetic resonance imaging

	Total	MVI group	Non-MVI group	*P* value
Tumors, *n* (%)	50 (100)	15 (30)	35 (70)	
Size (mm), mean (SD)		56.4 (34.6)	41.3 (29.1)	0.107
Multiplicity, *n* (%)				0.087
Single	43 (86)	15 (100)	28 (80)	
Multifocal	7 (14)	0	7 (20)	
T1 (unenhanced), *n* (%)				0.346
Hypointense	46 (92)	13 (87)	33 (94)	
Isointense	2 (4)	1 (7)	1 (3)	
Hyperintense	2 (4)	1 (7)	1 (3)	
T1 (arterial phase), *n* (%)				0.663
Hypointense	6 (12)	1 (7)	5 (14)	
Isointense	6 (12)	1 (7)	5 (14)	
Hyperintense	38 (76)	13 (87)	25 (71)	
T1 (portal venous phase), *n* (%)				0.231
Hypointense	42 (84)	14 (93)	28 (80)	
Isointense	6 (12)	0 (0)	6 (17)	
Hyperintense	2 (4)	1 (7)	1 (3)	
T1 (equilibrium phase), *n* (%)				0.654
Hypointense	45 (90)	14 (93)	31 (89)	
Isointense	4 (8)	1 (7)	3 (9)	
Hyperintense	0	0 (0)	0 (0)	
T1 (HPB phase), *n* (%)				0.664
Hypointense	33 (66)	9 (60)	24 (69)	
Isointense	1 (2)	0	1 (3)	
Not performed	16 (32)	6 (40)	10 (28)	
T2 hyperintensity, *n* (%)				0.451
Present	42 (84)	12 (80)	30 (86)	
Absent	8 (16)	3 (20)	5 (14)	
Restricted diffusion, *n* (%)				0.745
Present	44 (88)	13 (87)	31 (89)	
Absent	5 (10)	2 (13)	3 (9)	
Not performed	1 (2)	0 (0)	1 (3)	
Visible vessels (arterial phase), *n* (%)				0.001
Present	11 (22)	8 (53)	3 (9)	
Absent	39 (78)	7 (47)	32 (91)	
Visible vessels (portal venous phase), *n* (%)				0.043
Present	8 (16)	5 (33)	3 (9)	
Absent	42 (84)	10 (67)	32 (91)	
Peritumoral enhancement, *n* (%)				0.248
Present	15 (30)	6 (40)	9 (26)	
Absent	35 (70)	9 (60)	26 (74)	

Hypodense halo, *n* (%)				0.524
Present	5 (10)	1 (7)	4 (11)	
Absent	45 (90)	14 (93)	31 (89)	
Border between tumour and liver, *n* (%)				0.428
Sharp	34 (68)	11 (73)	23 (66)	
Ill-defined	16 (32)	4 (27)	12 (34)	
Tumor margins, *n* (%)				0.477
Smooth	28 (56)	9 (60)	19 (54)	
Non-smooth	22 (44)	6 (40)	16 (46)	
LI-RADS, *n* (%)				0.05
LR-4	10 (20)	0 (0)	10 (29)	
LR-5	27 (54)	10 (67)	17 (49)	
LR-M	13 (26)	5 (33)	8 (22)	

MVI: Microvascular invasion.

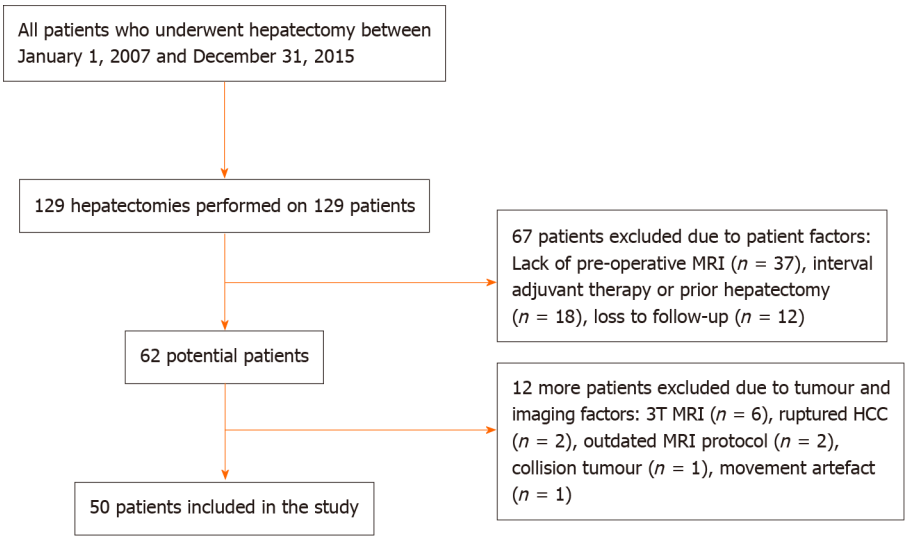

DOI: 10.5306/wjco.v13.i11.918

Figure 1 Flow chart of patient selection based on the inclusion and exclusion criteria. HCC: Hepatocellular carcinoma; MRI: Magnetic resonance imaging.

Methods 1, 2 and 3 exclusively used features from the arterial, PV, and equilibrium phase respectively. To optimise performance, 14 of the most significant features from methods 1-3 were manually selected and put through mutual information feature selection method for methods 4 and 5. Method 4 employed three features selected purely through mutual information, while study 5 incorporated recursive pruning and subsequent manual feature selection after mutual information. Method 5 eventually employed three features and was then tested with leave-one-out classification method to attain optimal performance.

Statistical analysis

Statistical analysis was performed using SPSS 20.0. The Mann-Whitney U-test or independent *t*-test were used for continuous variables, while the Fisher exact test was used for categorical variables.

RESULTS

Fifty patients (43 males, 7 females, and mean age 67 years, range 53-81 years) were included in the present study. All were new cases of histology-proven HCC in treatment-naive patients. The aetiologies

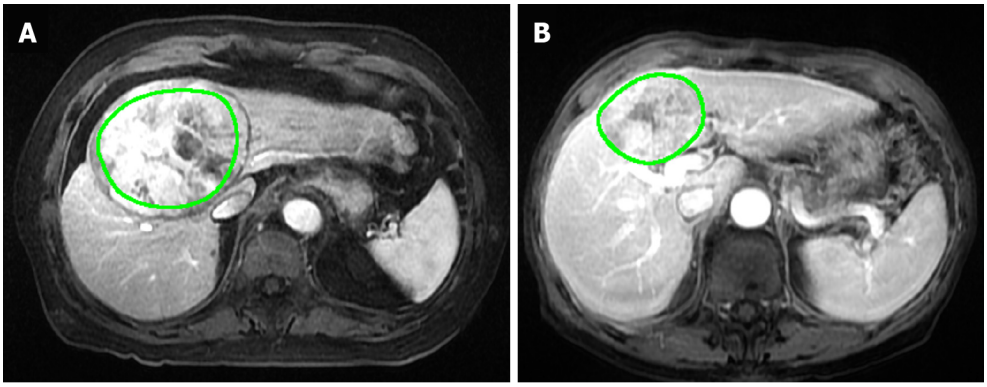

DOI: 10.5306/wjco.v13.i11.918

Figure 2 Segmentation of two different biopsy-proven hepatocellular carcinoma across the largest cross-sectional area of the tumor in the T1-arterial phase and T1-portovenous phase. A: T1-arterial phase; B: T1-portovenous phase.

include hepatitis B (n = 28%, 56%), hepatitis C (n = 3%, 6%), hepatitis B and C (n = 1%, 2%), *de novo* (n = 9%, 18%), cryptogenic (n = 5%, 10%), alcoholic cirrhosis (n = 3%, 6%), and non-alcoholic steatotic hepatitis (n = 1%, 2%).

MVI was present in 30% (n = 15) of the resected specimens. Univariate analysis between MVI group and non-MVI group is shown in Table 2. Univariate analysis was also performed for MR imaging features collected for qualitative analysis (Table 1). We found a statistically significant difference of the pre-operative serum ɣ-glutamyltranspeptidase (GGT; $P \leq 0.01$) level between the two groups. We also noted a statistically significant difference in the rates of the following imaging features between the two groups: Visible intra-tumoral vessels in arterial phase (P = 0.01) and in PV phase (P = 0.043).

Of the five methods, Method 5 achieved the highest accuracy of 87.8%. Method 5 also achieved a sensitivity of 73.3%, specificity of 94.1% with positive and negative predictive value of 85% and 89% respectively. Methods 1 through 4 achieved accuracies between 70.0% to 85.5%. The details and results of the 5 methods are summarized in Table 3. The three TA parameters in method 5 were Arterial S(4,0) Correlat, Arterial S(4,-4) InvDfMom and PV (3,0)SumAverg. Incidentally, these textural features are found in relatively close proximity along the horizontal and diagonal position of the image (at a distance of 3 and 4 pixels), which could imply particular areas of the tumours contribute more to accuracy than others.

DISCUSSION

The results of our study show that texture analysis of pre-operative MRI can predict the presence of MVI pre-operatively with an accuracy of up to 87.8%. Although the exact relationship between the selected texture parameters and the image appearance is not easily explainable, this study shows that the grey value variation in the horizontal and the diagonal direction show usable differences between the two groups. The study by Ahn *et al*[14] also showed that application of TA increased diagnostic performance [area under the curve (AUC) improved from 0.7 to 0.83]. Unlike ours, the same study also found sphericity and discrete compactness to be the texture analysis variables that are significantly associated with MVI[14]. Wilson *et al*[15] achieved an AUC of 0.83 with their final texture analysis model and found tumour entropy to be significantly associated with MVI. Other studies have also identified entropy on post-contrast CT images to be an independent predictor of disease-free survival and overall survival[17,18].

TA is a post-processing technique for quantification of tissue heterogeneity. The method is based on analysis of the grey value distribution and relationship of pixels within any given ROI. The potential applications of texture analysis and radiomics in general are expanding, especially in solid tumour imaging[19-22]. In its present state, this technique is able to achieve good results without the need to obtain additional sequences or interventions. TA can also potentially be incorporated into future predictive models that incorporate clinicoradiological risk factors and radiomic features; early work has shown some promise in predicting MVI[21].

Qualitative MRI features of HCC may be useful in predicting MVI. Kim *et al*[23] found irregular circumferential peritumoral enhancement to be the only significant variable in MVI-present HCC, while Chandarana *et al*[24] demonstrated tumor multifocality takes precedence over all other imaging features. The presence of the aforementioned imaging features leads to high specificity for diagnosis of MVI, but with low sensitivity[25,26]. Furthermore, interobserver agreement tends to be only fair to moderate[27].

Table 2 Patient demographics

Variable	Total	MVI		*P* value
		MVI group = 15	Non-MVI group = 35	
Age (yr), mean (SD)	67.0 (7.0)	68.3 (8.8)	66.4 (6.1)	0.491
Gender				0.348
Male, *n* (%)	43 (86)	12 (80)	31 (89)	
Female, *n* (%)	7 (14)	3 (20)	4 (11)	
Aetiology				0.377
Alcohol, *n* (%)	3 (6)	0 (0)	3 (8)	
Hepatitis B, *n* (%)	28 (56)	7 (46)	21 (60)	
Hepatitis C, *n* (%)	3 (6)	1 (7)	2 (6)	
Hepatitis B and C, *n* (%)	1 (2)	1 (7)	0 (0)	
NAon-alcoholic steatohepatitis, *n* (%)	1 (2)	1 (7)	0 (0)	
Cryptogenic cirrhosis, *n* (%)	5 (10)	2 (13)	3 (8)	
De novo, *n* (%)	9 (18)	3 (20)	6 (17)	
HbSAg				0.676
Positive, *n* (%)	27 (54)	7 (46)	20 (57)	
Negative, *n* (%)	22 (44)	8 (54)	14 (40)	
Unknown, *n* (%)	1 (2)	0 (0)	1 (3)	
Pre-operative serology				
Alpha-fetoprotein (UG/L), mean (SD)	248.0 (893.2)	777.7 (1571.4)	32.9 (105.6)	0.065
Albumin (g/L), mean (SD)	36.3 (5.8)	35.4 (5.6)	36.7 (5.9)	0.374
Bilirubin (μmol/L), mean (SD)	19.5 (12.1)	18.6 (7.1)	19.9 (13.8)	0.797

MVI: Microvascular invasion.

Table 3 Features and results of methods 1 to 5

	Method 1	Method 2	Method 3	Method 4	Method 5
Feature set used	Arterial phase	Portovenous phase	Equilibrium phase	Selected features from all phases	Selected features put through recursive pruning
Classification accuracy (%)	81.4	84.7	70	85.5	87.8

Most recently, Hong *et al*[28] conducted a systematic review and meta-analysis on MRI features for predicting MVI and found 7 MRI features to be significantly associated with MVI: Larger tumour size (> 5 cm), rim arterial enhancement, arterial peritumoral enhancement, peritumoral hypointensity on hepatobiliary phase, non-smooth tumour margin, multifocality and hypointensity on T1W imaging.

Our study evaluated most of the aforementioned features, but found that only intra-tumoral vessel visibility on arterial and PV phase was significantly associated with MVI. Interestingly, vessel visibility in post-contrast sequences has not been extensively studied and may be a subject of future study. Further analysis of these two statistically significant features show sensitivity of 53.3% and 33.3% for vessel visibility on arterial and PV phase respectively. Both features demonstrate specificity of 91.4%. Using these as a measure of the qualitative analysis by radiologists, our model outperforms both features, achieving sensitivity of 73.3% and specificity of 94.1%.

The imaging features described in other papers, such as peritumoral arterial phase hyperenhancement, were not found to be significant for diagnosis of MVI; this may be due to small sample size in our current study. Of note, none of the parameters selected for Methods 4 and 5 included features from the equilibrium phase. This is consistent with the observations in current literature, where arterial phase and hepatobiliary phase findings predominate[28].

Current diagnosis of MVI relies on histopathologic examination that is done post-operatively. The presence of MVI indicates more aggressive tumour behaviour and poorer prognosis[1,2]. Furthermore, our study cohort comprises a high proportion of Hepatitis B aetiology (n = 29%; 58%) which has been shown to be associated with development of vascular invasion[29]. The ability to diagnose pre-operative MVI can significantly alter the clinical management for patients in several ways. Firstly, the informed consent process could include equivalent non-invasive options (*e.g.* Chemoembolisation and/or ablation techniques) which have been shown to produce similar oncologic outcomes, but with the added benefit of lower morbidity[30]. Secondly, the presence of MVI may prompt the use of more aggressive treatment options such as extended surgical margins or additional bridging treatment while awaiting liver transplantation[31-34]. Additionally, adjuvant therapy after surgical resection have also been shown to improve survival in patients with MVI[35,36]. Lastly, these patients could be followed up more closely given the susceptibility for early recurrence.

This study is not without its limitations. Firstly, this is a retrospective single-institution study with a small sample size, limiting our ability to compare it against the diagnostic performance of visual analysis by radiologists. The low sample size may also account for the relative paucity of statistically significant differences among the two study groups in terms of both clinical and radiological characteristics. Despite this, TA was able to achieve relatively high accuracy rates while identifying features that were significantly associated with MVI. Secondly, this study included MR examinations that were done with two types of hepatobiliary contrast agents (gadoterate meglumine, gadoxetate and gadobenate dimeglumine). Utilising a single (hepatocyte-specific) contrast agent would have helped to reduce heterogeneity of the MR images and allowed further analysis of the hepatobiliary phase. Due to small sample size, sub-group analysis of scans performed with each type of contrast agent could not be performed. However, standard imaging parameters were performed, in particular fixed timing of contrast enhanced phases, which reduced technical variability. Lastly, TA was only done across the largest cross-sectional area of the tumour. While analysing the entire volume of the tumour and the peritumoral tissues, would have been ideal, enough information was extracted from just a two-dimensional representation of the HCC to yield relatively accurate results.

CONCLUSION

In conclusion, texture analysis of HCC performed on pre-operative MR images can accurately predict the presence of MVI with an accuracy of up to 87.8%. It has potential to be incorporated into clinical routine as a reliable tool for making pre-operative treatment decisions. Larger studies should be performed to validate the texture parameters and its value over qualitative visual analysis.

ARTICLE HIGHLIGHTS

Research background

Presence of microvascular invasion (MVI) indicates poorer prognosis post-curative resection of hepatocellular carcinoma (HCC), with an increased chance of tumour recurrence. By present standards, MVI can only be diagnosed post-operatively on histopathology.

Research motivation

Texture analysis potentially allows identification of patients who are considered 'high risk' through analysis of pre-operative magnetic resonance imaging (MRI) studies. These findings may or may not be readily apparent to the human eye, thus the need for an analytic software. This will in turn allow for better patient selection, improved individualised therapy (such as extended surgical margins or adjuvant therapy) and pre-operative prognostication.

Research objectives

To evaluate the accuracy of texture analysis on pre-operative MRI in predicting MVI in HCC.

Research methods

We recruited patients who underwent hepatectomy. Both qualitative (performed by radiologists) and quantitative data (performed by software) were obtained. Radiomics texture parameters were extracted based on the largest cross-sectional area of each tumor and analysed using MaZda software. Final histology of the tumour was used as ground truth.

Research results

Texture analysis of tumours on pre-operative MRI can predict presence of MVI in HCC with accuracies of up to 87.8%.

Research conclusions

Texture analysis of HCC performed on pre-operative MR images can accurately predict the presence of MVI with an accuracy of up to 87.8%. It has potential to be incorporated into clinical routine as a reliable tool for making pre-operative treatment decisions. Larger studies should be performed to validate the texture parameters and its value over qualitative visual analysis.

Research perspectives

This study demonstrates the utility of texture analysis on pre-operative MRI to potentially impact clinical management in patients with surgically resectable hepatocellular carcinoma.

FOOTNOTES

Author contributions: Sim JZT contributed to drafting of manuscript, critical revision; Hui TCH contributed to acquisition of data, analysis and interpretation of data; Chuah TK contributed to acquisition of data, analysis and interpretation of data; Low HM, Shelat VG, and Tan CH contributed to study conception and design, critical revision.

Institutional review board statement: IRB was obtained, the requirement to obtain written consent was waived.

Informed consent statement: All study participants or their legal guardian provided informed written consent about personal and medical data collection prior to study enrolment.

Conflict-of-interest statement: All the Authors have no conflict of interest related to the manuscript.

Data sharing statement: Not applicable.

STROBE statement: The authors have read the STROBE Statement – checklist of items, and the manuscript was prepared and revised according to the STROBE Statement – checklist of items.

Country/Territory of origin: Singapore

ORCID number: Jordan Zheng Ting Sim 0000-0002-4164-1643; Cher Heng Tan 0000-0003-3341-3111; Vishal G Shelat 0000-0003-3988-8142.

S-Editor: Liu JH
L-Editor: A
P-Editor: Liu JH

REFERENCES

1 **Ikai I**, Arii S, Kojiro M, Ichida T, Makuuchi M, Matsuyama Y, Nakanuma Y, Okita K, Omata M, Takayasu K, Yamaoka Y. Reevaluation of prognostic factors for survival after liver resection in patients with hepatocellular carcinoma in a Japanese nationwide survey. *Cancer* 2004; **101**: 796-802 [PMID: 15305412 DOI: 10.1002/cncr.20426]

2 **Lauwers GY**, Terris B, Balis UJ, Batts KP, Regimbeau JM, Chang Y, Graeme-Cook F, Yamabe H, Ikai I, Cleary KR, Fujita S, Flejou JF, Zukerberg LR, Nagorney DM, Belghiti J, Yamaoka Y, Vauthey JN; International Cooperative Study Group on Hepatocellular Carcinoma. Prognostic histologic indicators of curatively resected hepatocellular carcinomas: a multi-institutional analysis of 425 patients with definition of a histologic prognostic index. *Am J Surg Pathol* 2002; **26**: 25-34 [PMID: 11756766 DOI: 10.1097/00000478-200201000-00003]

3 **Lim KC**, Chow PK, Allen JC, Chia GS, Lim M, Cheow PC, Chung AY, Ooi LL, Tan SB. Microvascular invasion is a better predictor of tumor recurrence and overall survival following surgical resection for hepatocellular carcinoma compared to the Milan criteria. *Ann Surg* 2011; **254**: 108-113 [PMID: 21527845 DOI: 10.1097/SLA.0b013e31821ad884]

4 **Rodríguez-Perálvarez M**, Luong TV, Andreana L, Meyer T, Dhillon AP, Burroughs AK. A systematic review of microvascular invasion in hepatocellular carcinoma: diagnostic and prognostic variability. *Ann Surg Oncol* 2013; **20**: 325-339 [PMID: 23149850 DOI: 10.1245/s10434-012-2513-1]

5 **Wang W**, Guo Y, Zhong J, Wang Q, Wang X, Wei H, Li J, Xiu P. The clinical significance of microvascular invasion in the surgical planning and postoperative sequential treatment in hepatocellular carcinoma. *Sci Rep* 2021; **11**: 2415 [PMID: 33510294 DOI: 10.1038/s41598-021-82058-x]

6 **Zhou Y**, He L, Huang Y, Chen S, Wu P, Ye W, Liu Z, Liang C. CT-based radiomics signature: a potential biomarker for preoperative prediction of early recurrence in hepatocellular carcinoma. *Abdom Radiol (NY)* 2017; **42**: 1695-1704 [PMID:

28180924 DOI: 10.1007/s00261-017-1072-0]
7 **Hui TCH**, Chuah TK, Low HM, Tan CH. Predicting early recurrence of hepatocellular carcinoma with texture analysis of preoperative MRI: a radiomics study. *Clin Radiol* 2018; **73**: 1056.e11-1056.e16 [PMID: 30213434 DOI: 10.1016/j.crad.2018.07.109]
8 **Liu J**, Mao Y, Li Z, Zhang D, Zhang Z, Hao S, Li B. Use of texture analysis based on contrast-enhanced MRI to predict treatment response to chemoradiotherapy in nasopharyngeal carcinoma. *J Magn Reson Imaging* 2016; **44**: 445-455 [PMID: 26778191 DOI: 10.1002/jmri.25156]
9 **Ahmed A**, Gibbs P, Pickles M, Turnbull L. Texture analysis in assessment and prediction of chemotherapy response in breast cancer. *J Magn Reson Imaging* 2013; **38**: 89-101 [PMID: 23238914 DOI: 10.1002/jmri.23971]
10 **Yamashita Y**, Tsuijita E, Takeishi K, Fujiwara M, Kira S, Mori M, Aishima S, Taketomi A, Shirabe K, Ishida T, Maehara Y. Predictors for microinvasion of small hepatocellular carcinoma ≤ 2 cm. *Ann Surg Oncol* 2012; **19**: 2027-2034 [PMID: 22203184 DOI: 10.1245/s10434-011-2195-0]
11 **Cucchetti A**, Piscaglia F, Grigioni AD, Ravaioli M, Cescon M, Zanello M, Grazi GL, Golfieri R, Grigioni WF, Pinna AD. Preoperative prediction of hepatocellular carcinoma tumour grade and micro-vascular invasion by means of artificial neural network: a pilot study. *J Hepatol* 2010; **52**: 880-888 [PMID: 20409605 DOI: 10.1016/j.jhep.2009.12.037]
12 **Lei Z**, Li J, Wu D, Xia Y, Wang Q, Si A, Wang K, Wan X, Lau WY, Wu M, Shen F. Nomogram for Preoperative Estimation of Microvascular Invasion Risk in Hepatitis B Virus-Related Hepatocellular Carcinoma Within the Milan Criteria. *JAMA Surg* 2016; **151**: 356-363 [PMID: 26579636 DOI: 10.1001/jamasurg.2015.4257]
13 **Pawlik TM**, Gleisner AL, Anders RA, Assumpcao L, Maley W, Choti MA. Preoperative assessment of hepatocellular carcinoma tumor grade using needle biopsy: implications for transplant eligibility. *Ann Surg* 2007; **245**: 435-442 [PMID: 17435551 DOI: 10.1097/01.sla.0000250420.73854.ad]
14 **Ahn SJ**, Kim JH, Park SJ, Kim ST, Han JK. Hepatocellular carcinoma: preoperative gadoxetic acid-enhanced MR imaging can predict early recurrence after curative resection using image features and texture analysis. *Abdom Radiol (NY)* 2019; **44**: 539-548 [PMID: 30229421 DOI: 10.1007/s00261-018-1768-9]
15 **Wilson GC**, Cannella R, Fiorentini G, Shen C, Borhani A, Furlan A, Tsung A. Texture analysis on preoperative contrast-enhanced magnetic resonance imaging identifies microvascular invasion in hepatocellular carcinoma. *HPB (Oxford)* 2020; **22**: 1622-1630 [PMID: 32229091 DOI: 10.1016/j.hpb.2020.03.001]
16 **Strzelecki M**, Szczypinski P, Materka A, Klepaczko A. A software tool for automatic classification and segmentation of 2D/3D medical images. *Nucl Instruments Methods Phys Res Sect A Accel Spectrometers, Detect Assoc Equip* 2013; **702**: 137-140 [DOI: 10.1016/J.NIMA.2012.09.006]
17 **Mulé S**, Thiefin G, Costentin C, Durot C, Rahmouni A, Luciani A, Hoeffel C. Advanced Hepatocellular Carcinoma: Pretreatment Contrast-enhanced CT Texture Parameters as Predictive Biomarkers of Survival in Patients Treated with Sorafenib. *Radiology* 2018; **288**: 445-455 [PMID: 29584597 DOI: 10.1148/radiol.2018171320]
18 **Akai H**, Yasaka K, Kunimatsu A, Nojima M, Kokudo T, Kokudo N, Hasegawa K, Abe O, Ohtomo K, Kiryu S. Predicting prognosis of resected hepatocellular carcinoma by radiomics analysis with random survival forest. *Diagn Interv Imaging* 2018; **99**: 643-651 [PMID: 29910166 DOI: 10.1016/j.diii.2018.05.008]
19 **Lubner MG**, Smith AD, Sandrasegaran K, Sahani DV, Pickhardt PJ. CT Texture Analysis: Definitions, Applications, Biologic Correlates, and Challenges. *Radiographics* 2017; **37**: 1483-1503 [PMID: 28898189 DOI: 10.1148/rg.2017170056]
20 **Wei J**, Jiang H, Zeng M, Wang M, Niu M, Gu D, Chong H, Zhang Y, Fu F, Zhou M, Chen J, Lyv F, Wei H, Bashir MR, Song B, Li H, Tian J. Prediction of Microvascular Invasion in Hepatocellular Carcinoma *via* Deep Learning: A Multi-Center and Prospective Validation Study. *Cancers (Basel)* 2021; **13** [PMID: 34068972 DOI: 10.3390/cancers13102368]
21 **Yang L**, Gu D, Wei J, Yang C, Rao S, Wang W, Chen C, Ding Y, Tian J, Zeng M. A Radiomics Nomogram for Preoperative Prediction of Microvascular Invasion in Hepatocellular Carcinoma. *Liver Cancer* 2019; **8**: 373-386 [PMID: 31768346 DOI: 10.1159/000494099]
22 **Feng ST**, Jia Y, Liao B, Huang B, Zhou Q, Li X, Wei K, Chen L, Li B, Wang W, Chen S, He X, Wang H, Peng S, Chen ZB, Tang M, Chen Z, Hou Y, Peng Z, Kuang M. Preoperative prediction of microvascular invasion in hepatocellular cancer: a radiomics model using Gd-EOB-DTPA-enhanced MRI. *Eur Radiol* 2019; **29**: 4648-4659 [PMID: 30689032 DOI: 10.1007/s00330-018-5935-8]
23 **Kim H**, Park MS, Choi JY, Park YN, Kim MJ, Kim KS, Choi JS, Han KH, Kim E, Kim KW. Can microvessel invasion of hepatocellular carcinoma be predicted by pre-operative MRI? *Eur Radiol* 2009; **19**: 1744-1751 [PMID: 19247666 DOI: 10.1007/s00330-009-1331-8]
24 **Chandarana H**, Robinson E, Hajdu CH, Drozhinin L, Babb JS, Taouli B. Microvascular invasion in hepatocellular carcinoma: is it predictable with pretransplant MRI? *AJR Am J Roentgenol* 2011; **196**: 1083-1089 [PMID: 21512074 DOI: 10.2214/AJR.10.4720]
25 **Zhang L**, Yu X, Wei W, Pan X, Lu L, Xia J, Zheng W, Jia N, Huo L. Prediction of HCC microvascular invasion with gadobenate-enhanced MRI: correlation with pathology. *Eur Radiol* 2020; **30**: 5327-5336 [PMID: 32367417 DOI: 10.1007/s00330-020-06895-6]
26 **Hu HT**, Shen SL, Wang Z, Shan QY, Huang XW, Zheng Q, Xie XY, Lu MD, Wang W, Kuang M. Peritumoral tissue on preoperative imaging reveals microvascular invasion in hepatocellular carcinoma: a systematic review and meta-analysis. *Abdom Radiol (NY)* 2018; **43**: 3324-3330 [PMID: 29845312 DOI: 10.1007/s00261-018-1646-5]
27 **Min JH**, Lee MW, Park HS, Lee DH, Park HJ, Lim S, Choi SY, Lee J, Lee JE, Ha SY, Cha DI, Carriere KC, Ahn JH. Interobserver Variability and Diagnostic Performance of Gadoxetic Acid-enhanced MRI for Predicting Microvascular Invasion in Hepatocellular Carcinoma. *Radiology* 2020; **297**: 573-581 [PMID: 32990512 DOI: 10.1148/radiol.2020201940]
28 **Hong SB**, Choi SH, Kim SY, Shim JH, Lee SS, Byun JH, Park SH, Kim KW, Kim S, Lee NK. MRI Features for Predicting Microvascular Invasion of Hepatocellular Carcinoma: A Systematic Review and Meta-Analysis. *Liver Cancer* 2021; **10**: 94-106 [PMID: 33981625 DOI: 10.1159/000513704]
29 **Wei X**, Li N, Li S, Shi J, Guo W, Zheng Y, Cheng S. Hepatitis B virus infection and active replication promote the formation of vascular invasion in hepatocellular carcinoma. *BMC Cancer* 2017; **17**: 304 [PMID: 28464845 DOI: 10.1186/s12885-017-3293-6]

30 **Gui CH**, Baey S, D'cruz RT, Shelat VG. Trans-arterial chemoembolization + radiofrequency ablation *vs* surgical resection in hepatocellular carcinoma - A meta-analysis. *Eur J Surg Oncol* 2020; **46**: 763-771 [PMID: 31937433 DOI: 10.1016/j.ejso.2020.01.004]

31 **Iguchi T**, Shirabe K, Aishima S, Wang H, Fujita N, Ninomiya M, Yamashita Y, Ikegami T, Uchiyama H, Yoshizumi T, Oda Y, Maehara Y. New Pathologic Stratification of Microvascular Invasion in Hepatocellular Carcinoma: Predicting Prognosis After Living-donor Liver Transplantation. *Transplantation* 2015; **99**: 1236-1242 [PMID: 25427164 DOI: 10.1097/TP.0000000000000489]

32 **Erstad DJ**, Tanabe KK. Prognostic and Therapeutic Implications of Microvascular Invasion in Hepatocellular Carcinoma. *Ann Surg Oncol* 2019; **26**: 1474-1493 [PMID: 30788629 DOI: 10.1245/s10434-019-07227-9]

33 **Sumie S**, Nakashima O, Okuda K, Kuromatsu R, Kawaguchi A, Nakano M, Satani M, Yamada S, Okamura S, Hori M, Kakuma T, Torimura T, Sata M. The significance of classifying microvascular invasion in patients with hepatocellular carcinoma. *Ann Surg Oncol* 2014; **21**: 1002-1009 [PMID: 24254204 DOI: 10.1245/s10434-013-3376-9]

34 **Shi C**, Zhao Q, Liao B, Dong Z, Wang C, Yang J, Shen W. Anatomic resection and wide resection margin play an important role in hepatectomy for hepatocellular carcinoma with peritumoural micrometastasis. *ANZ J Surg* 2019; **89**: E482-E486 [PMID: 31618805 DOI: 10.1111/ans.15396]

35 **Zhang XP**, Chai ZT, Gao YZ, Chen ZH, Wang K, Shi J, Guo WX, Zhou TF, Ding J, Cong WM, Xie D, Lau WY, Cheng SQ. Postoperative adjuvant sorafenib improves survival outcomes in hepatocellular carcinoma patients with microvascular invasion after R0 Liver resection: a propensity score matching analysis. *HPB (Oxford)* 2019; **21**: 1687-1696 [PMID: 31153833 DOI: 10.1016/j.hpb.2019.04.014]

36 **Chen ZH**, Zhang XP, Zhou TF, Wang K, Wang H, Chai ZT, Shi J, Guo WX, Cheng SQ. Adjuvant transarterial chemoembolization improves survival outcomes in hepatocellular carcinoma with microvascular invasion: A systematic review and meta-analysis. *Eur J Surg Oncol* 2019; **45**: 2188-2196 [PMID: 31256949 DOI: 10.1016/j.ejso.2019.06.031]

World Journal of Clinical Oncology

Submit a Manuscript: https://www.f6publishing.com

World J Clin Oncol 2022 November 24; 13(11): 929-942

DOI: 10.5306/wjco.v13.i11.929

ISSN 2218-4333 (online)

SYSTEMATIC REVIEWS

Gut microbiota diversity and composition in predicting immunotherapy response and immunotherapy-related colitis in melanoma patients: A systematic review

Oliver Oey, Yu-Yang Liu, Angela Felicia Sunjaya, Daniel Martin Simadibrata, Muhammad Adnan Khattak, Elin Gray

Specialty type: Oncology

Provenance and peer review: Invited article; Externally peer reviewed.

Peer-review model: Single blind

Peer-review report's scientific quality classification
Grade A (Excellent): 0
Grade B (Very good): B, B
Grade C (Good): 0
Grade D (Fair): 0
Grade E (Poor): 0

P-Reviewer: MI SC, China; Wen XL, China

Received: October 19, 2022
Peer-review started: October 19, 2022
First decision: October 28, 2022
Revised: October 30, 2022
Accepted: November 6, 2022
Article in press: November 6, 2022
Published online: November 24, 2022

Oliver Oey, Department of Medical Oncology, St John of God Midland Public and Private Hospital, Midland, Perth 6004, WA, Australia

Oliver Oey, School of Medicine, University of Western Australia, Perth 6009, WA, Australia

Yu-Yang Liu, School of Medicine, University of Queensland, Brisbane 4072, QLD, Australia

Angela Felicia Sunjaya, Faculty of Medicine, Tarumanagara University, Jakarta 11440, Indonesia

Daniel Martin Simadibrata, School of Medicine, University of Indonesia, Jakarta 10430, Indonesia

Muhammad Adnan Khattak, Department of Medical Oncology, Fiona Stanley Hospital, Perth 6150, WA, Australia

Muhammad Adnan Khattak, Elin Gray, School of Medical Sciences, Edith Cowan University, Perth 6027, WA, Australia

Muhammad Adnan Khattak, Elin Gray, Centre for Precision Health, Edith Cowan University, Perth 6027, WA, Australia

Corresponding author: Oliver Oey, MD, Doctor, Researcher, Department of Internal Medicine, St John of God Midland Public and Private Hospital, Midland, No. 1 Clayton Street, Perth 6004, WA, Australia. oliver.oey@sjog.org.au

Abstract

BACKGROUND

Gut microbiome (GM) composition and diversity have recently been studied as a biomarker of response to immune checkpoint blockade therapy (ICB) and of ICB-related colitis.

AIM

To conduct a systematic review on the role of GM composition and diversity in predicting response and colitis in patients with melanoma treated with ICB.

METHODS

The review protocol was registered in PROSPERO: CRD42021228018. From a total of 300 studies, nine studies met inclusion criteria. Two studies were phase I clinical trials, while the remainder were prospective observational studies. All but one study has moderate risk of bias. In addition, we conducted a relevant search by Reference Citation Analysis (*RCA*) (https://www.referencecitationanalysis.com).

RESULTS

Fecal samples enriched in Firmicutes phylum were associated with good response to ICB, whereas the Bacteroidales family was associated with poor response to ICB. Samples with greater GM diversity were associated with more favorable response to ICB [hazard ratio (HR) = 3.57, 95% confidence interval = 1.02-12.52, $P < 0.05$]. Fecal samples with a higher abundance in Firmicutes were more susceptible to ICB-related colitis ($P < 0.01$) whereas samples enriched in *Bacteroidetes* were more resistant to ICB-related colitis ($P < 0.05$). Overall, there was limited concordance in the organisms in the GM identified to be associated with response to ICB, and studies evaluating GM diversity showed conflicting results.

CONCLUSION

This highlights the need for further prospective studies to confirm whether the GM could be used as a biomarker and potential intervention to modulate ICB response in melanoma patients.

Key Words: Melanoma; Gut microbiome; Microbiota; Immunotherapy; Biomarker; Immune checkpoint blockade therapy

Core Tip: Since the introduction of immune checkpoint inhibitors as part of standard of care for melanoma patients, there has been a growing interest in identifying biomarkers of response and immune related adverse events. Amongst these biomarkers, the composition of the gut microbiome has been one of the most intriguing discoveries. Our aim was to ascertain the current published evidence on the gut microbiome diversity and composition as a biomarker of response to immunotherapy. We demonstrated high variability in the results and limited concordance on the organisms identified. We highlight the conflicting aspects of these reports as well as their few commonalities.

Citation: Oey O, Liu YY, Sunjaya AF, Simadibrata DM, Khattak MA, Gray E. Gut microbiota diversity and composition in predicting immunotherapy response and immunotherapy-related colitis in melanoma patients: A systematic review. *World J Clin Oncol* 2022; 13(11): 929-942
URL: https://www.wjgnet.com/2218-4333/full/v13/i11/929.htm
DOI: https://dx.doi.org/10.5306/wjco.v13.i11.929

INTRODUCTION

Melanoma is the most lethal form of skin cancer accounting for 73% of skin-cancer related mortality and over 50000 deaths worldwide annually[1,2]. Survival for metastatic melanoma has significantly improved since the introduction of immunotherapy and targeted therapy with a 5-year survival rate of up to 50%[3-5]. Currently, the standard first-line therapy for metastatic melanoma include BRAF-targeted therapies and immune checkpoint blockade (ICB) consisting either anti-programmed death (PD)-1 monotherapy or combination of anti-PD-1 as well as anti-cytotoxic T lymphocyte-associated antigen-4 (CTLA-4) therapy[6]. Despite the considerable benefit of ICB, 40%-60% of melanoma patients do not experience objective responses to the therapy[7-9]. Thus, tremendous efforts are now focused on identifying novel biomarkers which could accurately predict the subset of patients who would benefit from ICB[10-14]. These biomarkers include tumor mutational burden, cytokines, circulating tumor DNA, human leukocyte antigen, gut microbiota (GM) diversity and composition, among many others [15].

The GM is a community of 100 trillion microorganisms of more than 1000 species mainly bacteria but also, archaea, viruses and fungi which colonize the human intestines[16]. The relationship which exists between GM and the host is a mutualistic relationship where one benefits the other[16]. In return for the nutrients derived from the host, the GM performs numerous critical functions such as fermentation of dietary fiber into short-chain fatty acids; synthesis of vitamins; protection against pathologic gut microbes; and induction and regulation of the immune system[17,18]. The gut microbial balance is pivotal in the optimal functioning of all of these roles and thus any discrepancy in this delicate

equilibrium could produce a state of dysbiosis which has been associated with many pathologies including cancer[19]. In the context of cancer, preclinical studies have demonstrated that some GM subpopulations have pro-tumorigenic effects, whereas others have tumor-suppressive effects[20-22]. Additionally, the GM has also been shown to modulate response to chemotherapy and immunotherapy [23-25]. This could be linked to the role of GM in metabolizing anti-cancer compounds and regulating the host's immune response[16]. Thus, GM has been studied intensely as a potential biomarker of response to ICB[12,26-31]. This is particularly relevant for melanoma, where ICB has become standard of care given its demonstrated pronounced effectiveness.

Studies investigating GM composition and/or diversity in patients with melanoma have identified distinct GM composition in responders to ICB compared to non-responders, offering hope of a novel biomarker for predicting response to ICB[12,26-32]. Additionally, studies exploring whether certain GM composition and diversity could be predictive of ICB-related colitis - one of the major factors of ICB treatment cessation and thus failure to derive full benefit of ICB - have also been conducted[27,33]. This systematic review will be the first to compile the existing data regarding the role of GM composition and diversity in predicting response to ICB and ICB-related colitis specifically in patients with melanoma. Notably previous reviews have combined multiple cancers.

MATERIALS AND METHODS

Literature search strategies

This review was conducted following the preferred reporting Items for systematic reviews and meta-analyses guidelines[34]. The review protocol was submitted to the international prospective register of systemic reviews (PROSPERO Registration number: CRD42021228018).

In this comprehensive literature search, original studies exploring the variation in GM community in fecal samples of melanoma patients who responded and did not respond to immunotherapy, experienced colitis and did not experience colitis were identified. Medline and Embase were searched for eligible papers published prior to December 2021 using the following search terms: (fecal OR gut) AND (microbiota OR microbiome) AND (melanoma) AND (immunotherapy OR checkpoint OR nivolumab OR ipilimumab OR pembrolizumab). OpenGrey and the Grey Literature Report were also searched for eligible unpublished papers and grey literature. The following keywords and its synonyms will be used for our search strategy: "fecal microbiota", "melanoma", "immunotherapy".

Duplicate and irrelevant publication types such as symposium agendas were removed from the initial search results. Titles and abstracts of relevant publications were screened independently by Oliver O and Simadibrata DM based on inclusion and exclusion criteria stated below. Subsequently, reference lists within each relevant publication were examined for further pertinent studies. The full texts of these publications were then reviewed.

Inclusion criteria

Inclusion criteria for the systematic review included randomized controlled trials (RCTs), original cohort, case-control studies published in a peer-reviewed journal exploring GM diversity and composition in fecal samples from melanoma patients treated with ICB which can be anti-PD-1 and/or anti-PD-L1 and/or anti-CTLA-4. Studies included should assess treatment outcome and/or ICB-related colitis incidence following treatment with ICB. Treatment outcomes should be determined by RECIST criteria and/or progression free survival (PFS) and/or overall survival (OS) and ICB-related colitis confirmed by colonoscopy.

Only studies which utilized fecal samples obtained from human subjects receiving ICB were included. Studies which assessed treatment response to immunotherapy in animal models were excluded. Two reviewers (Oliver O, Liu YY) independently screened and read the full text of the included articles for eligibility.

Data extraction

Two investigators (Oliver O, Liu YY) independently reviewed the eligible studies and extracted data from each study. Extracted variables included title, first author, year of publication, number of participants, type of immunotherapy received, GM analysis method, and study outcomes (GM composition and diversity in responders/non-responders and ICB-related colitis/non-ICB-related colitis patients). Extracted GM composition data included a list of the GM at the level of phyla, class, order, family, genus and species, whereas extracted GM diversity extracted included alpha diversity or the Shannon index. Any discrepancies found by the investigators on data extraction were resolved by consensus. In addition, we conducted a relevant search by Reference Citation Analysis (*RCA*) (https://www.referencecitationanalysis.com).

Quality assessment

Non-randomized studies, including cohort studies, case-control studies and single-arm clinical trial that

were included in this systematic review were independently evaluated by Oliver O and Simadibrata DM for any risk of bias using the Risk of Bias in Non-randomized Studies of interventions (ROBINS-I) assessment tool, a tool which assesses seven items: confounding, selection, intervention classification, deviation from intervention, missing data, measurement of outcome and selection of reported result. Each item was assessed according to the ROBINS-I guideline, where each bias domain can be classified as either low, moderate, serious or critical risk of bias, or no information mentioned.

RESULTS

Study selection and risk of bias assessment

The initial search from Medline, Embase, OpenGrey and Grey Literature retrieved 300 studies. After deduplication, the studies were screened by reviewing their abstracts and 10 articles selected for full assessment (Figure 1). One study by Vétizou *et al*[35] was excluded because while the fecal samples were obtained from patients treated with anti-CTLA-4, treatment response to ICB was assessed in an *in-vivo* mice model of melanoma following fecal transplantation rather than humans.

From the nine included studies, two studies were phase I clinical trials, while the remainder were prospective observational studies[26,28]. Unfortunately, no RCTs were available to date. According to the ROBINS-I assessment tool, all but one study was shown to have moderate risk of bias (Table 1). The study by Matson *et al*[29] had a serious risk of bias as there was a lack of clarity regarding the definition of intervention used.

GM composition and diversity in predicting immunotherapy response

Eight studies assessed the role of GM composition and/or diversity and response to ICB in melanoma patients (Table 2). Seven studies compared the GM between responders and non-responders to ICB, and two studies analyzed the GM in patients undergoing fecal microbiota transplant (FMT).

The study by Chaput *et al*[27] assessing fecal GM composition of 26 metastatic melanoma patients prior to and post commencing anti-CTLA-4 therapy revealed that GM composition varied according to response. Patients showing long term response to therapy (nine out of 26 patients) were found with fecal samples with significantly higher *Faecalibacterium* percentages ($P = 0.0092$) while patients with poor clinical benefit had higher proportions of *Bacteroides* ($P = 0.034$). When patients were grouped based on their microbiota composition, those with high prevalence of *Faecalibacterium* and other *Firmicutes* had a longer PFS ($P = 0.0039$) and to a lesser extent longer OS ($P = 0.051$) relative to patients whose fecal samples were abundant with *Bacteroides*. Additionally, these patient groups were noted to derive long-term clinical benefit compared to the latter (67% *vs* 0%; $P = 0.0017$)[28].

In an analysis of stool samples from 42 metastatic melanoma patients prior to treatment with anti-PD-1 ($n = 38$) and anti-CTLA-4 ($n = 4$) therapy, Matson *et al*[29] showed a significant difference in GM composition between responders (16 patients) and non-responders (26 patients) ($P < 0.01$). In responders, eight microbial species namely, *Enterococcus faecium*, *Collinsella aerofaciens*, *Bifidobacterium adolescentis*, *Klebsiella pneumoniae*, *Veillonella parvula*, *Parabacteroides merdae*, *Lactobacillus* sp. and *Bifidobacterium longum* were found to be more abundant in responders than in non-responders[29]. In non-responders, two microbial species, specifically, *Ruminococcus obeum* and *Roseburia intestinalis* were more abundant[29]. To further assess the applicability of GM composition as a biomarker of response to ICB, they explored the correlation between the ratio of total numbers of potentially "beneficial" and "nonbeneficial" operational taxonomic units (OTUs), and change in tumor size, as assessed by the RECIST[29]. Patients with an OTU ratio of greater than 1.5 demonstrated clinical response to ICB[29].

In another study by Gopalakrishnan *et al*[12], fecal samples of 43 metastatic melanoma patients prior to treatment with anti-PD-1 therapy were analyzed. In responders (30 patients), analysis of fecal samples revealed abundance of GM from *Ruminococcaceae* family of the *Clostridiales* order, whereas in non-responders (13 patients), abundance of GM from the *Bacteroidales* order was noted[12]. Further analyses demonstrated that *Faecalibacterium* genus was notably enriched in fecal samples from responders and *Bacteroides thetaiotaomicron*, *Escherichia coli*, and *Anaerotruncus colihominis* were enriched in non-responders[12]. In addition, to investigate durability of response, patients were stratified based on their fecal composition of *Faecalibacterium* genus and *Bacteroidales* order and correlated to their PFS [12]. Results demonstrated that patients with *Faecalibacterium*-enriched fecal samples have longer PFS than those with low abundance ($P = 0.03$) and patients with *Bacteroidales*-enriched fecal samples have shorter PFS than those with low abundance ($P = 0.05$). Beyond specific microbial taxa, GM diversity, as assessed by Simpson's reciprocal index, was higher in responders compared to non-responders ($P < 0.01$)[12]. Moreover, high GM diversity was significantly associated with anti-PD-1 therapy response, when compared to patient groups of intermediate diversity [hazard ratio (HR) = 3.60, 95% confidence interval (CI): 1.02-12.74, $P < 0.05$) and low diversity (HR = 3.57, 95%CI: 1.02-12.52, $P < 0.05$). Other important predictors of therapy response include abundance of *Faecalibacterium* (HR = 2.92, 95%CI: 1.08-7.89) and *Bacteroidales* (HR = 0.39, 95%CI: 0.15-1.03) in the fecal microbiome[12].

Table 1 Risk of bias assessment with Risk of Bias In Non-randomised Studies - of Interventions

Ref.	Confounding	Selection	Intervention classification	Deviation from intervention	Missing data	Measurement of outcome	Selection of reported result	Overall
Dubin *et al*[33], 2016	Moderate	Low	Low	Low	Low	Low	Low	Moderate
Chaput *et al*[27], 2017	Moderate	Low	Low	Moderate	Low	Low	Moderate	Moderate
Gopalakrishnan *et al*[12], 2018	Moderate	Low	No information	Low	Low	Low	Low	Moderate
Matson *et al*[29], 2018	Moderate	No information	Serious	No information	No information	Low	Moderate	Serious
Peters *et al*[30], 2019	Moderate	Low	No information	No information	Low	Low	Low	Moderate
Baruch *et al*[26], 2020	Moderate	Low	Low	Low	Moderate	Low	Low	Moderate
Wind *et al*[31], 2020	Moderate	No information	No information	No information	No information	Low	Low	Moderate
Davar *et al*[28], 2021	Moderate	Moderate	Low	Low	No information	Low	Low	Moderate
Andrews *et al*[36], 2021	Moderate	Low	Low	Low	Low	Low	Low	Moderate

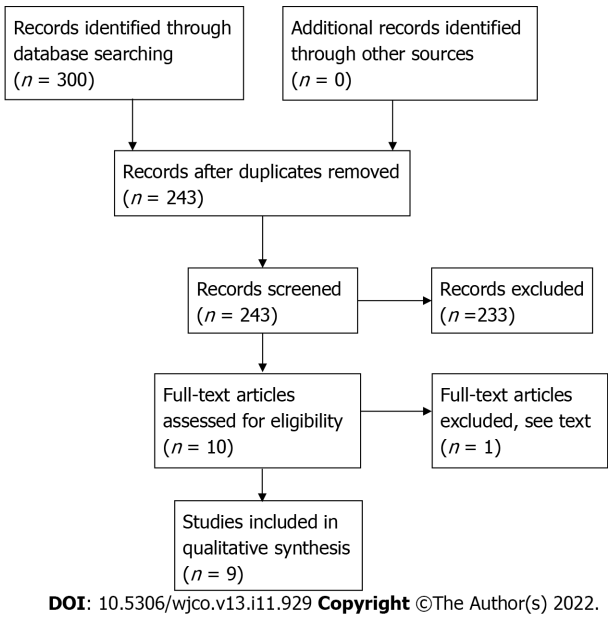

DOI: 10.5306/wjco.v13.i11.929

Figure 1 Prisma flow diagram of study selection.

Peters *et al*[30] examined the correlation between GM taxa and PFS in pre-treatment fecal samples of 27 metastatic melanoma patients receiving anti-PD-L1 and/or anti-CTLA-4. GM which was associated with shorter PFS included genera *Bacteroides* and *Bilophila*, and species *Bacteroides ovatus*, *Blautia producta*, and *Ruminococcus gnavus*, whereas those which correlated with longer PFS included genera *Faecalibacterium* and *Parabacteroides* and species *Faecalibacterium prausnitzii*[12]. With regards to GM richness the authors compared the β-diversity or between-sample microbiome diversity relative to survival. Multivariate analysis adjusting for age, sex, BMI, stage, number of sites of metastases, and antibiotic use in the last 6 mo revealed that higher GM richness was correlated with longer PFS (number of 16S sub - OTUs: HR [95%CI] = 0.97 [0.95, 1.00], P = 0.02; number of shotgun subspecies: HR [95%CI] = 0.89 [0.79, 0.99], P = 0.03)[30]. Furthermore, analysis of the 16S but not shotgun dataset showed that higher diversity of GM, as assessed by the Shannon index, was associated with longer PFS (P = 0.02)[12].

Table 2 Characteristics of included studies exploring link between gut microbiome composition and diversity and response to immune-checkpoint blockade therapy in metastatic melanoma patients treated with immune-checkpoint blockade therapy

Ref.	Year	Therapy	Method	Sample size/ time point	Dominant microbes	Microbial diversity
Chaput *et al*[27], 2017	2017	Anti-CTLA-4	16S rRNA gene sequencing of fecal samples	26 before tx	Responders: *Faecalibacterium* and *Firmicutes*	N/A
Matson *et al*[29], 2018	2018	Anti-PD-1 or anti-CTLA-4	16S rRNA gene and shotgun metagenome sequencing of fecal samples; qPCR on selected bacteria	42 before tx	Responders: *Bifidobacterium longum*, *Collinsella aerofaciens*, and *Enterococcus faecium* Non-responders: *Ruminococcus obeum* and *Roseburia intestinalis*	N/A
Gopalakrishnan *et al*[12], 2018	2018	Anti-PD-1	16S rRNA gene and shotgun metagenome sequencing of fecal samples	43 before tx	Responders: *Clostridiales*, in particular *Faecalibacterium* Non-responders: *Bacteroidales*, in particular *Bacteroides thetaiotaomicron*; as well as *Escherichia coli*, and *Anaerotruncus colihominis*	Higher alpha diversity in patients with longer PFS
Peters *et al*[30], 2019	2019	Anti-PD-1 or anti-CTLA-4	16S rRNA gene and shotgun metagenome sequencing of fecal samples	27 before tx	Responders: *Faecalibacterium, Parabacteroides*, and *Faecalibacterium prausnitzii* Non-responders: *Bacteroides* and *Biophilia*	Higher microbial community richness and diversity was associated with longer PFS
Wind *et al*[31], 2020	2020	Anti-PD-1 or anti-CTLA-4	Shotgun metagenome sequencing of fecal samples	25 before tx	Responders: *Ruminococcus gnavus, Streptococcus parasanguinis*, and *Bacteroides massiliensis*. Non-responders: *Bifidobacterium longum* and *Peptostreptococcaceae*	No significant difference in alpha-diversity between responder and non responders
Baruch *et al*[26], 2020	2020	Anti-PD-1 refractory	16S rRNA gene and shotgun metagenome sequencing of fecal samples	10 anti-PD-1 refractory patients	FMT donors (responders): *Lachnospiraceae, Veillonellaceae*, and *Ruminococcaceae* Post FMT Responders: *Enterococcaceae, Enterococcus*, and *Streptococcus australis* Non-responders: *Veillonella atypica*	No significant difference in GM composition prior to FMT, but significant difference post-FMT between responders and non-responders Lower microbial richness in the donor of responding recipients
Davar *et al*[28]. 2021	2021	Anti-PD-1 refractory	Shotgun metagenomic sequencing of fecal samples	15 anti-PD-1 refractory patients, before FMT	Responders: Firmicutes (*Lachnospiraceae* and *Ruminococcaceae* families) and *Actinobacteria* (*Bifidobacteriaceae* and *Coriobacteriaceae* families)	Higher GM diversity of donors who were complete responders compared to donors who were partial responders No significant difference in GM diversity between donors and recipients prior to FMT
Andrews *et al* [36], 2021	2021	Combined ICB - Anti-PD-1 and anti-CTLA-4	16S rRNA gene and shotgun metagenome sequencing of fecal samples	38	Responders: *Bacteroides stercoris*, *Parabacteroides distasonis*, *Fournierella massiliensis*. Non-responders: *Klebsiella aerogenes* and *Lactobacillus rogosae*	No significant difference in GM diversity between responders and non-responders

Anti-CTLA-4: Anti-cytotoxic T lymphocyte-associated antigen-4; N/A: Not applicable; Anti-PD-1: Anti-programmed death-1; qPCR: Quantitative real-time polymerase chain reaction; FMT: Fecal microbiota transplant; GM: Gut microbiome; ICB: Immune checkpoint blockade therapy.

Similarly, Wind *et al*[31] analyzed fecal samples from 25 metastatic melanoma patients - 12 responders, 13 non-responders - prior to start of treatment with anti-PD-1 or anti-CTLA-4. Analysis revealed that the fecal samples of responders were mainly enriched in *Ruminococcus gnavus*, *Escherichia coli*, *Eubacterium biforme*, *Phascolarctobacterium succinatutens* and *Streptococcus salivarius*, whereas samples from non-responders were abundant in *Bifidobacterium longum*, *Prevotella copri*, *Coprococus* sp, *Eggerthella unclassified* and *Eubacterium ramulus*[31]. When correlated with survival, fecal samples of participants enriched in *Bacteroides massiliensis* and *Streptococcus parasanguinis* were associated with longer PFS (HR: 3.79, 95%CI: 1.06-13.52 P = 0.04) and OS (HR: 5.05, 95%CI: 1.33-19.21, P = 0.017) respectively, whereas those who were carriers of *Peptostreptococcaceae* were associated with shorter PFS (HR: 0.18, 95%CI: 0.05-0.62, P = 0.007) and OS (HR: 0.12, 95%CI: 0.01-0.96, P = 0.046)[31]. In terms of GM diversity, as assessed by Shannon index, no significant difference between responders and non-responders was noted[31].

The study by Andrews *et al*[36] analyzed gut microbiome samples from a subset of 77 metastatic melanoma patients - 27 responders, 11 non-responders - who underwent combined ICB. There was no significant association in *Firmicutes* phyla and *Clostridiales* order and response to ICB (P = 0.39 and P = 0.38, respectively) and no significant difference in alpha diversity between responders and non-responders to ICB[36]. Fecal samples from responders were mainly enriched with *Bacteroides stercoris*,

Parabacteroides distasonis and *Fournierella massiliensis* (P = 0.03, P = 0.04 and P = 0.008, respectively) while fecal samples from non-responders were abundant in *Klebsiella aerogenes and Lactobacillus rogosae* (P = 0.04 and P = 0.02, respectively)[36].

In a first clinical trial of its kind (phase 1), Baruch *et al*[26] demonstrated that FMT from anti-PD-1 treated metastatic melanoma patients who were complete responders (2 donors), triggered response to anti-PD-1 therapy in metastatic melanoma patients who were refractory to at least one line of anti-PD-1 therapy. Out of 10 patients included in the trial, 3 patients demonstrated objective responses with 1 achieving complete response and 2 patients achieving partial response[26]. Notably, the PFS milestone of 6 mo was reached in all responders[26]. Upon analysis of pre-treatment fecal samples of donors, donor of the responding recipients had a lower microbial richness than the other donor of the non-responding patients[26]. There was no significant difference on the GM composition prior to FMT of recipients who responded compared to those who did not respond[26]. Metagenome sequencing found that recipients post FMT have higher proportions of *Veillonellaceae* family and a lower relative abundance of *Bifidobacterium bifidum*. Donors were found with high amounts of *Lachnospiraceae, Veillonellaceae*, and *Ruminococcaceae*. Comparison of a small subset of non-responders with responders, found statistically significant higher abundance of *Enterococcaceae, Enterococcus*, and *Streptococcus australis*, and a lower relative abundance of *Veillonella atypica*. However clear deductions on specific GM taxa cannot be made, as there were non-responders and pre-treatment fecal samples with similar dynamics. it is crucial to note that this trial was primarily designed to assess safety of FMT and not statistically powered to assess efficacy[26].

In a separate trial, Davar *et al*[28] showed that fecal microbial transplant (FMT) from metastatic melanoma patients (7 donors) who had complete (4 donors) or partial response (3 donors) to anti-PD-1 therapy helped overcome resistance in anti-PD-1 treatment-refractory metastatic melanoma patients (15 patients). Following FMT and anti-PD-1 therapy, 6 out of 15 patients achieved clinical benefit, with 3 patients achieving objective responses and 3 patients experiencing stable disease lasting more than 12 mo[28]. Analysis of stools after FMT revealed that samples from responders were abundant in the phyla, *Firmicutes* (*Lachnospiraceae* and *Ruminococcaceae*) and *Actinobacteria* (*Bifidobacteriaceae* and *Coriobacteriaceae*) and had decreased proportions in phylum *Bacteroidetes*[28]. In terms of GM diversity assessed with inverse Simpson index, GM diversity of donors who were complete responders were more diverse than donors who were partial responders. There was no significant difference in GM diversity between donors and recipients prior to FMT[28].

Gut microbiota composition and diversity in predicting ICB-related colitis

To date only three studies have reported on the correlation between pre-treatment GM composition and/or diversity and ICB-related colitis (Table 3).

Firstly, a prospective study by Dubin *et al*[33] explored the link between GM composition, and subsequent colitis development in 34 metastatic melanoma patients treated with ipilimumab, showed that the *Bacteroidetes* phylum was more abundant (P = < 0.05) in fecal samples of the 24 patients who did not develop ipilimumab-induced colitis compared to those who did. Further analysis revealed that within the *Bacteroidetes* phylum, the population of *Bacteroidaceae, Rikenellaceae* and *Barnesiellaceae* was significantly more abundant in the former than the latter (P < 0.01, P < 0.05 and P < 0.05 respectively)[33]. However, there was no significant difference in microbial richness and diversity, as assessed by Shannon and inverse Simpson indices, between those who developed ipilimumab-induced colitis relative to those who did not[33].

In a similar study by Chaput *et al*[27], analysis of fecal samples of metastatic melanoma patients receiving ipilimumab demonstrated high proportions of *Firmicutes* in patients who developed ipilimumab-induced colitis (P = 0.009). In contrast, fecal samples of those that did not develop colitis were mainly enriched with *Bacteroidetes* (P = 0.011)[27]. Accordingly, patients with the former GM composition also tend to have a shorter colitis-free cumulative incidence compared with patients with the latter composition[27]. Several OTUs known to be predictive to colitis such as *F. prausnitzii* L2-6, *butyrate producing bacterium* L2-21 and *G. formicilis* ATCC 27749 were associated with longer OS[27].

Finally, Andrews *et al*[36], analyzed gut microbiome samples in metastatic melanoma patients undergoing combined ICB and their link to ileitis and colitis events. No significant difference in alpha diversity was observed between those that did and did not develop colitis[36]. Fecal samples of patients developing colitis were enriched in *Bacteroides intestinalis* and *Intestinibacter bartlettii* (P = 0.009 and P = 0.009, respectively) while those that did not were abundant in *Anaerotignum lactatifermentans* and *Dorea formicigenerans* (P = 0.016 and P = 0.06, respectively)[36]. For both *B. intestinalis* and *D. formicigenerans*, associations with their risk of colitis were still maintained after adjustment using a logistic regression model [OR = 4.54 (95%CI = 1.06-24.7) and OR = 0.35 (95%CI = 0.082-1.35), respectively][36].

DISCUSSION

Our review of current reports assessing the GM composition relative to response to ICB, indicated high variability in the results and limited concordance on the organisms identified (Figure 2). Amongst the

Table 3 Characteristics studies exploring link between gut microbiome composition and diversity and immune-checkpoint blockade therapy-related colitis in metastatic melanoma patients treated with immune-checkpoint blockade therapy

Ref.	Year	Therapy	Method	Sample size/ timepoint	Dominant microbes	Microbial diversity
Dubin *et al* [33], 2015	2015	Anti-CTLA-4 immuno-therapy	16S rRNA gene and shotgun metagenome sequencing of fecal samples	34	Colitis-resistant: *Bacteroidetes* (*Bacteroidaceae, Rikenel-laceae* and *Barnesiellaceae*)	No significant difference in microbial richness and diversity
Chaput *et al* [27], 2017	2017	Anti-CTLA-4 immuno-therapy	16S rRNA gene sequencing of fecal samples	26	Colitis-resistant: *Bacteroidetes*; Colitis-prone: *Firmicutes*	Decreased bacterial diversity was associated with colitis
Andrews *et al*[36], 2021		Combined ICB - Anti-PD-1 and anti-CTLA-4	16S rRNA gene and shotgun metagenome sequencing of fecal samples	38	Colitis resistant: *Firmicutes* ; Colitis prone: *Bacteri-odetes*	No significant difference in alpha diversity

Anti-CTLA-4: Anti-cytotoxic T lymphocyte-associated antigen-4; N/A: Not applicable; Anti-PD-1: Anti-programmed death-1; qPCR: Quantitative real-time polymerase chain reaction; ICB: Immune checkpoint blockade therapy.

few commonalities, we found that fecal samples enriched in organisms from the *Firmicutes* phylum (*Lachnospiraceae* and *Ruminococcaceae* family) especially the *Faecalibacterium* genus were associated with ICB responders in 4 of 9 studies[12,27,28,31], while *Bacteroidetes* phylum was found in higher proportions in non-responders in 2 of the studies[12,30]. However, other than these two findings, there was no clear correlation between specific GM composition and response to ICB.

In fact, our analysis mainly identified inconsistencies in the GM composition reported to be associated with response to ICB. For instance, *Bifidobacterium longum* was found to be abundant in responders in the study by Wind *et al*[31], but found to be enriched in non-responders in the study by Matson *et al*[29]. Some species from the *Firmicutes* family were found in both responders and non-responders such as *Roseburia intestinalis*[29]. Similarly, species from the *Bacteroidales* order were found in both responders and non-responders, such as *Bacteroides massiliensis*[31]. The overlap in GM composition in responders and non-responders may suggest that the functional capacity of the GM may be more important than individual GM family/order/species in determining response to ICB[30].

In contrast to individual species or taxas, GM diversity have been heralded to a marker of good health[37]. Here four studies - Gopalakrishnan *et al*[12], Peters *et al*[30], Wind *et al*[31] and, Andrews *et al* [36] - assessed its potential to predict ICB responsiveness. The two first studies demonstrated that higher GM diversity in the responder group compared to non-responder arm[12,30]. However, the other two studies, Wind *et al*[31] and Andrews *et al*[36], found no differences in GM diversity between both groups. Nevertheless, in other cancer types such as renal cell carcinoma and non-small cell lung cancer, greater GM diversity has also been associated with improved responses to anti-PD-1 therapy[37-39].

Study results showing associations with GM diversity were consistent with previous studies which showed that greater GM diversity is prevalent in healthy state across multiple diseases, plausibly suggesting that a greater GM diversity produces the optimal immune environment needed for normal physiological functioning[40-42]. One major reason is the promotion of a favorable immune phenotype, as evidenced by the positive correlation between Shannon diversity index and several CD8+ T cell and NK cell signatures, required to produce a robust anti-tumoral response[38].

Previous studies have demonstrated that GM from *Firmicutes* family and *Bacteroidales* order play a significant role in mediating the response to immunotherapy in melanoma patients[12,27,29]. For instance, abundance of *Firmicutes* was associated with increased frequencies of CD4+, CD8+ T cells, CD 45+ myeloid and lymphoid tumor-infiltrating cells and preserved cytokine response to anti-PD-1 therapy[12]. Additionally, abundance of *Firmicutes* was linked with decreased frequency of intestinal and systemic regulatory T cells (Tregs) and $B7^+$ T cells, cells responsible for limiting immune response robustness[27]. This resulted in increased antigen presentation and effector T cell function in both the periphery and tumor microenvironment[12,27,29]. However, other GM such as *Bacteroidales* were unfavorable in terms of anti-tumoral response in that its abundance was associated with higher frequencies of Tregs and myeloid-derived suppressor cells and a blunted cytokine response[12]. These findings combined demonstrated that certain GM play a crucial role in mediating systemic and antitumor immune responses which have clear implications on efficacy on ICB therapy in metastatic melanoma patients.

Notably, GM has also been shown to potentially serve as not just a predictor of ICB therapy response, but also for boosting response to ICB therapy. FMT on anti-PD-1 treatment-refractory metastatic melanoma patients produced a complete response to anti-PD-1 therapy in one-third (9 out of 25 patients) of the otherwise therapy refractory patients[26,28].

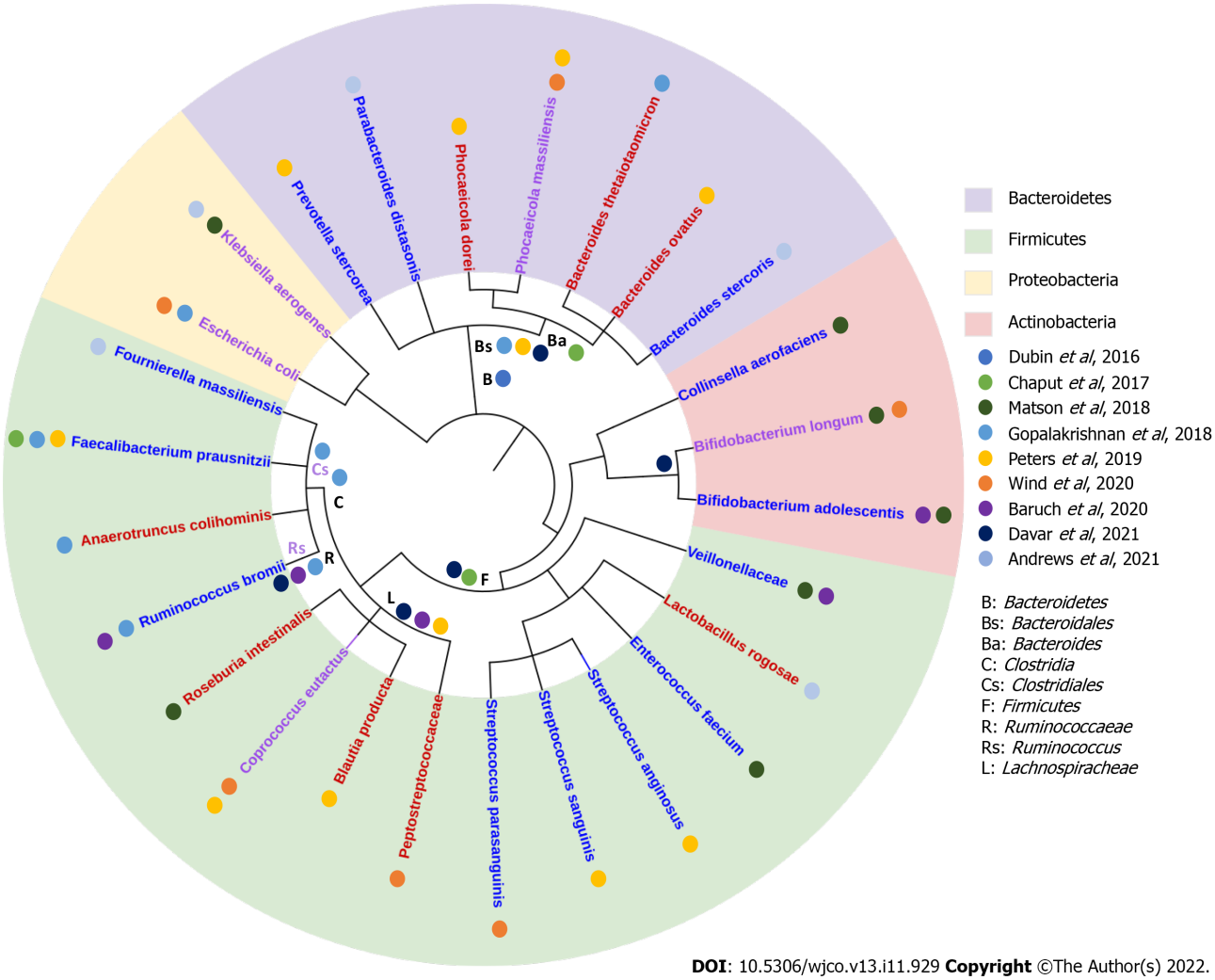

DOI: 10.5306/wjco.v13.i11.929

Figure 2 Phylogenetic tree showing family and species of gut microbiome abundant in responders and non-responders to immune-checkpoint blockade therapy in all included studies. Gut microbiome species highlighted in red: Abundant in non-responders to immune-checkpoint blockade therapy; blue: Abundant in responders to immune-checkpoint blockade therapy; purple: Abundant in both responders and non-responders.

Another aspect of the GM analyzed here, was its association with ICB-related colitis. The three studies included in this review demonstrated that GM which was abundant in ICB-related colitis-prone patients was enriched in responders to ICB (*Firmicutes*) while GM which was abundant in ICB-related colitis-resistant patients was enriched in non-responders to ICB (*Bacteroidetes*). This is consistent with the understanding that a more effective anti-tumoral response will produce greater off-target effects. The *Bacteroidetes* phyla has been linked with low-grade systemic inflammation, which could explain the observation that *Bacteroidetes* phyla was abundant in ICB-related colitis-resistant patients[27]. In line with this observation is the finding that level of *Bacteroidetes* is lower in inflammatory bowel disease - an autoimmune condition which produces chronic inflammation of the digestive tract - patients relative to healthy patients[43]. Conversely, *Firmicutes* phyla, especially *F. prausnitzii* has been associated with induction of Tregs which express high levels of CTLA-4, fueling speculation that it may cause sequestration of Tregs within the intestine[44]. Since Tregs express high levels of CTLA-4, their actions are inhibited, thereby limiting self-tolerance and promoting the development of colitis. These findings reiterate that GM has an immunomodulatory role, giving them the potential to be utilized as biomarkers of ICB-related colitis, in addition to response to ICB.

Our systematic review has several strengths. Firstly, unlike previous reviews which combined studies in various cancer types, this review focused solely on the effect of GM composition and diversity only in patients with melanoma. Secondly, we conducted a comprehensive search for RCTs and observational studies, performed a risk-of-bas assessment and studied clinically important outcomes - clinical response and ICB-related colitis - an adverse event reported in up to 25% of patients treated with ICB [45]. Thirdly, we only included studies which assessed response to immunotherapy in humans, not animals. However, several limitations exist in our systematic review. Studies which we included used distinct approaches when segregating patients into the responder and non-responder groups, using different response criteria to evaluate treatment response in patients. Additionally, there were

differences in methods of stool collection and analysis of GM composition and diversity. For example, Chaput *et al*[46] collected multiple stool samples every 3 wk of ICB, while other studies such as Dubin *et al*[33] and Matson *et al*[29] collected stool samples only prior to initiation of ICB. Furthermore, only 4 studies considered confounding factors such as variation in diet and antibiotic use[27,29-31]. Therefore, inter-study comparison of the GM composition and diversity in responders *vs* non-responders and those who experienced colitis *vs* non-colitis should be addressed with caution. Furthermore, included studies only enrolled a small number of patients, which could explain inconsistent results between studies.

CONCLUSION

In conclusion, GM composition and diversity holds some potential as a biomarker of response and toxicity to ICB in melanoma. Larger prospective studies with standardized experimental protocol ought to be conducted to elucidate whether distinct GM signatures are required for robust response to different ICB regimens. Additionally, more studies correlating metagenomic and metatranscriptomic data of GM to outcomes of melanoma patients on immunotherapy ought to be performed as the functional capacity may be more important rather than individual GM family/order/species. In addition, we eagerly await the outcome of multiple large-scale RCTs involving FMT in the context of ICB-refractory melanoma such as NCT04577729 and NCT04988841 (PICASSO) (ClinicalTrails.gov).We foresee that together with other promising biomarkers, GM composition and diversity will be integrated into a multiparameter model to accurately predict which subset of melanoma patients are likely to respond to ICB[10,11,47].

ARTICLE HIGHLIGHTS

Research background

Survival for metastatic melanoma has significantly improved since the introduction of immune checkpoint blockade (ICB) therapy. However, despite their considerable efficacy, 40%-60% of melanoma patients do not experience objective responses to the therapy. Additionally, some patients experience ICB-related colitis as a consequence of ICB therapy, preventing them from deriving the full benefit of ICB therapy. Recent studies have demonstrated that the gut microbiome (GM) may affect tumor immunity by regulating the host immune system and tumor micro-environment, thus suggesting that GM may affect response to ICB therapy and susceptibility of ICB-related colitis.

Research motivation

The GM has shown great potential as a biomarker of response to ICB therapy in melanoma patients. Previous studies investigating GM composition and/or diversity in patients with melanoma have identified distinct GM composition and diversity in responders to ICB compared to non-responders, as well as those more susceptible to ICB-related colitis than those who are not.

Research objectives

To be the first to compile the existing data regarding the role of GM composition and diversity in predicting response to ICB and ICB-related colitis specifically in patients with melanoma.

Research methods

Comprehensive literature search was done in various platforms using the following search terms: (fecal OR gut) AND (microbiota OR microbiome) AND (melanoma) AND (immunotherapy OR checkpoint OR nivolumab OR ipilimumab OR pembrolizumab). From a total of 300 studies, nine studies met inclusion criteria. Two studies were phase I clinical trials, while the remainder were prospective observational studies. All but one study has moderate risk of bias. Data from these studies including but not limited to, number of participants, type of immunotherapy received, GM analysis method, and GM composition and diversity were collected and interpreted.

Research results

Fecal samples enriched in *Firmicutes* phylum were associated with good response to ICB therapy, however they were associated with increased susceptibility to ICB-related colitis. Fecal samples enriched in *Bacteroidales* family were associated with poor response to ICB. Samples with greater GM diversity were associated with more favorable response to ICB. Fecal samples enriched in *Bacteroidetes* were associated with decreased incidence of ICB-related colitis. Overall, there was limited concordance in the organisms in the GM identified to be associated with response to ICB, and studies evaluating GM diversity showed conflicting results.

Research conclusions

GM composition and diversity holds some potential as a biomarker of response and toxicity to ICB in melanoma. Further prospective studies, including several RCTs that are underway, are needed to confirm whether the GM could be used as a biomarker and potential intervention to modulate ICB response in melanoma patients.

Research perspectives

With other promising biomarkers, GM composition and diversity holds potential to be integrated into a multiparameter model to accurately predict which subset of melanoma patients are likely to respond to ICB.

FOOTNOTES

Author contributions: Oey O, Simadibrata DM, Gray E and Khattak MA contributed to the study conception and design; Oey O and Liu Y performed data extraction; Oey O and Simadibrata DM performed risk of bias assessment; Oey O, Liu Y, Sunjaya AF, Simadibrata DM, Khattak MA and Gray E performed data analysis; Oey O written the first draft of the manuscript; all authors commented on previous versions of the manuscript, read and approved the final manuscript.

Conflict-of-interest statement: Khattak MA reports receiving travel support from Merck Sharp and Dohme (MSD), Bristol-Myers Squibb and Merck Serono. Gray E reports receiving travel sponsorship from MSD. Oey O, Liu Y, Sunjaya AF, and Simadibrata DM report no competing interests.

PRISMA 2009 Checklist statement: All authors have read the PRISMA 2009 Checklist, and the manuscript was prepared and revised according to the PRISMA 2009 Checklist.

Country/Territory of origin: Australia

ORCID number: Oliver Oey 0000-0003-0673-6804; Yu-Yang Liu 0000-0002-7438-7258; Angela Felicia Sunjaya 0000-0001-8831-0449; Daniel Martin Simadibrata 0000-0002-7512-2112; Elin Gray 0000-0002-8613-3570.

Corresponding Author's Membership in Professional Societies: American Society of Clinical Oncology; American Association for Cancer Research.

S-Editor: Wang LL
L-Editor: A
P-Editor: Wang LL

REFERENCES

1 **Gershenwald JE**, Guy GP Jr. Stemming the Rising Incidence of Melanoma: Calling Prevention to Action. *J Natl Cancer Inst* 2016; **108** [PMID: 26563358 DOI: 10.1093/jnci/djv381]
2 **Sung H**, Ferlay J, Siegel RL, Laversanne M, Soerjomataram I, Jemal A, Bray F. Global Cancer Statistics 2020: GLOBOCAN Estimates of Incidence and Mortality Worldwide for 36 Cancers in 185 Countries. *CA Cancer J Clin* 2021; **71**: 209-249 [PMID: 33538338 DOI: 10.3322/caac.21660]
3 **Hamid O**, Robert C, Daud A, Hodi FS, Hwu WJ, Kefford R, Wolchok JD, Hersey P, Joseph R, Weber JS, Dronca R, Mitchell TC, Patnaik A, Zarour HM, Joshua AM, Zhao Q, Jensen E, Ahsan S, Ibrahim N, Ribas A. Five-year survival outcomes for patients with advanced melanoma treated with pembrolizumab in KEYNOTE-001. *Ann Oncol* 2019; **30**: 582-588 [PMID: 30715153 DOI: 10.1093/annonc/mdz011]
4 **Larkin J**, Chiarion-Sileni V, Gonzalez R, Grob JJ, Rutkowski P, Lao CD, Cowey CL, Schadendorf D, Wagstaff J, Dummer R, Ferrucci PF, Smylie M, Hogg D, Hill A, Márquez-Rodas I, Haanen J, Guidoboni M, Maio M, Schöffski P, Carlino MS, Lebbé C, McArthur G, Ascierto PA, Daniels GA, Long GV, Bastholt L, Rizzo JI, Balogh A, Moshyk A, Hodi FS, Wolchok JD. Five-Year Survival with Combined Nivolumab and Ipilimumab in Advanced Melanoma. *N Engl J Med* 2019; **381**: 1535-1546 [PMID: 31562797 DOI: 10.1056/NEJMoa1910836]
5 **Robert C**, Grob JJ, Stroyakovskiy D, Karaszewska B, Hauschild A, Levchenko E, Chiarion Sileni V, Schachter J, Garbe C, Bondarenko I, Gogas H, Mandalá M, Haanen JBAG, Lebbé C, Mackiewicz A, Rutkowski P, Nathan PD, Ribas A, Davies MA, Flaherty KT, Burgess P, Tan M, Gasal E, Voi M, Schadendorf D, Long GV. Five-Year Outcomes with Dabrafenib plus Trametinib in Metastatic Melanoma. *N Engl J Med* 2019; **381**: 626-636 [PMID: 31166680 DOI:

10.1056/NEJMoa1904059]
6 **Domingues B**, Lopes JM, Soares P, Pópulo H. Melanoma treatment in review. *Immunotargets Ther* 2018; **7**: 35-49 [PMID: 29922629 DOI: 10.2147/ITT.S134842]
7 **Hodi FS**, O'Day SJ, McDermott DF, Weber RW, Sosman JA, Haanen JB, Gonzalez R, Robert C, Schadendorf D, Hassel JC, Akerley W, van den Eertwegh AJ, Lutzky J, Lorigan P, Vaubel JM, Linette GP, Hogg D, Ottensmeier CH, Lebbé C, Peschel C, Quirt I, Clark JI, Wolchok JD, Weber JS, Tian J, Yellin MJ, Nichol GM, Hoos A, Urba WJ. Improved survival with ipilimumab in patients with metastatic melanoma. *N Engl J Med* 2010; **363**: 711-723 [PMID: 20525992 DOI: 10.1056/NEJMoa1003466]
8 **Larkin J**, Chiarion-Sileni V, Gonzalez R, Grob JJ, Cowey CL, Lao CD, Schadendorf D, Dummer R, Smylie M, Rutkowski P, Ferrucci PF, Hill A, Wagstaff J, Carlino MS, Haanen JB, Maio M, Marquez-Rodas I, McArthur GA, Ascierto PA, Long GV, Callahan MK, Postow MA, Grossmann K, Sznol M, Dreno B, Bastholt L, Yang A, Rollin LM, Horak C, Hodi FS, Wolchok JD. Combined Nivolumab and Ipilimumab or Monotherapy in Untreated Melanoma. *N Engl J Med* 2015; **373**: 23-34 [PMID: 26027431 DOI: 10.1056/NEJMoa1504030]
9 **Robert C**, Schachter J, Long GV, Arance A, Grob JJ, Mortier L, Daud A, Carlino MS, McNeil C, Lotem M, Larkin J, Lorigan P, Neyns B, Blank CU, Hamid O, Mateus C, Shapira-Frommer R, Kosh M, Zhou H, Ibrahim N, Ebbinghaus S, Ribas A; KEYNOTE-006 investigators. Pembrolizumab versus Ipilimumab in Advanced Melanoma. *N Engl J Med* 2015; **372**: 2521-2532 [PMID: 25891173 DOI: 10.1056/NEJMoa1503093]
10 **Chan TA**, Yarchoan M, Jaffee E, Swanton C, Quezada SA, Stenzinger A, Peters S. Development of tumor mutation burden as an immunotherapy biomarker: utility for the oncology clinic. *Ann Oncol* 2019; **30**: 44-56 [PMID: 30395155 DOI: 10.1093/annonc/mdy495]
11 **Chowell D**, Morris LGT, Grigg CM, Weber JK, Samstein RM, Makarov V, Kuo F, Kendall SM, Requena D, Riaz N, Greenbaum B, Carroll J, Garon E, Hyman DM, Zehir A, Solit D, Berger M, Zhou R, Rizvi NA, Chan TA. Patient HLA class I genotype influences cancer response to checkpoint blockade immunotherapy. *Science* 2018; **359**: 582-587 [PMID: 29217585 DOI: 10.1126/science.aao4572]
12 **Gopalakrishnan V**, Spencer CN, Nezi L, Reuben A, Andrews MC, Karpinets TV, Prieto PA, Vicente D, Hoffman K, Wei SC, Cogdill AP, Zhao L, Hudgens CW, Hutchinson DS, Manzo T, Petaccia de Macedo M, Cotechini T, Kumar T, Chen WS, Reddy SM, Szczepaniak Sloane R, Galloway-Pena J, Jiang H, Chen PL, Shpall EJ, Rezvani K, Alousi AM, Chemaly RF, Shelburne S, Vence LM, Okhuysen PC, Jensen VB, Swennes AG, McAllister F, Marcelo Riquelme Sanchez E, Zhang Y, Le Chatelier E, Zitvogel L, Pons N, Austin-Breneman JL, Haydu LE, Burton EM, Gardner JM, Sirmans E, Hu J, Lazar AJ, Tsujikawa T, Diab A, Tawbi H, Glitza IC, Hwu WJ, Patel SP, Woodman SE, Amaria RN, Davies MA, Gershenwald JE, Hwu P, Lee JE, Zhang J, Coussens LM, Cooper ZA, Futreal PA, Daniel CR, Ajami NJ, Petrosino JF, Tetzlaff MT, Sharma P, Allison JP, Jenq RR, Wargo JA. Gut microbiome modulates response to anti-PD-1 immunotherapy in melanoma patients. *Science* 2018; **359**: 97-103 [PMID: 29097493 DOI: 10.1126/science.aan4236]
13 **Pavlick AC**, Fecher L, Ascierto PA, Sullivan RJ. Frontline Therapy for *BRAF*-Mutated Metastatic Melanoma: How Do You Choose, and Is There One Correct Answer? *Am Soc Clin Oncol Educ Book* 2019; **39**: 564-571 [PMID: 31099689 DOI: 10.1200/EDBK_243071]
14 **Marsavela G**, Lee J, Calapre L, Wong SQ, Pereira MR, McEvoy AC, Reid AL, Robinson C, Warburton L, Abed A, Khattak MA, Meniawy TM, Dawson SJ, Sandhu S, Carlino MS, Menzies AM, Scolyer RA, Long GV, Amanuel B, Millward M, Ziman MR, Rizos H, Gray ES. Circulating Tumor DNA Predicts Outcome from First-, but not Second-line Treatment and Identifies Melanoma Patients Who May Benefit from Combination Immunotherapy. *Clin Cancer Res* 2020; **26**: 5926-5933 [PMID: 33067256 DOI: 10.1158/1078-0432.CCR-20-2251]
15 **Morad G**, Helmink BA, Sharma P, Wargo JA. Hallmarks of response, resistance, and toxicity to immune checkpoint blockade. *Cell* 2021; **184**: 5309-5337 [PMID: 34624224 DOI: 10.1016/j.cell.2021.09.020]
16 **Lepage P**, Leclerc MC, Joossens M, Mondot S, Blottière HM, Raes J, Ehrlich D, Doré J. A metagenomic insight into our gut's microbiome. *Gut* 2013; **62**: 146-158 [PMID: 22525886 DOI: 10.1136/gutjnl-2011-301805]
17 **Belkaid Y**, Hand TW. Role of the microbiota in immunity and inflammation. *Cell* 2014; **157**: 121-141 [PMID: 24679531 DOI: 10.1016/j.cell.2014.03.011]
18 **Morowitz MJ**, Carlisle EM, Alverdy JC. Contributions of intestinal bacteria to nutrition and metabolism in the critically ill. *Surg Clin North Am* 2011; **91**: 771-785, viii [PMID: 21787967 DOI: 10.1016/j.suc.2011.05.001]
19 **Sheflin AM**, Whitney AK, Weir TL. Cancer-promoting effects of microbial dysbiosis. *Curr Oncol Rep* 2014; **16**: 406 [PMID: 25123079 DOI: 10.1007/s11912-014-0406-0]
20 **Jan G**, Belzacq AS, Haouzi D, Rouault A, Métivier D, Kroemer G, Brenner C. Propionibacteria induce apoptosis of colorectal carcinoma cells *via* short-chain fatty acids acting on mitochondria. *Cell Death Differ* 2002; **9**: 179-188 [PMID: 11840168 DOI: 10.1038/sj.cdd.4400935]
21 **Lara-Tejero M**, Galán JE. A bacterial toxin that controls cell cycle progression as a deoxyribonuclease I-like protein. *Science* 2000; **290**: 354-357 [PMID: 11030657 DOI: 10.1126/science.290.5490.354]
22 **Paulos CM**, Wrzesinski C, Kaiser A, Hinrichs CS, Chieppa M, Cassard L, Palmer DC, Boni A, Muranski P, Yu Z, Gattinoni L, Antony PA, Rosenberg SA, Restifo NP. Microbial translocation augments the function of adoptively transferred self/tumor-specific CD8+ T cells *via* TLR4 signaling. *J Clin Invest* 2007; **117**: 2197-2204 [PMID: 17657310 DOI: 10.1172/JCI32205]
23 **Viaud S**, Saccheri F, Mignot G, Yamazaki T, Daillère R, Hannani D, Enot DP, Pfirschke C, Engblom C, Pittet MJ, Schlitzer A, Ginhoux F, Apetoh L, Chachaty E, Woerther PL, Eberl G, Bérard M, Ecobichon C, Clermont D, Bizet C, Gaboriau-Routhiau V, Cerf-Bensussan N, Opolon P, Yessaad N, Vivier E, Ryffel B, Elson CO, Doré J, Kroemer G, Lepage P, Boneca IG, Ghiringhelli F, Zitvogel L. The intestinal microbiota modulates the anticancer immune effects of cyclophosphamide. *Science* 2013; **342**: 971-976 [PMID: 24264990 DOI: 10.1126/science.1240537]
24 **Yu T**, Guo F, Yu Y, Sun T, Ma D, Han J, Qian Y, Kryczek I, Sun D, Nagarsheth N, Chen Y, Chen H, Hong J, Zou W, Fang JY. Fusobacterium nucleatum Promotes Chemoresistance to Colorectal Cancer by Modulating Autophagy. *Cell* 2017; **170**: 548-563.e16 [PMID: 28753429 DOI: 10.1016/j.cell.2017.07.008]
25 **Zheng Y**, Wang T, Tu X, Huang Y, Zhang H, Tan D, Jiang W, Cai S, Zhao P, Song R, Li P, Qin N, Fang W. Gut

microbiome affects the response to anti-PD-1 immunotherapy in patients with hepatocellular carcinoma. *J Immunother Cancer* 2019; **7**: 193 [PMID: 31337439 DOI: 10.1186/s40425-019-0650-9]

26 **Baruch EN**, Youngster I, Ben-Betzalel G, Ortenberg R, Lahat A, Katz L, Adler K, Dick-Necula D, Raskin S, Bloch N, Rotin D, Anafi L, Avivi C, Melnichenko J, Steinberg-Silman Y, Mamtani R, Harati H, Asher N, Shapira-Frommer R, Brosh-Nissimov T, Eshet Y, Ben-Simon S, Ziv O, Khan MAW, Amit M, Ajami NJ, Barshack I, Schachter J, Wargo JA, Koren O, Markel G, Boursi B. Fecal microbiota transplant promotes response in immunotherapy-refractory melanoma patients. *Science* 2021; **371**: 602-609 [PMID: 33303685 DOI: 10.1126/science.abb5920]

27 **Chaput N**, Lepage P, Coutzac C, Soularue E, Le Roux K, Monot C, Boselli L, Routier E, Cassard L, Collins M, Vaysse T, Marthey L, Eggermont A, Asvatourian V, Lanoy E, Mateus C, Robert C, Carbonnel F. Baseline gut microbiota predicts clinical response and colitis in metastatic melanoma patients treated with ipilimumab. *Ann Oncol* 2017; **28**: 1368-1379 [PMID: 28368458 DOI: 10.1093/annonc/mdx108]

28 **Davar D**, Dzutsev AK, McCulloch JA, Rodrigues RR, Chauvin JM, Morrison RM, Deblasio RN, Menna C, Ding Q, Pagliano O, Zidi B, Zhang S, Badger JH, Vetizou M, Cole AM, Fernandes MR, Prescott S, Costa RGF, Balaji AK, Morgun A, Vujkovic-Cvijin I, Wang H, Borhani AA, Schwartz MB, Dubner HM, Ernst SJ, Rose A, Najjar YG, Belkaid Y, Kirkwood JM, Trinchieri G, Zarour HM. Fecal microbiota transplant overcomes resistance to anti-PD-1 therapy in melanoma patients. *Science* 2021; **371**: 595-602 [PMID: 33542131 DOI: 10.1126/science.abf3363]

29 **Matson V**, Fessler J, Bao R, Chongsuwat T, Zha Y, Alegre ML, Luke JJ, Gajewski TF. The commensal microbiome is associated with anti-PD-1 efficacy in metastatic melanoma patients. *Science* 2018; **359**: 104-108 [PMID: 29302014 DOI: 10.1126/science.aao3290]

30 **Peters BA**, Wilson M, Moran U, Pavlick A, Izsak A, Wechter T, Weber JS, Osman I, Ahn J. Relating the gut metagenome and metatranscriptome to immunotherapy responses in melanoma patients. *Genome Med* 2019; **11**: 61 [PMID: 31597568 DOI: 10.1186/s13073-019-0672-4]

31 **Wind TT**, Gacesa R, Vich Vila A, de Haan JJ, Jalving M, Weersma RK, Hospers GAP. Gut microbial species and metabolic pathways associated with response to treatment with immune checkpoint inhibitors in metastatic melanoma. *Melanoma Res* 2020; **30**: 235-246 [PMID: 31990790 DOI: 10.1097/CMR.0000000000000656]

32 **Carlino MS**, Larkin J, Long GV. Immune checkpoint inhibitors in melanoma. *Lancet* 2021; **398**: 1002-1014 [PMID: 34509219 DOI: 10.1016/S0140-6736(21)01206-X]

33 **Dubin K**, Callahan MK, Ren B, Khanin R, Viale A, Ling L, No D, Gobourne A, Littmann E, Huttenhower C, Pamer EG, Wolchok JD. Intestinal microbiome analyses identify melanoma patients at risk for checkpoint-blockade-induced colitis. *Nat Commun* 2016; **7**: 10391 [PMID: 26837003 DOI: 10.1038/ncomms10391]

34 **Liberati A**, Altman DG, Tetzlaff J, Mulrow C, Gøtzsche PC, Ioannidis JP, Clarke M, Devereaux PJ, Kleijnen J, Moher D. The PRISMA statement for reporting systematic reviews and meta-analyses of studies that evaluate health care interventions: explanation and elaboration. *J Clin Epidemiol* 2009; **62**: e1-34 [PMID: 19631507 DOI: 10.1016/j.jclinepi.2009.06.006]

35 **Vétizou M**, Pitt JM, Daillère R, Lepage P, Waldschmitt N, Flament C, Rusakiewicz S, Routy B, Roberti MP, Duong CP, Poirier-Colame V, Roux A, Becharef S, Formenti S, Golden E, Cording S, Eberl G, Schlitzer A, Ginhoux F, Mani S, Yamazaki T, Jacquelot N, Enot DP, Bérard M, Nigou J, Opolon P, Eggermont A, Woerther PL, Chachaty E, Chaput N, Robert C, Mateus C, Kroemer G, Raoult D, Boneca IG, Carbonnel F, Chamaillard M, Zitvogel L. Anticancer immunotherapy by CTLA-4 blockade relies on the gut microbiota. *Science* 2015; **350**: 1079-1084 [PMID: 26541610 DOI: 10.1126/science.aad1329]

36 **Andrews MC**, Duong CPM, Gopalakrishnan V, Iebba V, Chen WS, Derosa L, Khan MAW, Cogdill AP, White MG, Wong MC, Ferrere G, Fluckiger A, Roberti MP, Opolon P, Alou MT, Yonekura S, Roh W, Spencer CN, Curbelo IF, Vence L, Reuben A, Johnson S, Arora R, Morad G, Lastrapes M, Baruch EN, Little L, Gumbs C, Cooper ZA, Prieto PA, Wani K, Lazar AJ, Tetzlaff MT, Hudgens CW, Callahan MK, Adamow M, Postow MA, Ariyan CE, Gaudreau PO, Nezi L, Raoult D, Mihalcioiu C, Elkrief A, Pezo RC, Haydu LE, Simon JM, Tawbi HA, McQuade J, Hwu P, Hwu WJ, Amaria RN, Burton EM, Woodman SE, Watowich S, Diab A, Patel SP, Glitza IC, Wong MK, Zhao L, Zhang J, Ajami NJ, Petrosino J, Jenq RR, Davies MA, Gershenwald JE, Futreal PA, Sharma P, Allison JP, Routy B, Zitvogel L, Wargo JA. Gut microbiota signatures are associated with toxicity to combined CTLA-4 and PD-1 blockade. *Nat Med* 2021; **27**: 1432-1441 [PMID: 34239137 DOI: 10.1038/s41591-021-01406-6]

37 **Valdes AM**, Walter J, Segal E, Spector TD. Role of the gut microbiota in nutrition and health. *BMJ* 2018; **361**: k2179 [PMID: 29899036 DOI: 10.1136/bmj.k2179]

38 **Jin Y**, Dong H, Xia L, Yang Y, Zhu Y, Shen Y, Zheng H, Yao C, Wang Y, Lu S. The Diversity of Gut Microbiome is Associated With Favorable Responses to Anti-Programmed Death 1 Immunotherapy in Chinese Patients With NSCLC. *J Thorac Oncol* 2019; **14**: 1378-1389 [PMID: 31026576 DOI: 10.1016/j.jtho.2019.04.007]

39 **Salgia NJ**, Bergerot PG, Maia MC, Dizman N, Hsu J, Gillece JD, Folkerts M, Reining L, Trent J, Highlander SK, Pal SK. Stool Microbiome Profiling of Patients with Metastatic Renal Cell Carcinoma Receiving Anti-PD-1 Immune Checkpoint Inhibitors. *Eur Urol* 2020; **78**: 498-502 [PMID: 32828600 DOI: 10.1016/j.eururo.2020.07.011]

40 **Mosca A**, Leclerc M, Hugot JP. Gut Microbiota Diversity and Human Diseases: Should We Reintroduce Key Predators in Our Ecosystem? *Front Microbiol* 2016; **7**: 455 [PMID: 27065999 DOI: 10.3389/fmicb.2016.00455]

41 **Turnbaugh PJ**, Hamady M, Yatsunenko T, Cantarel BL, Duncan A, Ley RE, Sogin ML, Jones WJ, Roe BA, Affourtit JP, Egholm M, Henrissat B, Heath AC, Knight R, Gordon JI. A core gut microbiome in obese and lean twins. *Nature* 2009; **457**: 480-484 [PMID: 19043404 DOI: 10.1038/nature07540]

42 **Vincent C**, Stephens DA, Loo VG, Edens TJ, Behr MA, Dewar K, Manges AR. Reductions in intestinal Clostridiales precede the development of nosocomial Clostridium difficile infection. *Microbiome* 2013; **1**: 18 [PMID: 24450844 DOI: 10.1186/2049-2618-1-18]

43 **Verma R**, Verma AK, Ahuja V, Paul J. Real-time analysis of mucosal flora in patients with inflammatory bowel disease in India. *J Clin Microbiol* 2010; **48**: 4279-4282 [PMID: 20861337 DOI: 10.1128/JCM.01360-10]

44 **Romano E**, Kusio-Kobialka M, Foukas PG, Baumgaertner P, Meyer C, Ballabeni P, Michielin O, Weide B, Romero P, Speiser DE. Ipilimumab-dependent cell-mediated cytotoxicity of regulatory T cells ex vivo by nonclassical monocytes in

melanoma patients. *Proc Natl Acad Sci U S A* 2015; **112**: 6140-6145 [PMID: 25918390 DOI: 10.1073/pnas.1417320112]

45 **Som A**, Mandaliya R, Alsaadi D, Farshidpour M, Charabaty A, Malhotra N, Mattar MC. Immune checkpoint inhibitor-induced colitis: A comprehensive review. *World J Clin Cases* 2019; **7**: 405-418 [PMID: 30842952 DOI: 10.12998/wjcc.v7.i4.405]

46 **Nel Van Zyl K**, Whitelaw AC, Newton-Foot M. The effect of storage conditions on microbial communities in stool. *PLoS One* 2020; **15**: e0227486 [PMID: 31935223 DOI: 10.1371/journal.pone.0227486]

47 **Pedersen JG**, Madsen AT, Gammelgaard KR, Aggerholm-Pedersen N, Sørensen BS, Øllegaard TH, Jakobsen MR. Inflammatory Cytokines and ctDNA Are Biomarkers for Progression in Advanced-Stage Melanoma Patients Receiving Checkpoint Inhibitors. *Cancers (Basel)* 2020; **12** [PMID: 32486146 DOI: 10.3390/cancers12061414]

Published by **Baishideng Publishing Group Inc**
7041 Koll Center Parkway, Suite 160, Pleasanton, CA 94566, USA
Telephone: +1-925-3991568
E-mail: bpgoffice@wjgnet.com
Help Desk: https://www.f6publishing.com/helpdesk
https://www.wjgnet.com